


For Reference

NOT TO BE TAKEN FROM THIS ROOM

Ex LIBRIS
UNIVERSITATIS
ALBERTAENSIS





Digitized by the Internet Archive
in 2022 with funding from
University of Alberta Library

<https://archive.org/details/Ferguson1983>

THE UNIVERSITY OF ALBERTA

The Postnatal Development of Sarcolemmal Invaginations and
Dyadic Couplings in the Right Atrial Myocardium of the Rat:
A Qualitative and Quantitative Study.

by

 Donald G. Ferguson

A THESIS

SUBMITTED TO THE FACULTY OF GRADUATE STUDIES AND RESEARCH
IN PARTIAL FULFILMENT OF THE REQUIREMENTS FOR THE DEGREE
OF Doctor of Philosophy

Department of Anatomy

Edmonton, Alberta
Spring, 1983

DEDICATION

This thesis is dedicated to the memory of the late Nancy Jotcham. Her positive outlook and uncomplaining strength in the face of painful adversity and her unflagging encouragement helped, in no small measure, to inspire me throughout the course of this project.

ABSTRACT

The fine structure of developing right atrial myocardium of the rat has been studied during the early postnatal period. Tannic acid has been used to enhance membrane contrast and act as an extracellular space marker. This procedure clearly delineated the sarcolemmal invaginations, caveolae and T-tubules, from the tubules of the SR. Sarcolemmal invaginations were rare until the middle of the second week postnatally. Then there was a rapid proliferation of caveolae to assume complex forms, with up to a dozen caveolae sharing the same opening to the cell surface. There was also a development of short, branching, convoluted tubular invaginations of the sarcolemma at this time. The T-tubules never achieved the abundance, or degree of complexity seen in mammalian ventricular myocardial cells. Dyadic couplings between cisternal elements of the SR and the sarcolemma (peripheral couplings) were seen to occur, fully differentiated, at all stages. These gradually increased in abundance during the first two postnatal weeks. A rapid increase in the numbers of peripheral couplings appeared to occur during the middle of the second postnatal week. Dyadic couplings between the SR and the sarcolemmal invaginations gradually increased over the second and third week of the postnatal period. The above results were confirmed using stereological techniques. Developmental changes in fine structure were discussed in relation to postnatal changes in surface to volume ratios and abundance

of myofibrillar protein. The results were also discussed in relation to the physiological changes known to occur during the early postnatal period.

ACKNOWLEDGEMENTS

I would like to thank Dr. T. S. Leeson, who gave me the opportunity to do this project, for his valuable advice and assistance throughout the course of the research.

I would also like to thank Mr. Gary Higgs for many useful suggestions and references concerning stereology and Mr. Greg Morrison for providing expert photographic assistance during the preparation of the figures.

Finally I would like to thank Dr. B. R. MacPherson for critical evaluation of the manuscript during preparation.

The project was supported by a studentship from the Alberta Heritage Foundation for Medical Research.

Table of Contents

Chapter	Page
I. INTRODUCTION	1
II. METHODS	23
Animals: Care and Housing	23
Tissue Preparation for Electron Microscopy:	23
Experimental Design: Descriptive Morphology	25
Quantitative Morphology	26
III. RESULTS	31
A. Descriptive Morphology	31
Adult Right Atrial Myocardium	31
Neonatal Right Atrial Myocardium	35
7 Day Postnatal Right Atrial Myocardium	37
14 Day Postnatal Right Atrial Myocardium	39
16-21 Day Postnatal Right Atrial Myocardium	39
B. Morphometry	43
Weight Measurements	43
Stereology	43
Calculation of surface/volume ratios	46
IV. Discussion	49
A. Summary and Conclusions	70
V. TABLES	74
VI. FIGURES	76
BIBLIOGRAPHY	157
APPENDIX 1	173
APPENDIX 2	196

LIST OF TABLES

Table 1. Means and Standard Deviations of Body, Heart and Right Atrial Weight as as Function of Postnatal Age	74
Table 2. Means and Standard Deviations of Cell Diameter as a Function of Postnatal Age.....	74
Table 3. Means and Standard Deviations of Volume Density of Myofibrils, and Surface Density of Peripheral Couplings, Internal Couplings and Sarcolemmal Invaginations as a Function of Postnatal Age.....	75

LIST OF FIGURES

Figure 1. Adult Right Atrial Myocardium, Low Magnification, Longitudinal Section	78
Figure 2. Adult Right Atrial Myocardium, Longitudinal Section	80
Figure 3. Adult Right Atrial Myocardium, Endocardial Surface	82
Figure 4. Adult Right Atrial Myocardium, Trabecular Surface, Oblique Section	84
Figure 5. Adult Right Atrial Myocardium, Oblique Section	86
Figure 6. Adult Right Atrial Myocardium, Transverse Section	88
Figure 7. Adult Right Atrial Myocardium, High Magnification	90
Figure 8. Adult Right Atrial Myocardium, Caveolar Complexes and T-tubules	92
Figure 9. Neonatal Right Atrial Myocardium, Low Magnification, Transverse Section	94
Figure 10. Neonatal Right Atrial Myocardium, Endocardial Surface	96
Figure 11. Neonatal Right Atrial Myocardium, High Magnification, Transverse Section	98
figure 12. Neonatal Right Atrial Myocardium, Transverse Section, Endocardial Surface	100
Figure 13. Neonatal Right Atrial Myocardium, Trabecular Surface	102

Figure 14. Seven Day Postnatal Right Atrial Myocardium, Trabecular Surface	104
Figure 15. Seven Day Postnatal Right Atrial Myocardium, Longitudinal Section	106
Figure 16. Seven Day Postnatal Right Atrial Myocardium, Transverse Section	108
Figure 17. Seven Day Postnatal Right Atrial Myocardium, Trabecular Surface	110
Figure 18. Seven Day Postnatal Right Atrial Myocardium, Epicardial Surface	112
Figure 19. Fourteen Day Postnatal Right Atrial Myocardium, Low Magnification, Trabecular Surface ...	114
Figure 20. Fourteen Day Postnatal Right Atrial Myocardium, Oblique Section	116
Figure 21. Fourteen Day Postnatal Right Atrial Myocardium, Transverse Section, Distribution of Sarcoplasmic Reticulum	118
Figure 22. Fourteen Day Postnatal Right Atrial Myocardium, Development of Caveolae and Tubular Invaginations	120
Figure 23. Sixteen Day Postnatal Right Atrial Myocardium, Oblique Section	122
Figure 24. Sixteen Day Postnatal Right Atrial Myocardium, Transverse Section, Myofibrillar Development	124
Figure 25. Sixteen Day Postnatal Right Atrial Myocardium, Caveolar Complexes	126
Figure 26. Sixteen Day Postnatal Right Atrial Myocardium, T-tubules and Internal Couplings	128

Figure 27. Eighteen Day Postnatal Right Atrial Myocardium, Low Magnification, Longitudinal Section	.130
Figure 28. Eighteen Day Postnatal Right Atrial Myocardium, Endocardial Surface132
Figure 29. Eighteen Day Postnatal Right Atrial Myocardium, Transverse Section134
Figure 30. Eighteen Day Postnatal Right Atrial Myocardium, Development of Myofibrils and Sarcoplasmic Reticulum136
Figure 31. Eighteen Day Postnatal Right Atrial Myocardium, Caveolae and T-tubules138
Figure 32. Eighteen Day Postnatal Right Atrial Myocardium, Caveolar Complexes and T-tubules140
Figure 33. Twenty One Day Postnatal Right Atrial Myocardium, Low Magnification, Oblique Section142
Figure 34. Twenty One Day Postnatal Right Atrial Myocardium, Longitudinal Section144
Figure 35. Twenty One Day Postnatal Right Atrial Myocardium, Transverse Section, Development of Myofibrils and Sarcoplasmic Reticulum146
Figure 36. Twenty One Day Postnatal Right Atrial Myocardium, Caveolar Complexes, T-tubules and Internal Couplings148
Figure 37. Diagram Indicating Grid Spaces Used for Morphometry150
Figure 38. Plots of Means and Standard Deviations of Surface Density of Peripheral Couplings, Internal Couplings and Sarcolemmal Invaginations as a Function of Postnatal Age152
Figure 39. Plots of Means and Standard Deviations of	

Cell Diameter and Volume Density of Myofibrils as a Function of Postnatal Age	154
--	-----

Figure 40. The MOP-3 Digitizer	156
--------------------------------------	-----

LIST OF ABBREVIATIONS AND SYMBOLS

AP = Action Potential

Ca^{2+} = Calcium Ion

EC coupling = Excitation Contraction Coupling

IC = Internal Coupling

PC = Peripheral Coupling

SL = Sarcolemma

SR = Sarcoplasmic Reticulum

Sv = Surface Density

T-system = Transverse Tubule System

T-tubule = Transverse Tubule

TC = Terminal Cisternae

TEM = Transmission Electron Microscope

Vv = Volume Density

nm = Nanometer

μm = Micrometer

I. INTRODUCTION

The most striking fine structural feature of striated muscle cells seen in longitudinal section is the banding pattern of cross-striations formed by the protein filaments that comprise the contractile apparatus. These filaments often fill 60% of the cell's sarcoplasm. There are two major myofilaments. Thick ones, approximately 12-15 nm in diameter and 1.3-1.5 μm long and thin ones 5-6 nm in diameter that are approximately 1.0 μm in length. The myofilaments are oriented parallel to the long axis of the cell. When seen in cross-section each thick filament is surrounded by a number of thin filaments. In cardiac muscle there are twice as many thin filaments and each thick filament appears to be surrounded by 6 thin filaments in a hexagonal pattern. The banding patterns seen in electron micrographs are caused by the regular arrangement of the myofilaments into repeating units called sarcomeres. There are alternating, lighter staining I-bands and more darkly stained A-bands. In the middle of the I-band is a dense transverse line, the Z-line. Each sarcomere runs from Z-line to Z-line. In the middle of the A-band there is usually a lighter H-band. The I-band is a region where there are only thin filaments, the darker A-band contains thick filaments as well as thin ones. The Z-lines represent a site of junction between the thin filaments of adjacent sarcomeres and are strengthened by intermediate filaments, approximately 10 nm in diameter. The H-band, a lighter central region in the A-band is a region

where thin and thick filaments do not overlap. The myofilaments are collected into cylindrical bundles of approximately 1 to 2 μm in diameter, called myofibrils (156).

Each thick filament is composed of large numbers of molecules of the protein myosin bundled together in a regular manner. The individual myosin molecules are composed of two lighter meromyosin chains and two heavier meromyosin chains wrapped in a helical fashion. The light chains are woven together to form the backbone of the thick filaments. The heavy chains project out from the thick filament at periodic intervals of 143 nm. The myosin subunits are arranged so that the projecting heavy chains make an angle of 60° with each adjacent projection when viewed in cross-section. Thus the heavy myosin chains spiral radially around the thick filament in a regular, periodic manner. The heavy meromyosin chains terminate in a globular head that contains ATPase which can interact with active sites on the thin filament during the contractile process (155).

Each thin filament is comprised of several forms of the protein actin as well as the proteins tropomyosin and troponin. Globular actin subunits (G-actin) are polymerized to form thin filaments of F-actin. Two strands of F-actin are wrapped helically to form the backbone of the thin filament. Very thin strands of tropomyosin lie end to end in the grooves of the helix formed by the F-actin strands. At the points of discontinuity between tropomyosin strands,

globular troponin molecules are complexed with globular molecules of C-actin and I-actin to form the active sites. The I-actin is oriented to block access to the active site. The C-actin binds with Ca^{2+} during the activation of contraction and this then causes a change in the tertiary structure of the I-actin. The active site is now exposed and reacts with the ATPase of the head of the heavy myosin chains providing the energy for contraction (155).

There are isomeric forms of all the contractile proteins which have slightly different physiological, biochemical and biomechanical properties. Thus some of the different contractile properties that have been reported to exist between atrial and ventricular cells and between fetal, neonatal and adult muscle cells can be explained on the basis of the change from fetal to adult isomeric forms of the contractile proteins (157, 158).

Striated muscle cells possess two morphologically and functionally distinct types of intracellular tubules which are involved in the activation and co-ordination of the contractile apparatus. These are the T-system and the sarcoplasmic reticulum (SR). It now is generally accepted that the T-system consists of a network of tubules invaginated from the surface membrane (SL). The SR is considered to be a modified form of endoplasmic reticulum, peculiar to muscle cells (1, 13, 32, 58, 59, 60, 77, 125, 139, 144).

There are specialized junctions where the membranes of the T-system and the SR lie in close apposition separated by a gap of 20 nm. In transmission electron microscope (TEM) preparations dense projections with a 30 nm periodicity are seen to bridge the gap. These junctional regions are called couplings (18, 19, 23, 37, 49, 51, 57, 59, 78, 138, 140).

Several recent review articles have dealt at length with the complex mechanisms underlying the activation of the contractile apparatus in cardiac muscle cells (1, 2, 12, 28, 33, 37, 42, 48, 81, 99, 100). Briefly, it is now felt that each muscle cell is activated by a depolarization of the sarcolemma. The ensuing action potential (AP) is passed to the interior of the cell along the tubules of the T-system. Although the mechanisms are unclear, it is thought that a message is passed from the T-tubules to the SR at the couplings. This results in the release of Ca^{2+} which has been sequestered in the lumen of the SR. The released Ca^{2+} interacts with the myofibrillar proteins causing contraction. This whole process has come to be known as excitation-contraction (EC) coupling.

The fine structure of the T-system has been well studied in ventricular myocardial tissue. A classical study by Fawcett and McNutt (49) described the organelle as a network of relatively large diameter (150-200 nm) tubules that invaginated from the cell surface membrane at the level

of the Z-line. These large diameter tubules appear to contain glycoprotein continuous with the glycocalyx of the sarcolemma (65). Longitudinal connections were described and the authors suggested that these smaller diameter connections were quite numerous. Forssmann and Girardier (53) used horseradish peroxidase (HRP) as an extracellular marker to study the T-system of rat myocardium. They found that ventricular myocardial cells had a very extensive network with many relatively wide longitudinal branches connecting the transverse tubules. This was confirmed by Sperelakis, Forbes and Rubio (142) and Sommer and Waugh (140). Ayettey and Navaratnam (10) performed a very extensive study of the T-system in rat heart myocytes again using HRP as a tracer. In ventricular muscle they described several levels of branching. Primary tubules were those large diameter tubules that ran transversely at the Z-lines. Secondary tubules were of smaller diameter, but still ran transversely at the Z-lines and interconnected the primary tubules. Longitudinal branches were of slightly smaller diameter than the primary tubules and joined the primary tubules of adjacent Z-lines. All of these levels of branching were seen to contain glycocalyx material but this was not a constant feature. Tertiary branches were very small and interconnected the longitudinal branches. Sommer and Johnson (139) summarized these studies and also reported on the three dimensional appearance of the T-system of cardiac muscle cells seen using high voltage electron

microscopy. This technique confirms the T-system to be a fairly irregular array of interconnected tubules of various sizes oriented primarily in a transverse direction at the Z-lines with many longitudinal interconnections. Specialized junctions or couplings between cisternal elements of SR and the T-tubules were described by all of the above authors but Sommer and Johnson (138) specifically noted the great abundance in myocardial cells of junctions between SR and the cell surface sarcolemma. These authors defined internal couplings as those junctions between SR and T-tubules. Junctions between the SR and sarcolemmal membranes are called peripheral couplings. Forbes and Sperelakis (51) studied these structures in mouse myocardium. Couplings, whether peripheral (PC) or internal (IC) were seen to have a very similar appearance. The element of the SR was apposed closely to the T-tubule or the sarcolemma (SL). The gap was consistently 20 nm and with the TEM dense projections called bridges or feet could be seen. In some preparations these feet appeared as two outer dense lines with a less dense center, and in grazing or oblique sections the feet were seen as electron dense circles with a less dense core. These dense bridges appeared to run completely across the gap and have a periodicity of approximately 30 nm. The presence of these feet as bridging particles in freeze fracture preparations is controversial. Rayns, Devine and Sutherland (118) reported seeing them but showed no examples while Shibata and Page (131) and Ashraf and Halverson (8) were not

able to locate junctional specializations in freeze fracture preparations of the myocardial sarcolemma. Forbes and Sperelakis (58) suggested that all the couplings (IC and PC) have a similar TEM appearance, consisting of flattened cisternae of SR filled with moderately electron dense granular material. The feet seem to be a feature of the SR membrane. SR membranes containing the feet have been defined as junctional SR (jSR). Elements of jSR which are not in apposition to T-tubule or SL membranes and are thus not involved in the formation of couplings are a relatively common occurrence in cardiac muscle. The nonjunctional SR is called longitudinal or lSR. The ICs of ventricular myocardial cells show a certain amount of variability in organization. Some are seen to be true triads with a T-tubule interposed between two cisternal expansions of jSR. More often the arrangement is in the form of a dyad with cisternae of jSR wrapping around the T-tubule. Occasionally reversed triads are seen with one jSR element sharing two T-tubules. There is much less variation in the fine structural appearance of the PCs which generally consist of flattened subsarcolemmal cisternae of jSR (51, 138, 139).

The T-system is the most striking of the membrane specializations of myocardial sarcolemma but McNutt (97), and Gabella (63) reported on another form of membrane invagination that warrants consideration. These consist of small vesicles each approximately 80 nm in diameter,

connected to the extracellular space (ECS) by a short, narrow neck. Originally these were thought to be micropinocytotic vesicles but tracer studies have shown that the vesicles are a permanent feature of the SL and these structures are now called caveolae. Often more than one caveola opens into a single neck.

It has yet to be determined what specific functions caveolae serve but it has been suggested that they may act as a reservoir for SL membranes (34). Alternatively, the caveolae may act as analogs of the T-system in cells of small diameter such as non-mammalian cardiac muscle cells, mammalian atrial muscle cells and smooth muscle cells (32, 63, 139). Caveolae do greatly increase the surface area of the SL membrane (63, 89, 95).

Most descriptions of the fine structure of mammalian myocardium note differences between ventricular and atrial cells (10, 16, 27, 53, 67, 70, 86, 88, 98, 130, 139). Atrial cells are much smaller with average diameters of 5-6 μm compared to 12-15 μm for ventricular cells. Contractile proteins of atrial cells are less abundant and are less well-ordered into myofibrils. This leaves more clear cytoplasm, generally towards the central portions of the cell in the perinuclear region. The sarcoplasm contains more glycogen. A better developed Golgi apparatus is also present. One striking feature is the presence of electron dense specific granules. The precise contents of the

granules and their function is not completely understood but they are now thought to contain glycoprotein (20, 21, 120, 121, 151, 152, 153). The SR is less abundant and less well organized in atrial cells. Many authors report that the T-system is scarce or absent in these cells and, therefore, ICs are rare (27, 53, 67, 98, 139). Several studies suggest that there may be different populations of atrial cells some with and some without a T-system (9, 16, 41, 74, 94, 98, 139). Recent studies using tracers have shown that many atrial cells do contain tubular invaginations of the sarcolemma and that ICs are not as rare as was thought previously (10, 16, 87).

In summary, atrial myocardium can be seen to consist of small diameter cells. The myofibrillar material is abundant but does not completely fill each cell. Myofibrils are often restricted to the peripheral portions of the cells. The SR and T-tubules are less abundant and less well-organized, and there are relatively more peripheral couplings in comparison to ventricular cells. These fine structural differences are reflected in differences in the physiological processes which underly EC coupling in the two types of cardiac muscle cell. During electrophysiological recording of the events which take place during the depolarization of the sarcolemma in ventricular cells the action potential (AP) is seen to consist of a rapid upstroke, reflecting changes in K^+ permeability. This is followed by a long plateau caused

primarily by the entry of Ca^{2+} through slow channels. In atrium the AP is shorter and has almost no plateau, thus less Ca^{2+} enters through slow channels from the ECS and the duration of the contraction is not as long. The latency to contraction is much shorter, the velocity of shortening is quicker, but the maximum contractile force developed is lower.

The definitive work on the morphology of the developing T-system has been performed using skeletal muscle. Ezerman and Ishikawa (43) investigated the differentiation of sarcoplasmic reticulum and T-system in cultured muscle cells from 11 day chick embryos. The SR in the early myotube was seen as distended vesicles of rough endoplasmic reticulum (RER). As the myofibrils increased the RER vesicles formed multiple, narrow, smooth surfaced tubular projections in various directions. The tubules grew and branched, interconnecting around the developing myofibrils until there was an elaborate network continuous with the RER vesicles.

The arrangement and distribution of the T-tubules in the early stages was very irregular. They appeared first as invaginations of the sarcolemma and later extend farther into the myotubes. The surfaces of the T-tubules were curved and beaded, they entered radially and often turned obliquely or longitudinally; often the tubules were very tortuous near the sarcolemma.

In the earliest stages of development there was no particular relation of the T-system to the SR. However, soon after differentiation of the T-tubules, dilated SR resembling terminal cisternae became associated with elements of the T-system in a seemingly random manner, with no relationship to the developing myofibrils. At first this junction between T-tubules and SR was just apposition of the membranes 10-12 nm apart. Later, dense structures (bridges) started appearing in the gap. In the later stages of development the triads were seen to be localized in the I-band near the A-I junction. Ishikawa (72) continued the investigation of the development of the T-system in cultured chick muscle. He described elaborate membrane systems which at higher magnifications appeared to consist of tubular units with a diameter of approximately 55 nm, in a roughly hexagonal array. This tubular network had a well-defined limiting membrane and a clear lumen which was accessible to ferritin. T-tubules were seen to be continuous with this elaborate structure. Ishikawa (72) noted that in developing myotubes there were many inpocketings of the sarcolemma which resembled caveolae. These caveolae were often seen to communicate with each other to form multilobed structures. All of these vesicles were accessible to ferritin infiltration. The dimensions of the elaborate hexagonal intracellular arrays were similar to caveolae. Ishikawa (72) suggested that the T-system developed by repeated caveolation at the cell membrane. He suggested that the

membranous structures seen inside the developing cell were proliferations of the T-system formed by caveolation of the T-tubules. This, possibly due to a rapid and unbalanced growth of the T-system in tissue culture. This mechanism seemed to be somewhat inadequately explained. The author appeared to be suggesting that the caveolae were budding off at the sarcolemma and stringing together. On the basis of current thinking as to the processes of *de novo* membrane synthesis, this would seem unlikely (160). Presumably caveolae formed as membraneous vesicles at the Golgi apparatus and migrated to the cell surface. Unless T-tubule formation is haphazard, a very complicated recognition process which causes some caveolae to string together in a regular manner must be postulated.

Although Chacko (24) reported that the T-system and SR started to appear in 11-day rat embryos, most authors seem to agree that neonatal rat muscle had little or no T-system or SR. Significant quantities of these organelles only began to appear 8-10 days postnatally (35, 69, 70, 73, 110, 113, 125, 130, 139, 142). *In vivo* studies by Schiaffino and Margreth (125) and Kelly (77) on developing rat skeletal muscle found that SR was seen much earlier than the T-system. It was continuous with RER at very early stages which confirmed *in vitro* findings. There were no T-tubules before 10 days postnatally but frequent peripheral couplings between the sarcolemma and SR were seen. Even at this early stage the myofibrils were beginning to form the regular

banding patterns typical of adult muscle fibers. Ten to fifteen days postnatally T-tubules started to develop at the sarcolemma as short, beaded, branching tubules. Caveolae and complexes of caveolae were often seen to be continuous with developing tubules. At this stage the T-tubules were oriented obliquely or longitudinally and all couplings with the SR were peripheral (77, 125). Later in development the T-tubules became more transverse, true triads began to appear and peripheral couplings became scarce. In the adult skeletal muscle cell peripheral couplings were not seen. Kelly (77) noted two important differences between the *in vivo* studies and the cultured cells of Ishikawa (72). Ishikawa saw no peripheral couplings and the T-system was seen to develop at a very early stage, even before there was much myofibrillar development.

Edge (35) studied the *in vivo* development of triads in skeletal muscle cells. She confirmed that they formed at the surface of the cell as simple apposition of SR and sarcolemmal membranes with a gap of 10-15 nm. Periodic densities formed in the gap at a slightly later stage. The T-system appeared several days after birth as inpocketings of the SL with many branchings budding off in many directions. The tubules of the T-system and the SR formed close associations and couplings were developed soon after the T-tubules began to differentiate. During the first two postnatal weeks the triads were oriented longitudinally and still lay in the sarcoplasm relatively close to the SL. The

triads became transversely oriented between 10-15 days postnatally and were then found at A-I junctions. Peripheral couplings disappeared while this was occurring. Schiaffino *et al.* (126) wished to show that the differences in the development of cultured muscle cells and *in vivo* muscle cells were not attributable to species differences. Ishikawa (72) had used chicken skeletal muscle cells while Schiaffino and Margreth (125) and Kelly (77) had studied rat skeletal muscle. Schiaffino *et al.* (126) confirmed that with rat embryonic muscle in tissue culture T-tubules developed very early, independently of SR. The T-system was deep into the cell before couplings started to arise. No peripheral couplings were seen between SR and sarcolemma. They also confirmed that, *in vitro*, elaborate membranous networks continuous with T-systems did occur.

Ishikawa and Yamada (73) studied the differentiation of the SR and the T-system in mouse ventricular myocardium. They reported that at birth the SR was continuous with large amounts of RER. The SR remained poorly developed as late as ten days after birth. Many peripheral couplings were noted with dense bridges spanning the gap between the SR and the sarcolemma. As the myofibrils became more highly developed the SR proliferated and surrounded them in the region of the I-band, and later extended into the A-band. At birth there was no T-system. Approximately five days postnatally slender T-tubules began to appear. In the early stages they were confined to the periphery and assumed beaded shapes. As in

skeletal muscle there was a proliferation of caveolae and extensions of caveolar complexes extended to the interior of the cell. There was much branching and many interconnections between developing T-tubules. At 15 days, large preferential channels (primary T-tubules) lined with basal lamina became prominent. Horseradish peroxidase infiltrated all the caveolar complexes and the branching tubules which were presumed to be T-tubules. Using freeze-fracture, Ishikawa and Yamada (73) showed caveolae preferentially grouped at the level of the I-band; slender tortuous T-tubules were seen continuous with the sarcolemma although the actual openings were difficult to distinguish from caveolae. The SR developed earlier than the T-tubules but proliferation occurred at the same time and coupling between the SR and T-system was seen at very early stages. In cardiac muscle peripheral couplings between the SR and the sarcolemma persisted in the adult.

Moses and Kasten (104) studied the development of T-tubules in cultured cardiac myocytes taken from the ventricles of three to four-day-old neonatal rats. No extensive T-system was seen but approximately 10% of the cells developed short tubular invaginations of the sarcolemma two to three days after they were plated out. Morphogenesis was reported to be similar to that reported for *in vivo* cells but the tubules remained short and branching was minimal.

Mizuhara and Futaesako (101) introduced the use of tannic acid as a fixative combined with gluteraldehyde. They suggested that since tannic acid was known to precipitate proteins from solutions it should be an effective fixative agent when combined with aldehydes, producing crossbridges between the proteins. Simionescu and Simionescu (133, 134) suggested that tannic acid acts as a mordant during fixation. They suggested that the tannic acid binds to osmium during fixation and then binds particularly well to lead during the staining process. Several studies using this technique noted that it markedly enhanced contrast and definition of membranes. A useful byproduct of the procedures using tannic acid was noted by Bonilla (14) and Leeson (83, 84, 85). Tannic acid seemed to act as an extracellular-space marker and muscle tissue prepared using these procedures may have the T-system filled with very electron dense material. Leeson (83, 84, 85, 86) used this tracer effect to perform extensive studies on the morphology of the T-system in skeletal muscles and cardiac muscles of adult animals of several species.

Despite the moderately large body of work performed to clarify the fine structure of the T-system in cardiac muscle, many questions remain unanswered. The reported sparseness of the T-system of atrial cells has been questioned recently. T-tubules may be more abundant than was previously thought but have not been recognized because it

was difficult to see their connections to the sarcolemma and they were easily confused with tubular elements of the SR. The development of of the T-system in cardiac muscle had not been studied extensively. Those investigations that considered this topic were largely comparisons to skeletal muscle processes. The development of sarcolemmal membrane specializations in atrial muscle cells had not been studied. Having developed a preparation technique using tannic acid that allowed clear visualization of the T-tubules and permitted absolute differentiation between the T-system and SR, it was decided to investigate the development of these structures in atrial muscle cells. It was also felt that the developmental process might be more easily followed in atrial cells as the contractile apparatus did not fill the cytoplasm to as great an extent and other structures would be more visible.

The development of stereologic procedures has stimulated many quantitative morphological studies. Briefly, stereology consists of the prediction of the three-dimensional structures of tissue from information measured on the two dimensional representations of sections or micrographs. The techniques use mathematical formulae based on the laws of geometric probability to estimate various parameters such as volume density or surface density of particular fine structural entities (17, 39, 40, 96, 145, 149).

There have been a number of morphometric studies that have estimated the volume density of various organelles in mammalian myocardium. Singh, White and Bloor (159) summarized those studies that have reported on the volume density of myofibrils, mitochondria, SR and T-tubules for ventricular tissue. Page (111) reviewed the quantitative ultrastructural work that had dealt with cardiac cell membranes. Specifically he summarized the studies that measured the surface density of the sarcolemma, T-system and SR membranes, and mitochondrial inner and outer membranes in ventricular myocardium. Levin and Page (89) estimated that the contribution of caveolae to the surface density of the sarcolemma was approximately 20% in rabbit right ventricular papillary muscle. Page and Surdyk-Droske (115) investigated the distribution, surface density and membrane areas of couplings in ventricular tissue and reported that there were four to six times as many ICs as PCs. They estimated that as much as 50% of the T-system was involved in dyadic junctions.

Several studies have reported on the quantitative morphology of adult atrial cells (7, 16, 56, 70). Volume density of myofibrils, mitochondria, SR and PCs have been studied for different mammalian species. Generally volume density of myofibrils and PCs were comparable to the values obtained for ventricular myocardial tissue. Mitochondrial and SR volume density were found to be much lower than in ventricle. Bossen *et al.* (16) reported that the volume

density of the T-system in atrium was approximately 10-20% lower than in ventricle and the value for right atrium was approximately half of that for the left atrium. Masson-Pevet *et al* (95) investigated the relative abundance of caveolae in atrial and ventricular cells. They reported that the contribution of caveolae to S₁ surface area was approximately twice as much in atrium (56%), as in ventricle (25%).

Developing myocardial tissue has also been studied using morphometric techniques (5, 6, 31, 69, 70, 80, 111, 112, 114, 129, 130). Investigations of fetal heart tissue in rats showed that cellular contractile components were not abundant before birth and intracellular membranous components were very sparse. In quantitative morphological studies of the postnatal development of ventricular myocardial tissue there is general agreement that cell diameters increased gradually and that as cells reached an average diameter of approximately 7 μ a T-system began to develop. This was reported to occur in rats at eight to ten days after birth and slightly later in cats and rabbits (68, 69, 70, 139). As the cell diameters increased during postnatal development cell volume increased exponentially. Even after taking into consideration the contribution of the T-tubules, the surface to volume ratio of the cells began a gradual progressive decline to adult levels (71, 112, 114, 129, 130).

Volume density of the myofibrils and SR was relatively constant. As the cells increased in size the myofibrils and SR gradually increased in abundance and degree of organization. Page and Buecker (112) investigated the development of dyadic couplings in the left ventricular cells of the rabbit. They found that the surface density of PCs gradually increased during the fetal period and achieved adult levels shortly after birth. As the T-system began to develop ten days after birth, ICs became numerous. By the fourteenth postnatal day ICs were four to five times as abundant as PCs. This ratio was maintained to adulthood.

Morphometric studies on developing atrial myocardium are not numerous. Hirakow *et al.* (70) looked at rat and guinea pig atrial myocardium during postnatal development. This study involved comparisons of left with right atrium, concentrating on cell size and volume density of myofibrils, mitochondria, glycogen and atrial specific granules at various ages.

There have been two main suggestions as to the factors which may act as stimuli for T-system development. Several authors have noted a correlation between the increase in cell diameter and decreasing surface to volume ratios (71, 112, 130, 139). This has led to speculation that at some point, for example, when the cells reached an average diameter of 6-8 μ , the T-system became necessary to maintain the surface to volume ratio. None of these studies

considered the contribution of caveolae to surface area of the sarcolemma. Forssmann and Girardier (53) and Sommer and Johnson (139) noted that this was probably not the sole factor. There were many fairly large diameter atrial cells which appeared to have no T-system and in the adult ventricle many cells of relatively small diameters have an extensive, well-developed network of T-tubules. Hibbs and Ferrans (67) reported that the T-system was only present in those atrial cells which have the most myofibrils. They suggested that the development of abundant amounts of contractile protein and the subsequent organization of myofibrils may be the stimulus that caused T-tubule formation. There have been suggestions that the T-tubules and caveolae may be functionally related specializations of the sarcolemma of cardiac muscle cells (63, 139) and morphometric studies of this relationship have been carried out for adult animals (94, 95).

In summary, the morphology of the developing T-system has not been well-studied in cardiac muscle cells. It has been described only for ventricular myocardium and the investigations have depended on comparisons with those developmental processes which were seen in skeletal muscle. The development of T-tubules in atrial cells has not been studied at all. The stimuli involved in the initiation of T-tubule development, (for example, the influence of increasing cell diameter and the degree of myofibrillar

development) remain to be clarified. Further, the relationships between caveolae and T-tubules, and between internal and peripheral couplings during the development and differentiation of atrial muscle cells remains unclear. It was thus decided that a comprehensive descriptive and morphometric study of the ultrastructure of atrial muscle cells during postnatal development would serve to unravel some of the uncertainty which still surrounds these relationships, and provide useful information concerning the effects of the appearance of the T-tubules on the adjustments in the excitation-contraction coupling process which have been reported to occur in neonatal cardiac muscle.

II. METHODS

Animals: Care and Housing

Sprague-Dawley albino rats were used throughout the project. Some neonatal rats were obtained by breeding animals in the departmental holding rooms, but this proved unreliable. Most of the neonatal rats were obtained by ordering pregnant females during the second week of gestation from the Health Sciences Animal Care Facility of the University of Alberta. The pregnant females were held in individual cages and given *ad lib* purina rat chow and tap water. The photoperiod was maintained at 12 hours of light using an automatic timer. Litter sizes are known to affect chronology of development (117) so an attempt was made to maintain litter size at 6-8 siblings by removing an appropriate number of animals immediately following birth.

Tissue Preparation for Electron Microscopy:

The procedures used were identical for each batch of tissue. Each animal was anesthetized with ether and the body weight measured and recorded. The animal was killed by spine dislocation to minimize suffering. The chest cavity was opened and the heart exposed. The heart was perfused by very slowly injecting several milliliters of 3% gluteraldehyde-3% formaldehyde buffered in 0.1 M sodium cacodylate into the left ventricle from a 10-mL syringe. The heart was excised rapidly and the right atrium was dissected, minced, patted

dry and placed in a tared vial containing 1 mL of the fixative solution. The vial was reweighed and the right atrial weight recorded. The remainder of the heart was patted dry with an absorptive tissue, weighed and the weight recorded. Total heart weight was the sum of these two values.

Fixation in buffered 3% gluteraldehyde-3% formaldehyde was continued for 2 hours at room temperature. The tissue was then washed for 30 minutes in 0.16 M sodium cacodylate. Three changes of wash solution were performed at 10-minute intervals. The tissue was post-fixed in 1% osmium tetroxide buffered in 0.1 M sodium cacodylate for one hour at room temperature and again washed in 0.16 M sodium cacodylate for three 10-minute periods. The tissue was then mordanted with 1.2% tannic acid in 0.1 M sodium cacodylate. This fixation procedure was a slight modification of that recommended in Simionescu and Simionescu (133).

The tissue was dehydrated through a graded series of ethanol, 50%, 70%, 95%, 10 minutes in each case and then in 100% ethanol, three changes each of 10-minute duration. The final dehydration step consisted of two 15-minute washes in dried propylene oxide.

Infiltration was initiated by placing the tissue in a 1:1 mixture of propylene oxide and epoxy resin for 2 hours at room temperature on a tissue rotator. The resin was an epon-araldite mixture (2 parts araldite:2.5 parts epon:6 parts DDSA:0.25 parts DMP30). This was followed by 1:3

propylene oxide:epon-araldite for two hours at room temperature. The final infiltration was accomplished using pure epon-araldite for 16-20 hours in a vacuum desiccator.

The tissue was embedded as blocks approximately 1 mm³ in beam capsules. The plastic was polymerized overnight in a 45°C oven and then for 48 hours at 60°C.

Blocks were sectioned using glass knives on a Porter-Blum MT-2 ultramicrotome. Sections approximately 60 nm thick (silver grey) were collected on uncoated 300 mesh copper grids. The grids were stained for 7 minutes on drops of Reynold's lead citrate.

The grids were examined using a Philips EM200 at 60 KV or a Philips EM410 at 80 KV. Electron micrographs were obtained using 35 mm positive release film (Kodak 5132). Prints were made using an Omega D2 enlarger. Kodak RCII polycontrast paper was used for all prints.

Experimental Design: Descriptive Morphology

Initially, right atrial myocardium of adult rats was examined to confirm that tubular invaginations of the sarcolemma were a characteristic feature of enough cells to warrant further study. Then the right atrial myocardium of neonatal rats, two to three hours after birth, was examined to confirm the absence of T-tubules at this age. Finally, a comprehensive examination of the fine structural appearance of right atrial cells from rats of every age from birth to 21 post natal days was carried out to select stages at which

significant developmental changes were apparent. The groups selected for more comprehensive study were neonate, 7, 14, 16, 18, and 21 postnatal days and adult. The right atrial tissue from five to ten animals of each age was examined in great detail and qualitative morphological differences were noted.

Quantitative Morphology

Stereological principles and techniques have been reviewed periodically over the last two decades (17, 39, 40, 96, 145, 149); applications to striated muscle tissue have been considered by several authors (15, 38, 91, 102, 111, 150). Briefly, mathematical formulae have been derived to show that areal density on a section is directly proportional to volume density in tissue. Thus the volume of any fine structural component in a given volume of tissue can be determined by measuring the area of that component on a sufficiently large number of randomly chosen sections to obtain the average area of the component as a function of test area. Similarly the average length of the boundary trace of a structure in sections as a function of test area, is directly related to the surface area of that structure in a given volume of tissue.

The specific morphometric measurements performed for this project gave estimates of average cell diameters, and volume density of myofibrils. Estimates of surface densities of sarcolemma, T-tubules and caveolae, peripheral and

internal couplings were also obtained. The measurements were carried out using a Zeiss MOP-3 digitizer. This is an automatic planimeter consisting of a tablet with a magnetized grid, a sensitive magnetic stylus and a preprogrammed console/printer (Fig. 40). Using this device it was possible to obtain quite accurate measurements (relative standard errors $< 10\%$) of the area of selected fine structural components as a function of cell area for a large sample of randomly selected sections and then estimate the volume density of these structures. By tracing the boundaries of sarcolemma, T-tubules and caveolae and averaging them as a function of cell area it was also possible to estimate surface density.

The measurements were conducted on 5" x 8" electron micrographs obtained in the following manner. Right atrial tissue was collected from five rats at each of six age levels: neonates, 7 days, 14 days, 18 days and 21 days postnatal, as well as adults. Numbers were assigned to all the blocks taken from the right atrium of each animal and then four blocks per animal were selected using a random number table. Sections from each selected block were viewed to ensure good fixation and a reasonable degree of relaxation. Blocks poorly fixed or with a sarcolemmal length outside the range 2.20 to 2.30 μm were rejected and replaced with blocks from the same animal. Several medium sized sections (large enough to cover 8-10 grid spaces) were collected from each block on grids with a central arrow to

allow orientation. Five micrographs were taken from each grid in a systematic manner. Micrographs were obtained from the five grid spaces immediately to the right and below the central arrow (Fig. 37). Electron micrographs of two magnifications were taken of all the selected grid spaces. Low power micrographs (approximately 5000x) were used to obtain average cell diameters. Higher power micrographs (approximately 15000x) were used to obtain measurements of areal density of myofibrils, and boundary traces of sarcolemma, T-tubules and caveolae, PCs and ICs.

The morphometric data for all of the variables was subjected to Cochran's test for homogeneity of variance (105). For all of the parameters except volume density of the myofibrils, the different age groups were found to have nonhomogeneous variances. Since between group variances were often quite different for different ages and this would unduly affect the results of any parametric statistical tests it was felt that nonparametric statistical tests should be used to analyze the data. The Kruskal-Wallis one way analysis of variance (132) was deemed to be most appropriate. This test circumvents the problems caused by the highly variable values obtained for the lower age groups by assigning ranks to each value. The large variations in the absolute values, many of which may be zero, have relatively less effect on the group means when converted to rankings. The rankings of the values for each age group are the statistic which is tested A sample of the calculations

used in these tests is presented in appendix 2. Briefly, for each variable the measured values from all age groups were assigned ranks from lowest to highest (1-600). Tied scores were given the mean value of the ranks for which they were tied. The ranks for each age group were then summed and the values were applied to the Kruskal-Wallis Formula:

$$H = \frac{12}{N(N+1)} \sum_{j=1}^k \frac{R_j^2}{n_j} - 3(N+1)$$

where:

H = the Kruskal-Wallis statistic

K = number of groups

n_j = number of cases in the j th group

N = total number of cases in all groups

R_j = sum of the ranks in the j th group

$\sum_{j=1}^k$ = the operation of summing the data from k groups

The Kruskal-Wallis test was used to determine whether the sums of the ranks for the different age groups were so disparate that they were not likely to have come from samples which were all drawn from the same population.

It has been shown that if the k samples are from the same or identical populations then H is distributed as chi-square with degrees of freedom equal to one less than the number of groups, provided that the sample sizes are not too small (132).

Ties influence the value of H, but they can be corrected for by dividing H by $1 - \Sigma T / N^3 - N$ where $T = t^3 - t$ (t being the total number of ties) and N = the total number of

values in all the groups. All of the H values were corrected for ties and were compared to chi-square values to test for statistical significance.

All of the Kuskal-Wallis tests were confirmed using the MIDAS statistical package available from Computing Services at the University of Alberta.

III. RESULTS

A. Descriptive Morphology

Adult Right Atrial Myocardium

A number of descriptions of the fine structural appearance of adult myocardial cells from mammalian atria are available in the literature (16, 27, 41, 67, 86, 94, 98, 139). Virtually all of these were comparisons of atrial structures to those found in ventricular cells.

As Figure 1 demonstrates, well fixed adult atrial cells were seen to be of small diameter (5-6 μm), and were tightly packed, leaving relatively little intercellular space. The extracellular space was filled with fine reticular fibers of the endomysium and the glycoprotein coat which invested each muscle cell. In some areas collagen fibrils of the endomysium became more robust (Figs. 3B, 4). The endocardium was characterized by a thin layer of endothelial cells with a moderate accumulation of collagen fibrils and relatively large amounts of elastic fibres (seen as very dense black patches and strands in Fig. 3B and Fig. 4) lying between the endocardial and myocardial cells.

There have been some suggestions that there are two atrial cell types, particularly in the right atrium (9, 16, 41, 74, 92, 116, 127). Some right atrial cells near the endocardial surface did appear to contain less contractile protein and these cells did not appear to have tubular

invaginations (Fig. 3B) but it was not possible to see clearly defined specific tracts of these cells.

Capillaries were abundant and often small unmyelinated axons were seen adjacent to the blood vessels (Fig. 1, upper left; Fig. 2, center). The endothelial cells often contained many vesicles of the type which are generally considered to be micropinocytotic, although these were often seen to be filled to a greater or lesser extent with tannic acid. These were probably in communication with the ECS but usually the vesicles were not as darkly stained as caveolae in adjacent muscle cells (Fig. 8C).

Intercalated discs were seen to cross transversely at the ends of many cells but many junctional contacts were seen along the lateral edges of tapering cells (Figs. 1, 2, 3A, 4).

It had been reported that the myofilaments of atrial muscle cells were only partially organized into myofibrils (98,139). This was seen in some areas characterized by thinner diameter of myofibril-like arrangements which branch. The Z lines were not in register and the myofibrils were only partially separated by rows of mitochondria. The myofibrils were incompletely invested with sleeves of anastomosing tubules of the SR (Figs. 1, 2, 3, 6A, 7A). This was well demonstrated in transverse sections (Fig. 6A)

A characteristic feature of atrial cells was the presence of a well-developed Golgi apparatus which in the adult was usually associated with aggregations of dense

granules that were remarkably like secretory granules in appearance (Figs. 1, 2, 5). These have been previously described and called specific granules (20,21,120,121,151,152,153). At higher magnifications glycogen granules seemed to be quite abundant but it was difficult to differentiate between free ribosomes and glycogen particles. (Figs. 4, 5, 7, 8).

At low magnifications caveolae and tubular invaginations of the sarcolemma were not obvious (Figs. 1, 2, 3 at small black arrowheads) but were much easier to see in material well-mordanted with tannic acid (Fig. 1, 3) than in material where the penetration of tannic acid was less evident (Fig. 2). The penetration of tannic acid was not uniform (Fig. 3B, Fig. 4, Fig. 6). It tended to be best at superficial areas (Figs. 3B, 6) and in thinner trabeculae (Fig. 4). It was noted that tissue which was well penetrated with tannic acid, (as evidenced by heavy electron dense deposits in the ECS, caveolae and T-tubules), tended to be better fixed than material where infiltration was less apparent.

Caveolae were most frequently seen as single or double vesicles opening into a single neck (Figs. 1, 3B, 6, 8B, 8C). Even at relatively low magnifications complex arrangements were noticeable (Fig. 3A large white arrowheads, Fig. 4 small black arrowheads). There did not seem to be any preferential location of caveolae in relation to the sarcomeres. Tubular invaginations were not obvious

but at moderate magnification in well-mordanted material these structures were visible in many cells (Fig. 4, small black arrowheads and elsewhere). At higher magnifications the caveolar complexes, consisting of as many as a dozen vesicles joined in a cluster, were seen to be quite numerous (Figs. 5, 7A, 8A, 8C). Tubular invaginations were also present and seemed, in adult atrial cells, to be tortuous convoluted structures primarily in the subsarcolemmal sarcoplasm (Figs. 4, 6B, 8B). These tubules sometimes appeared to be opening from caveolae or sometimes to be strings of caveolae (Fig. 8B). Tubules were not seen deep inside the cell frequently, but in well mordanted material even at lower magnifications it was possible to see areas where tubules seemed to contain more electrondense deposits than tubules of the SR (Fig. 3A, large black arrowheads). At higher magnifications it was possible to confirm that at least some of these tubules did contain tannic acid deposits and were probably in continuity with the ECS (Fig. 6A, Fig. 7A & B). Peripheral couplings between SR and the sarcolemma were frequently seen (Fig. 1, 6A large white arrowheads and elsewhere). Internal couplings between tubular invaginations and jSR were not frequent but were seen in well-mordanted material (Fig. 7A & B). At lower magnifications it was possible to see SR tubules in relation to caveolae and caveolar complexes (Fig. 1, small white arrowheads, lower right). At moderate magnifications this apposition was often seen to be quite intimate but junctional specializations

were hard to see (Figs. 6A, 6B, 8A). At higher magnifications at least some of the SR which was in apposition to the caveolae appeared to have junctional specializations as described for internal couplings (Fig. 7A small white arrowhead, Fig. 8C large black arrowhead). For the purposes of morphometry an apposition between jSR and caveolae was considered to be an internal coupling as it was not, strictly speaking, a junction with the surface sarcolemma.

Neonatal Right Atrial Myocardium

Neonatal right atrial myocardium showed several major differences in comparison to adult tissue. The cells were much smaller (3.28 μm average diameter). The extracellular space in some areas was very large, forming what appear to be clefts between the cells. These clefts appeared to be filled with finely granular or amorphous flocculent material but these may have been fixation artefacts due to tannic acid (Figs. 9, 10). Collagen fibrils were not abundant even in subendocardial and subepicardial areas (Figs. 10, 12, 13A, and 13B) but large numbers of active fibroblasts were routinely seen (Figs. 9, 10, 13B). Many cell-to-cell contacts were apparent but these appeared to be incompletely developed intercalated discs (Figs. 10, 12, 13A).

The hearts of neonates were small but were functioning effectively so it was not surprising to see that some cells appeared to be relatively well-developed (Fig. 9). There was

some well-organized contractile protein collected into myofibril-like bundles, oriented along the longitudinal axis of many of the cells. This material tended to be restricted mainly to the peripheral areas of the cell adjacent to the sarcolemma (Fig. 9). Other cells appeared much less mature with relatively sparse development of the myofilaments and irregular orientation of the filaments that were present (Figs. 11, 12). Even those cells in which the contractile apparatus appeared well-organized at lower magnifications (Fig. 9) were seen to be less highly organized at higher magnifications (Fig. 11). Nuclei seemed to be only slightly smaller but did appear to have irregular shapes when seen in transverse section compared to the regular elongated configuration of the nuclei seen in adult atrial cells.

Although the contractile protein appeared to be partially organized into myofibril-like units there was very little development of the SR at birth (Figs. 11, 12). The tubules of endoplasmic reticulum that were present seemed to be mainly granular ER. Peripheral couplings were seen but were rare compared to their abundance in adult atrial myocardium; internal couplings were not seen.

Golgi bodies were seen frequently but many appeared to be very active in the elaboration of vesicles with relatively electron lucent cores as well as the production of atrial specific granules (Fig. 12). These specific granules were abundant but seemed smaller than those seen in adult cells; the granules were not clustered primarily at

the nuclear poles but seemed to be scattered randomly throughout the sarcoplasm. Mitochondria were numerous but were also scattered throughout the cell and not lined up into rows between the myofibril-like bundles. Caveolae were not abundant and were almost all single, one vesicle to a neck. Tubular invaginations were extremely rare and those that were seen seemed to be clefts caused by folding of the cell rather than true invaginations of the sarcolemma (Fig. 11).

Lipid droplets were regularly seen although they were not abundant (Fig. 12). Lipid droplets were not seen in adult material.

7 Day Postnatal Right Atrial Myocardium

Atrial cells of this age group were seen to be slightly larger and intercellular clefts had decreased in size and number (Figs. 14, 15, 16, 17, 18). Fibroblasts were still numerous and more robust collagen fibrils were being laid down between cells (Fig. 14) and at endocardial and epicardial surfaces (Fig. 18B). Capillaries were numerous but the endothelial cells were still immature, being thick-walled compared to the attenuated endothelial walls seen in adult blood vessels (Fig. 16). Myocardial cell-cell junctions were numerous and while many were still immature some began to resemble the intercalated discs seen between adult cells (Figs. 15, 17A and B).

Some of the nuclei were beginning to appear more rounded when seen in cross-section but many still had irregular profiles. Myofilaments were seen to be more abundant and were increasingly organized into myofibril-like units of relatively small diameter ($<0.25\ \mu\text{m}$). The contractile protein was still primarily restricted to peripheral locations but myofibrils were becoming organized more centrally within some of the cells (Figs. 14, 15, 16).

Interspersed with the cells in which myofilaments were becoming more abundant and better organized were many cells that retained an immature appearance (Figs. 16, 17A and B) with central areas incompletely filled with organized structures.

A striking difference between the right atrial cells of one week old and newborn rats was the abundance and degree of organization of the SR. A moderate amount of the ER did still seem to be granular in nature but there were now large amounts of what appeared to be true SR; many of the myofibril-like units were now partially delineated by sleeves of SR tubules (Fig. 16, 18A). Peripheral couplings were seen more frequently (Figs. 14, 18A small white arrowheads). Caveolae seemed more abundant. Although these were usually single vesicles, very occasionally complex shapes were seen (Figs. 14, 15, 17A & B; small black arrowheads). Tubular invaginations were virtually non-existent but very infrequently a short tubule was seen at or near a Z-line; internal couplings would be presumed

for these structures but none were seen clearly (Fig. 15, at star).

Mitochondria had begun to line up into rows between the contractile material (Figs. 15, 17A & B).

14 Day Postnatal Right Atrial Myocardium

The right atrial tissue of 2 week old rats was not found to be remarkably different from that of one week old animals (Figs. 19, 20, 21, 22). There seemed to have been a gradual increase in cell size and concomitant decrease in the size and number of intercellular clefts. The contractile protein was becoming more abundant and increasingly more highly organized but relatively immature cells were still seen. Granular ER was increasingly replaced by SR but peripheral couplings seemed no more abundant than for week old atrial cells. Caveolae appeared to be more numerous; caveolar complexes and tubules were seen more frequently (Fig. 22B, lower left) but were still not sufficiently abundant to be considered significant structures. Associations between jSR and caveolar complexes were seen more frequently.

16-21 Day Postnatal Right Atrial Myocardium

Throughout the third postnatal week there was a further gradual increase in cell diameter. The ECS became less noticeable and intercellular clefts were much reduced (Figs. 23, 27, 28, 33, 34). Many capillaries retained an immature

appearance with thickened endothelial cells (Figs. 23, 30, 33). Cell to cell contacts increasingly resembled adult intercalated discs (Figs. 27, 31B, 36A). The abundance of the myofilaments appeared to increase and the myofibril-like units were certainly becoming more organized and clearly delineated by increased amounts of SR (Figs. 24, 29B, 30A, 35A & B). By the end of the third week many areas were indistinguishable from adult tissue (Fig. 34). However, areas were also seen where cells were less well-developed (Figs. 24A, 25, 29A, 30B, 33B). In figure 33B there seemed to be several cells clustered together surrounded, partially by a moderately well-developed amount of connective tissue. This might be have been taken as evidence for the existence of internodal pathways, but may just have indicated inadequate penetration of fixative solution to the cells that were partially isolated by the thickness of the connective tissue surrounding them. Active fibroblasts remained relatively abundant (Figs. 23, 24A, 25A, 27, 28, 30B, 33A & B).

While no dramatic increase in cell diameter or in abundance of myofibrillar material appeared to be taking place over this period there seemed to be striking changes taking place in the abundance and complexity of the invaginations of the sarcolemma. Caveolae and particularly complexes of various sizes and shapes were becoming more abundant (Figs. 24A, 25A & B, 28, 30A, 32B, 36A). Tubular invaginations of the sarcolemma became moderately frequent

(Figs. 26A, 31A & B, 36) and occasionally could be seen to branch (Fig. 26B). Peripheral couplings appeared to be more numerous (Figs. 24B, 29B, 35A & B) and with the increased development of caveolar complexes and tubular invaginations of the sarcolemma, associations between jSR and these structures seemed to increase in number (Figs. 25B, 30A, 31A & B, 36A; white arrowheads). Increasingly, true internal couplings were seen (Figs. 26C, 36B & C).

In summary, adult right atrial cells were seen to be relatively small and tightly packed. They contained abundant filamentous contractile protein organized partially into myofibrils which were incompletely delineated by tubules of SR and rows of mitochondria. These structures filled the bulk of the sarcoplasm. The central areas of the cell contained a nucleus, a well developed Golgi apparatus and aggregations of specific granules, though many granules could be also be seen scattered throughout the sarcoplasm. There were many caveolae and caveolar complexes; tubular invaginations of the sarcolemma while not universal were often seen. The jSR made many specialized couplings with the sarcolemma and appeared to be associated with caveolar complexes. Where tubules invaginated, even if only for a short distance from the sarcolemma, internal couplings were seen.

Atrial muscle cells from newborn rats were much smaller, with irregular-shaped nuclei. There was some

development and organization of the myofilaments but the bundles were located at the periphery of the cell and were not delineated by SR or rows of mitochondria. The SR was mainly granular, there were few PCs and ICs were nonexistent. Caveolae were not abundant and no true tubular invaginations of the sarcolemma were seen.

The right atrial cells of 7 day postnatal rats were slightly larger than those of neonates. The contractile protein was more abundant and better organized. The SR had started to develop and was moderately well-organized. Peripheral couplings and caveolae were more abundant at the sarcolemma but tubular invaginations and internal couplings were not significant features. During the second week of postnatal development the right atrial cells gradually became mature in appearance. The myofilaments became more abundant and were increasingly organized into myofibril-like bundles in central as well as peripheral regions of the sarcoplasm. The SR seemed better organized around the myofilaments. At the cell surface caveolae appeared to be slightly more numerous, primarily due to the increased frequency of very simple aggregations of vesicles sharing the same neck. T-tubules were seen but were still quite rare. PCs were more apparent and ICs, though infrequent, were now seen.

During the third week of postnatal development no dramatic changes in cell size or abundance and organization of myofilaments appeared to take place. However, while the

cells still seemed to be of relatively small diameter, more of them were beginning to resemble mature cells. Caveolae, caveolar complexes and tubular invaginations of the sarcolemma did seem to be considerably more numerous. Both peripheral and internal couplings were seen much more frequently.

B. Morphometry

Weight Measurements

The means and standard deviations for postnatal body weight, heart weight and right atrial weight for the various age groups are presented in Table 1. There was a gradual increase in all of these variables over the first four weeks. By the end of the fourth postnatal week both the heart and the right atrium had achieved approximately 60% of adult levels. The differences were all significant ($p < 0.01$).

Stereology

Measurements from low power electron micrographs:

The mean cell diameters, obtained using micrographs of approximately 5000x magnification are presented in Table 2. The values used to obtain the means are presented in Appendix 1:Table A1.1. Each data point in Table A1.1 represents the average cell diameters as measured from all

the cell profiles in one micrograph. This data confirmed that there was a steady, gradual increase in atrial cell diameter over the first three postnatal weeks. This difference was found to be significant at $p < 0.01$ using the Kruskal-Wallis test. An example of this test is presented in Appendix 1:Table A2.1. Volume density (V_v) of the myofibrillar protein for adult animals, estimated using low power micrographs was found to be $55.85 \pm 5.44\%$ of the total cell volume.

Measurements from high power electron micrographs:

Table 3 contains the mean estimates of Volume Density (V_v) for myofibrillar protein as a percentage of cell volume and the surface density (S_v) of peripheral couplings, internal couplings and of caveolae+T-tubules calculated as a percentage of sarcolemmal boundary. These means were obtained from measurements performed on electron micrographs of approximately 15,000x magnification. Measurements of the cell area, myofibrillar area; PC, IC, sarcolemmal and caveolar boundary length are contained in Tables A1.2, A1.3, A1.5, A1.7, A1.9 and A1.10 respectively. Areal density of myofibrillar protein estimated for each micrograph were listed in Table A1.4. Each individual data point was obtained by dividing the values in Table A1.3 by the values in Table A1.2. Surface densities for PCs, ICs and Cav + T were estimated by dividing individual values in Tables A1.6, A1.8, and A1.10 by the corresponding values in Table A1.5. Surface densities of PCs, ICs, and Cav + T were listed in

Tables A1.7, A1.9 and A1.11 respectively.

As can be seen from Table 3, there was a gradual increase in volume density of the myofilaments over the first two postnatal weeks then a slight decline followed by another gradual increase. The change over the first 14 postnatal days and again the changes between 18 postnatal days to the adult were found to be significant ($p < .01$). The value estimated for volume density of the myofilaments for adult atrial cells was not significantly different from the value estimated using low power electron micrographs.

Surface density of the peripheral couplings increased slightly, but significantly ($p < 0.01$) over the first two postnatal weeks, then increased dramatically between the fourteenth and eighteenth postnatal day ($p < 0.01$). There was a significant increase between the eighteenth and twenty-first postnatal day and a decrease to adult levels ($p < 0.01$).

Surface density of the internal couplings, which was comprised of couplings between SR and caveolae as well as between SR and tubular invaginations, increased significantly over the first three postnatal weeks ($p < 0.01$) in a regular manner.

SvCAV was an estimate of the contribution that invaginations of the sarcolemma were making to the surface area of the cell. The means in Table 3 were calculated using the sum of the caveolar and tubular boundary traces as a single value. The values for neonatal, 7 and 14 day postnatal were all due to estimated caveolar surface area;

the contribution of tubular invaginations to the values obtained at 18 and 21 postnatal days was approximately 5 percent and for adult cells was less than 10 percent of the contribution of caveolae. There was no difference in tubular area measured for the latter three age groups. As can be seen in Table 3, there was very little increase in the percentage of surface area contributed by caveolae over the first two postnatal weeks. There was a dramatic increase between the 14th and 18th postnatal day and a subsequent gradual increase to adult levels ($p < 0.01$).

The general trends of the means for the four variables, across all of the age groups, are presented in Figure 38. It can be seen that the measurements generally support the impressions obtained from the micrographs (Figs. 1 - 36).

Calculation of surface/volume ratios

Surface/volume (S/V) ratios of the developing atrial cells can be estimated using the average boundary length of the sarcolemma and the average cell area. As was mentioned previously, S/V is directly proportional to sarcolemmal boundary trace/ average cell area as measured from a sample of micrographs. Estimates of sarcolemmal boundary and cell area at each age level can be obtained using the values for average cell diameters (Table 2). For example, assuming perfect cross sections one can use the formula which gives the circumference of a circle ($C = \pi \times D$) to estimate the sarcolemmal boundary. For neonates this was calculated to be

$3.28 \times \pi = 10.30 \mu\text{m}$. Similarly sarcolemmal boundary lengths for other age groups were calculated to be 7d = $10.62 \mu\text{m}$, 14d = $11.78 \mu\text{m}$, 18d = $12.69 \mu\text{m}$, 21d = $13.76 \mu\text{m}$ and adult = $23.53 \mu\text{m}$. The average cell area was calculated using the formula for area of a circle ($A = \pi r^2$). These values were determined to be N = $8.45 \mu\text{m}^2$, 7d = $8.97 \mu\text{m}^2$, 14d = $11.04 \mu\text{m}^2$, 18d = $12.69 \mu\text{m}^2$, 21d = $15.07 \mu\text{m}^2$ and A = $44.06 \mu\text{m}^2$. It was not possible to estimate the contribution of the caveolae and the T-tubules to the sarcolemmal boundary from the low power micrographs as these structures were too small to measure accurately at those magnifications.

Estimates of the percentage contribution of caveolae and T-tubules to sarcolemmal boundary were available from the higher power micrographs. It was possible to estimate the values for total sarcolemmal boundary by multiplying the average SvCav values (Table 3) by the values of sarcolemmal boundary calculated above and then combining these two estimates. For example, for neonates total sarcolemmal boundary = $(10.34 \times 0.127) + 10.34 = 1.309 + 10.34 = 11.613$. Similarly total sarcolemmal boundaries were calculated for the other age groups: 7d = $11.98 \mu\text{m}$, 14d = $13.388 \mu\text{m}$, 18d = $16.491 \mu\text{m}$, 21d = $18.731 \mu\text{m}$ and A = $34.323 \mu\text{m}$.

Dividing the values for total sarcolemmal boundary by the value calculated for average cell area gave estimates for S/V ratio at all age levels: N = $1.374 \mu\text{m}^2/\mu\text{m}^3$, 7d = $1.336 \mu\text{m}^2/\mu\text{m}^3$, 14d = $1.213 \mu\text{m}^2/\mu\text{m}^3$, 18d = $1.299 \mu\text{m}^2/\mu\text{m}^3$, 21d = $1.243 \mu\text{m}^2/\mu\text{m}^3$ and A = $0.779 \mu\text{m}^2/\mu\text{m}^3$. It appeared that S/V

ratio remained relatively constant during the early postnatal period with perhaps a slight decline and was much reduced for adult atrial cells.

Cells grow in length as well as in diameter but Korecky and Rakusan (80) showed that the increase in length was proportional to the increase in diameter. The estimates of S/V ratios calculated above using only cell diameters should be reasonably accurate.

IV. Discussion

The right atrium may have seemed an unusual choice for the study of the development of the T-system since it was the heart chamber reported to have the least development of this organelle (16, 139). As mentioned previously, preliminary studies had shown that T-tubules were more prevalent than had been previously suggested (10, 16, 86) and it was felt that the development could be followed more easily in the atrial cells which were filled relatively less completely with myofilaments. A further reason was the discovery of an unusual filamentous structure which appeared to be restricted entirely to right atrial cells (87). It was thought that this structure might be related to internodal conducting pathways and that by following its appearance and differentiation postnatally it might have proven possible to clarify this controversial area. This filamentous material was not observed in the heart tissue from neonatal to four week old animals and a subsequent paper (50) described this filament as a characteristic of ageing myocardium.

Previous studies have shown that tannic acid mordanting enhances membrane structure and, further, deposits in the T-system to act as an extracellular space tracer (14, 84, 85, 86, 87, 122, 133, 134, 136). Other investigators have used horseradish peroxidase (HRP) as a tracer but results with tannic acid were comparable to those reported for HRP (10, 53, 106, 140) and fixation seemed better. Tannic acid penetration was not even and was restricted mainly to a

depth of several micrometers around the larger vessels and at epicardial and endocardial surfaces. Most of the tissue which was studied came from these areas. It was true that the tissue which was well-penetrated with tannic acid tended to be better fixed than surrounding non-mordanted tissue but this may have meant that the penetration properties of the fixative solution and the mordanting solutions were similar rather than suggesting that tannic acid was improving fixation. Nonetheless, in those areas where tannic acid did penetrate the T-tubules and the caveolae were spectacularly demonstrated and differences between tubular invaginations of the sarcolemma and subsarcolemmal tubules of the SR were unmistakable.

The variability in appearance of adult right atrial cells has been well documented. Most authors describe two main cell types; one a smaller cell with abundant myofibrillar protein and T-tubules and the other a larger cell with fewer myofilaments and no T-tubules (4, 9, 16, 41, 53, 74, 92, 98, 116, 139, 148). Sherf and James (127) have even characterized six different cell types. All of the above investigations were studying the morphology of right atrial cells in an attempt to demonstrate the existence of internodal conducting pathways. These preferential transmission pathways have been suggested on the basis of electrophysiological recording (127) and by differential staining experiments (41). The morphological evidence for the existence of these tracts is controversial; Anderson and

his coworkers still feel that they have yet to be demonstrated (4, 74). All of the above investigators agree, however, that there were no clearly delineated tracts of morphologically distinguishable cells; in fact even though two main cell types were described, a broad transition between the two, consisting of many intermediate types was acknowledged. The presumption seems to have been that the pathways are derived from what was embryologically the sinus muscle, yet this muscle was reported to become morphologically indistinguishable from other atrial cells in the adult (148). The existence of a large population of specialized conducting cells without T-tubules in recognizable areas of the right atrium would greatly influence the study of the development of the T-system. Tissue from areas which contained these tracts would, perhaps, best be omitted from this investigation. During the preliminary stages of the project an attempt was made to locate the pathways ultrastructurally. However, it did not prove possible to differentiate these areas in either adult or neonatal right atria. The range in cell type from cells with a large number of myofibrils to those with relatively few was gradual and some cells that had few myofibrils contained T-tubules. After unsuccessful preliminary attempts to distinguish these tracts morphologically no further efforts were made to account for the presence of preferential conducting pathways. For the most part, the whole right atrium was excised and minced. Blocks were

selected randomly from all of the material available from each animal without regard to the specific location in the atrium from which the block was taken. It proved difficult to obtain well-fixed heart tissue from early neonatal animals. One of the concerns was that neonatal heart tissue may have had an appearance which suggested poor fixation; every attempt was made not to equate adult-like appearance of neonatal cells with good fixation and thus introduce bias into the descriptions of the typical ultrastructure of neonatal right atrium.

It has been reported that the T-system in ventricular myocardial cells starts to develop when the individual cells reach a mean diameter of 7-8 μm (68, 69, 111, 139). This occurred in rats at approximately the tenth postnatal day (69, 73). The present investigation has found that, while short tubular invaginations of the sarcolemma were visible in atrial cells on rare occasions prior to the fourteenth postnatal day, it was only at the sixteenth day of postnatal development that tubules began to proliferate. This was almost a full week later than had been reported for ventricular cells. This may have been due to the relatively small size of the atrial cells, although even adult cells barely achieve the average diameter reported to be the point at which T-tubules develop. Eighteen day postnatal atrial cells were estimated to have average diameters of only slightly more than 4 μm . This suggested that cell size alone was unlikely to be the only factor initiating T-tubule

development.

The development of the T-system in skeletal muscle cells and ventricular myocardium was reported to involve repeated caveolation of the surface sarcolemma (43, 73, 78, 125, 126). While a dramatic proliferation of the caveolae and the formation of caveolar complexes occurred at the same time (16-18 days postnatally) as the formation of T-tubules the two processes seemed to be relatively independent in atrial muscle cells. Short tubular invaginations of the sarcolemma were seen and even though some of the tubules were highly twisted most did not seem to form from strings of caveolae joined together. Such strings of caveolae did arise at this time but the caveolar complexes seemed to be permanent structures which persisted in the adult atrial cells. Since caveolar complexes and T-tubules are both invaginations of the sarcolemma and the chronology of their development is identical it may be reasonable to speculate that they are related functionally. In fact, Masson-Pevet *et al.* (95) have shown that caveolae are much more abundant in atrial cells while ventricular cells, having a well-developed T-system, have fewer caveolae. Further, the caveolar complexes were found not to persist to the same extent in adult ventricle (63, 85, 89, 94) as they were seen to do in right atrium in this investigation.

The freeze-fracture appearance of caveolae have not been extensively studied but some studies have reported that the P-face of caveolae and T-tubules in ventricular cells

are quite smooth and are thus distinguishable from both the SR and the sarcolemma which have abundant IMPs in their P-faces (8, 63, 89, 90, 118, 119). This may be taken as further suggestive evidence that caveolae and T-tubules are related invaginations of the sarcolemma.

The fine structural appearance of the couplings in adult heart muscle has been well studied (51, 138) but the morphology of the couplings in developing cardiac muscle cells has only been superficially described.

In skeletal muscle the couplings were seen to arise at the cell surface as simple apposition of SR tubules with the cell membrane; periodic densities formed later (35). As the T-system developed, internal couplings were seen to appear and peripheral couplings decreased in abundance (78, 125). In atrial cells couplings between SR and the sarcolemma were seen at the earliest stages (Fig. 12); these structures appeared identical to the peripheral couplings seen in adult atrial cells. In some planes of section there were views where tubules of the SR were seen in proximity to the sarcolemma with an absence of dense bridges in the gap, but this may or may not be taken as the initial stage of dyadic development. Peripheral couplings and jSR were not abundant in neonatal animals but they were present. This was also reported for neonatal ventricular cells (73). It seems reasonable to suggest that jSR differentiates first and then associates with specialized areas of the sarcolemma and the T-tubules.

Stereological techniques have gained a wide acceptance over the last two decades but there are a number of uncertainties which arise due partly to some of the assumptions underlying the derivations of the formulae as well as problems caused by inadequately prepared tissue.

Swelling or shrinkage of cells can greatly affect the values obtained for cell volume. Every effort was made to select tissue that was uniformly well-fixed to avoid this problem. Section thickness can also greatly influence the results of a morphometric study. Where section thickness is greater than the thickness of the structure being measured, there is a tendency to overestimate the abundance of the structure. Again every effort was made to maintain a consistent section thickness so that any over-estimation would be equivalent for the various age groups.

One of the main assumptions underlying the stereological formulae is that the distribution of structures within the cell is random, that is, the orientation of the tissue is isotropic. Striated muscle is a highly anisotropic tissue and thus violates this assumption. Suggestions for overcoming this difficulty have included oblique sectioning to cancel out the periodicity introduced by the sarcomeres (91, 150) and using longitudinal sections but orienting the point counting grid at two different predetermined angles to the myofilaments (38, 102). Bossen *et al.* (16) suggested that no special techniques were required as long as large sample sizes were used. Atrial

muscle is much less anisotropic than skeletal muscle or ventricular muscle (86) but still most T-tubules were found at Z-lines and cells in some areas of the atrial myocardium do show highly oriented structural organization. It was felt that the random sectioning angles and the relatively large samples used in this study avoided any major violation of the assumptions underlying stereological principles. Mayhew *et al.* (96) suggested that relative standard errors of the mean of 5-10% were acceptable for morphometric work. The RSE's for measurements reported here fell within this range, verifying acceptable levels of accuracy. The use of the MOP-3 also decreased systematic error as all of the pertinent structures on any given micrograph were measured, as opposed to the field sampling inherent when using point-counting methods (66). In any case, it was felt that systematic errors would be the same at each age group and should cancel out. Caution must be used when comparing the results of this study to values reported by investigators using different methods.

The heart to body weight ratios for developing rats were similar to those reported by Hirakow *et al.* (70) and Anversa *et al.* (5, 6) and though slightly larger than those reported by Zak (154) and Page *et al.* (113), were in the same range as accepted values.

The volume density of myofibrillar protein in adult heart cells has been frequently reported (5, 6, 7, 15, 16, 31, 56, 64, 69, 70, 88, 91, 93, 110, 113, 129, 130). Values

reported ranged from 35% to 62% of sarcoplasmic volume. The majority of studies reported that the volume density of myofibrils for adult myocardial cells (both atrial and ventricular) were in the range of 53% to 58%. The values obtained for this investigation fell within this range.

The volume density of right atrial myofibrils was found to increase slightly during the postnatal period. This was in keeping with the results of Nakata (108) and Hirakow *et al.* (70). The estimations were consistently several percentage points lower than the above authors' but Hirakow *et al.* (70) measured only those cells that showed a nucleus and then estimated the volume density as a function of non-nuclear sarcoplasm. At no point during the postnatal period was there a sudden large increase in the volume density of myofibrillar protein. There was a slight decrease in the volume density of the myofilaments between the fourteenth and the eighteenth postnatal day. This could be put down to inaccurate measurement but it could also be an indication that the cells were involved in synthetic activity that inhibited or diminished the synthesis of contractile proteins. It is interesting to note that there was a rapid development of the sarcolemmal invaginations and couplings which was taking place over the same period.

Hirakow *et al.* (70) found that during postnatal development of right atria average cell diameters increased from 5.6 μm in neonates to 8.7 μm in adult. Again it must be remembered that these authors measured only cell profiles

which contained a nucleus so their values represented diameters through the thickest part of the cells. Nakata (108) reported values much closer ($4.5\text{ }\mu\text{m}$ neonatal - $6.0\text{ }\mu\text{m}$ adults) to the cell diameters reported in Table 2. These were obtained from all portions of the tapering atrial cells.

Several studies reported on changes in surface/volume ratios in developing ventricular muscle cells. Sheridan *et al.* (130) using cats found a decrease from $1.01\text{ }\mu\text{m}$ for neonates to $0.74\text{ }\mu\text{m}$ for infants to $0.47\text{ }\mu\text{m}$ for adult cells. These authors did not account for contributions of caveolae or T-tubules. Hoerter *et al.* (71) reported virtually identical values of surface/volume ratio using rabbits. This study did account for the contribution of T-tubules but ignored caveolae. Page *et al.* (113) looked at S/V ratios in rat ventricle and reported values of $0.5\text{ }\mu\text{m}$ for weanlings and a slight decrease for adults to $0.36\text{ }\mu\text{m}$. These authors included T-tubules in their determination of surface area but ignored caveolae. It was difficult to tell whether the differences in the values between rats and cats and rabbits were real species differences or due to different measurement techniques.

The present study found little change in S/V ratios during the early post natal period with perhaps a slight decrease. There was a relatively large decrease in S/V ratios for adult atrial cells. The increase in volume of the cell during the early postnatal period was balanced by a

dramatic increase in caveolar and T-tubular surface at the eighteenth post natal day. Accumulating the boundary length of caveolae and T-tubules as one variable was not meant to imply a firmly established functional relationship between the two structures. Rather it was just more convenient to measure all the sarcolemmal invaginations at the same time. Such a functional relationship may in fact exist but biochemical characterization or immunological labelling of membrane proteins would be needed to confirm this.

The values for S/V at all ages were approximately 30-40% higher than reported values for ventricle. A proliferation of caveolae during the development of the T-system in ventricular cells has been reported (73) but no estimations of surface area were reported. The fact that Sheridan *et al.* (130) and Hoerter *et al.* (71) ignored caveolae may explain why the S/V ratios of early postnatal ventricle cells were found to decline but the S/V ratios of postnatal atrial cells in this study remained relatively constant. The fact that atrial S/V values were found to be consistently higher than those for ventricle may reflect a real difference. This study found that caveolar and T-tubule surface area increased the surface area of the sarcolemma by 45.9% in adult atrial cells. This was comparable to the value of 56% reported by Masson-Pevet *et al.* (95). Levin and Page (89) estimated that caveolar contributions increased the cell surface area by approximately 16-20% in adult ventricular cells. Page *et al.* (113) report the contribution

of T-tubules to total cell surface area of adult ventricle cells to be approximately 25%. Thus tubular invaginations and caveolae increase the surface area by similar amounts in atrial and ventricular cells. Ventricular cells, however, were of much larger diameter and the contribution of caveolae and T-tubules to surface area was not enough to compensate for the exponential increase in volume, thus S/V ratios of rat ventricular cells are roughly half those of atrial cells.

The association seen between jSR and caveolae leads to a further area of speculation. Many of the short tubular invaginations seem to have a vesicular expansion at the end (Figs. 8B, 22B, 26A, 31A, 36C). One is led to postulate that, perhaps this was originally a caveola which was associated with an area of jSR. As the myofibrillar protein began to develop in the interior portions of the cell the SR may have moved deeper into the cell to become organized as a sleeve around the myofibril. The associated caveolae could have been drawn along with the jSR, forming a tubular invagination.

Page and his coworkers have performed several morphometric investigations concerned with development of the dyads in ventricular muscle cells (112, 113, 115). Page and Surdyk-Droske (115) reported that the surface density (S_v) of peripheral couplings was $0.023 \mu\text{m}/\mu\text{m SL}$ and of internal couplings was $0.069 \mu\text{m}/\mu\text{m SL}$ for rat ventricular muscle. Thus total surface density of couplings was 0.093

μm . From Table 3 it can be seen that for adult atrial cells surface densities of PCs ($0.055 \mu\text{m}/\mu\text{m SL}$) were much higher and of ICs ($0.022 \mu\text{m}/\mu\text{m SL}$) were much lower than for ventricular cells, giving a total of $0.077 \mu\text{m}/\mu\text{m SL}$. This was somewhat lower than the total reported for ventricle and may reflect the relative sparsity of the SR in atrial cells in comparison to the cells of the ventricular myocardium.

During postnatal development of ventricular cells, Page and Beucker (112) found that the Sv of the PCs as a function of sarcolemmal surface increased slightly during the postnatal period and then declined to adult levels. The Sv of PCs showed a rapid and large increase during the period of T-tubule appearance and then levelled off at adult values. From Table 3 it can be seen that the surface density (Sv) of the PCs increased slightly during the first two postnatal weeks and then increased dramatically at the same time that there was a proliferation of caveolae (16-18 days). The Sv of ICs in atrial cells showed a steady increase over the early postnatal period. For both ventricular and atrial cells there was a rapid increase in the total Sv of couplings which was correlated with the proliferation of sarcolemmal invaginations. In ventricle this occurred at approximately the tenth postnatal day and involved mainly ICs (113) while in atrial cells this occurred at approximately the eighteenth postnatal day and was caused primarily by a large increase in the numbers of PCs (Table 3).

The measurements performed in this study were intended to clarify what stimuli may be initiating the proliferation of sarcolemmal invaginations. It had been suggested that the T-system developed to allow the spread of the wave of excitation to myofibrils that were forming in the deeper areas of the cell or alternatively that more surface area was needed to maintain the S/V ratio of the sarcolemma. However, no dramatic increase in volume density of myofibrils or decrease in S/V ratio was seen to occur at the time the sarcolemmal invaginations began to proliferate in atrial cells. This had been reported for ventricular cells as well but not stated explicitly (5, 6, 7, 30, 31, 53, 69, 70, 71, 73, 93, 110, 111, 113, 129, 130, 139). Unless a critical value for volume density of the myofilaments or S/V ratio or a critical combination of the two above which a rapid proliferation of sarcolemmal invaginations occurs is postulated, then there is nothing in the data that provides much information as to the stimuli which lead to T-tubule development or caveolar proliferation. It would seem as logical to predict a gradual increase in T-tubules and caveolae to accompany the gradual increase in volume density of myofibrils and the gradual decline in S/V ratios of the cells. Furthermore, one is forced to wonder what functions this increased surface area might be performing if the freeze fracture data is accurate and there were very few intramembraneous particles in the p-faces of the T-tubules and caveolae.

It may be possible to clarify these matters by looking at the physiological changes which take place in cardiac muscle during postnatal development.

There have been several studies dealing with the physiological changes that take place in the excitation-contraction coupling process during the first few postnatal weeks in heart muscle cells. Excitation-contraction coupling in mammalian cardiac muscle appears to involve a Ca^{2+} -induced release of calcium from the sarcoplasmic reticulum (42, 44-48). Fabiato (45) has found that this process is not developed at birth but becomes established during the early postnatal period. Sheridan (128) reported that the resting potential of cardiac cells increased during the early postnatal period and heart tissue became increasingly sensitive to lowered Ca^{2+} concentrations extracellularly. This suggests that an event was taking place whereby the interiors of the cells were becoming more negative with respect to the exterior. These results were consistent with a decrease in the internal concentration of free Ca^{2+} . It was becoming increasingly necessary to provide Ca^{2+} from external stores.

It has been shown that Na^{+} - Ca^{2+} exchange at the sarcolemma is more important to the contractile processes which occur in non-mammalian cardiac muscle (1, 28) and in mammalian atrial cells (33, 79) than it is in ventricular tissue. Hoerter *et al.* (71) report that this is also the case for neonatal mammalian cardiac muscle. The relaxation

process in tissue taken from neonates and infants was found to be much more susceptible to reduced levels of Na^+ in the perfusate. The relaxation process was severely retarded under the above conditions. This suggested that neonatal heart cells were much less able to deal with higher levels of intracellular Ca^{2+} if they could not exchange it with Na^+ at the sarcolemma.

The results of Fabiato (45), Sheridan (130), and Hoerter *et al.* (71) were all consistent with the relative sparsity of the SR at birth and its proliferation and differentiation during the postnatal period. This has been reported by a number of authors (13, 53, 111, 113, 125, 130, 139, 144) as well as being described in the present study. During the postnatal period the SR increases in abundance and maturity (13, 144). This was reflected in the changes seen in the developing myocardial tissue's response to variations in the external ionic environment and the appearance of Ca^{2+} -induced stimulation of contraction. The physiological differences between adult atrial and ventricular cells (28, 33, 79) are also partially understandable in light of differences in the abundance of the SR. Volume density of the SR in adult atrial cells was found to be approximately half of the value reported for ventricular cells (16, 56, 111, 113). Thus Ca^{2+} -induced calcium release from SR would be expected to be less effective in atrial cells, as has been reported (45). As would also be expected the contractile processes of atrial

cells were found to be more susceptible to alterations in the extracellular ionic environment (28, 33, 71).

It is generally accepted that the LSR of muscle contains large amounts of a Ca^{2+} -dependent ATPase which acts as a calcium pump, clearing Ca^{2+} away from the myofibrils and allowing the muscle cells to relax. The Ca^{2+} is sequestered in the cisternal SR and released when the sarcolemma and the T-tubules are depolarized. Without a well developed SR, muscle cells are dependent on trans-sarcolemmal movements of Ca^{2+} for the contraction-relaxation cycle. This is the case in early postnatal heart muscle cells.

The physiological studies on early postnatal development of cardiac muscle have looked at variables which can, perhaps, be best understood in light of the structural changes taking place in the SR. However, the information may also be useful in helping to understand the processes underlying the development of sarcolemmal invaginations. A physiological function one would associate with increased surface area would be increased transport of ions across the cell surface membrane. Higher proportions of PCs as opposed to ICs should lead to marginally shorter latencies to contraction. These differences were seen when comparing adult atrial cells to adult ventricular cells (28,33,79); no information was found concerning changes in these physiological processes which may be occurring during the early postnatal period.

The high degree of development of the caveolae in atrial cells must compensate to a certain extent for the relative sparsity of the SR. The cells need to be more efficient in transsarcolemmal transport of ions. The proliferation of caveolar complexes during postnatal development and their persistence in adult atrial cells would act to keep S/V ratios particularly high and help compensate for the less well-developed ability to regulate intracellular Ca^{2+} concentrations by sequestration in an intracellular compartment.

The latency to contraction was found to be considerably shorter for adult atrial cells than it was for adult ventricular cells. This may be an indication that transport of Ca^{2+} across the sarcolemma of the smaller atrial cell and subsequent diffusion of the ion to the vicinity of the myofibrils is a moderately rapid process. This is possible as the atrial cells are of small diameter and the myofibrils are all relatively close to the cell surface, compared to the internal myofibrils of the much larger ventricular cells. The fact that the great majority of atrial couplings are peripheral may also shorten the latency as the wave of depolarization does not have to spread throughout the T-system. Although no evidence was found concerning changes in contraction latency during the early postnatal period, it may be presumed that in neonates contraction occurs very rapidly in the relatively small atrial and ventricular cells. As the cells increase in volume and couplings form,

the processes underlying contraction become more complex and latencies to contraction would be expected to lengthen. As the ratio of PCs to ICs falls during postnatal development the latencies probably become even longer; the transport of the wave of depolarization through the T-system must take a finite, albeit a very short, time.

The data presented in Tables 1, 2 and 3 demonstrated that there were only two structures that showed rapid spurts of growth during the early postnatal period. These were the SR and the invaginations of the sarcolemma. In ventricular cells this was seen as a rapid development of the T-tubules, and a proliferation of SR and internal couplings (69, 112); in atrial cells this was seen as a formation of short tubular invaginations and a rapid proliferation of caveolae, SR tubules and peripheral couplings (Table 3). It has been suggested that the formation of SR from the granular ER present in the neonatal state takes a certain length of time. Even the smooth ER seen during the early stages of postnatal development may not be functioning as SR (13). It may be that it is only when the bulk of the SR is fully matured (presumably at the tenth postnatal day in ventricles and at the sixteenth postnatal day in atrium) that it is able to form couplings. While some SR may be mature in neonatal animals the vast majority remains as granular ER and is acting to synthesize proteins for the dividing cells. Ventricular cells became larger at an earlier age and it may be that more of the ER becomes

actively engaged in the regulation of Ca^{2+} movements at an earlier age to allow coordination of contractile events at the interior of these larger cells. Thus the SR may undergo a rapid maturation at the tenth postnatal day, peripheral couplings may be formed and T-tubules drawn into the cell. Proliferation and branching of the T-system in ventricular cells must be a more complex process than the formation of the simple tubules seen in atrial cells. In atrium the cells are smaller and perhaps more of the ER is involved in the production of specific granules and less available for maturation and formation of couplings. This may explain the week's delay in the formation of peripheral couplings and the proliferation of the caveolar complexes in atrial cells. In any case, it seems reasonable to suggest that it is the proliferation and maturation of the SR and the ability of the jSR to form couplings which is the stimulus which initiates proliferation of sarcolemmal invaginations. The other factors such as S/V ratios and degree of development and organization of myofibrillar protein are likely secondary to the maturation of the SR. They may themselves be dependent on this maturation.

Claycomb (29) found that at approximately the middle of the second postnatal week DNA replication stopped and the growth of the heart was no longer hyperplastic but became dominated by hypertrophy of existing cells. This might explain why the nuclei of atrial cells began to exhibit less irregular shapes in the heart tissue taken from sixteen to

eighteen day postnatal animals. It also corresponds with the chronology of caveolar proliferation in atrial cells. This may indicate that the development of the invaginations are related to the maturational state of the genetic apparatus. The earlier proliferation of the T-tubules in ventricular cells (8- 10 days postnatally) argues against this interpretation. Perhaps, even as early as the tenth postnatal day some of the ventricular cells have become terminally differentiated and the T-tubules develop in these cells.

Further studies on the morphology of the T-tubules and the caveolae, and their relation to the SR are certainly necessary. Recently, differences have been demonstrated between SR and sarcolemmal Ca^{2+} -ATPases using indirect immunofluorescent labelling techniques (75). These and other antibody labelling techniques should prove useful in demonstrating the contrasting morphology of caveolae, T-tubules and the sarcolemma of atrial and ventricular muscle cells. The freeze-fracture appearance of the caveolae and T-system needs to be clarified; comparisons between the freeze fracture appearance of the sarcolemma and its invaginations should provide useful morphological information. The freeze-fracture morphology of the couplings in cardiac muscle is considerably less well understood than that of the triads of skeletal muscle. In conclusion, although some useful information concerning the morphology

of developing T-tubules in cardiac muscle has been provided considerable work remains to be done.

A. Summary and Conclusions

It has been suggested that the T-tubules in ventricular myocardium developed by a repeated caveolation of the sarcolemma. It has also been generally reported that mammalian adult atrial cells have few, if any, T-tubules. Preliminary studies have shown that tannic acid mordanting is extremely effective at delineating sarcolemmal invaginations, the caveolae and the T-tubules, and has demonstrated that T-tubules are not as rare as had been suggested. It is felt by the author that repeated caveolation at the sarcolemma might not adequately explain the process of T-system development. The aim of the study was to investigate the postnatal development of sarcolemmal invaginations in the atrial myocardium of the rat using tannic acid mordanting to aid in the visualization of the early stages of T-tubule development.

The present study has shown that, indeed, a proliferation of caveolae and the formation of complex clusters of caveolae did occur during the third week of postnatal development, approximately at the same time tubules appear. Although the processes are chronologically correlated they do not seem to be sequential. It is thus suggested that the formation of caveolar complexes is unlikely to be the first step of T-tubule formation; tubules

do not often appear as strings of caveolae and the caveolar complexes persist in the adult.

T-tubules are reported to start appearing in significant numbers in ventricular cells at approximately the tenth postnatal day. The proliferation of sarcolemmal invaginations in atrial cells is found to occur several days later. It has been speculated that increasing cell diameters during the postnatal period might induce T-system formation as a means of maintaining constant surface to volume ratios. Alternatively, it was felt that the progressive development of centrally located myofibrils would require a T-system to permit co-ordination of the contractile process. In an attempt to differentiate between these possibilities a morphometric study has been carried out. Measurements of cell diameter, volume density of myofibrillar protein, and surface density of caveolae and T-tubules, as well as surface density of internal and peripheral couplings have been performed. It was found that cell diameter and volume density of the myofilaments increased gradually throughout the first three postnatal weeks. Both the caveolae and T-tubules and the junctional SR (in the form of couplings) increased in abundance dramatically between the fourteenth and sixteenth postnatal day.

T-tubules were seen to develop in small diameter cells (of much smaller diameter than had been suggested to be necessary to induce development of the T-tubules in ventricle) and often atrial cells containing sparsely

developed myofilaments had a relatively extensive T-system. For these reasons as well as the fact that no large increase in surface/volume ratio or level of myofibrillar development is seen to occur postnatally, it is felt that the development of sarcolemmal invaginations may be induced by some other factor.

The morphometric data suggested that the proliferation of sarcolemmal invaginations was related, at least chronologically, to the development of the jSR and the formation of couplings. The physiological changes that have been reported to occur during the postnatal period are consistent with these observations. Thus the maturation of the SR and the proliferation of the T-tubules and caveolae are seen to occur at the same time.

It is felt that while mechanical, chemical, and electrical events may greatly influence the maturation of the SR, this maturation is ultimately under the control of genetically coded processes. As the jSR matures and peripheral couplings form, the Golgi bodies would have been producing membrane vesicles to augment the formation of caveolar complexes. This latter process occurs, perhaps, as a response to decreasing surface to volume ratios. The T-tubule invaginations are possibly formed as elements of jSR involved in peripheral couplings are being drawn into the interior portions of the cell during the organization of the SR into sleeves around centrally located myofibrils.

Thus it is concluded that, at least in atrial cells, the formation of the T-tubules is not by repeated caveolation at the sarcolemmal surface. The maturation of the SR and the proliferation of the caveolar complexes are chronologically synchronized as genetically coded postnatal changes. The maturation of the jSR and the formation of couplings are likely major factors in the inducement of T-tubule invagination.

V. TABLES

Table 1. Means and standard deviations of body weight, heart weight and right atrial weight for rats of various postnatal ages.

POSTNATAL AGE	NEONATE	7 DAYS	14 DAYS	18 DAYS	21 DAYS	ADULT
Body Wt. (g)	6.26± 1.71	17.78± 1.49	34.93± 2.56	57.05± 3.30	94.66± 6.29	291.20± 23.09
Heart Wt. (mg)	61.8± 8.8	168.2± 21.0	333.6± 14.6	434.0± 33.6	750.0± 38.1	1274.0± 147.9
Right Atr. Wt. (mg)	3.4± 0.6	12.4± 2.7	28.4± 2.2	39.8± 5.5	73.8± 4.4	116.3± 13.0

Table 2. Mean right atrial cell diameters measured from low power (1000X) electron micrographs for rats of various postnatal ages.

POSTNATAL AGE	NEONATE	7 DAYS	14 DAYS	18 DAYS	21 DAYS	ADULT
Cell Diameter (μm)	3.28± 0.55	3.38± 0.54	3.75± 0.71	4.02± 0.75	4.38± 0.73	7.49± 1.70

Table 3. Means and standard deviations of myofibrillar volume density (VvMYOF) and surface density (Sv) of peripheral couplings, internal couplings and caveolae + T-tubules estimated from electron micrographs (magnification = 15,000X) of rat right atrial myocardium.

POSTNATAL AGE	NEONATE	7 DAYS	14 DAYS	18 DAYS	21 DAYS	ADULT
VvMYOF (% cell volume)	35.16± 8.68	38.28± 8.72	41.07± 8.93	40.79± 8.93	44.06± 8.53	56.41± 7.73
SvPC ($\mu\text{m}/\mu\text{m}$ SL)	0.017± 0.014	0.021± 0.016	0.024± 0.018	0.50± 0.036	0.067± 0.028	0.054± 0.031
SvIC ($\mu\text{m}/\mu\text{m}$ SL)	0.0 0.0	0.001± 0.002	0.004± 0.007	0.010± 0.010	0.016± 0.014	0.022± 0.025
SvCav+T ($\mu\text{m}/\mu\text{m}$ SL)	0.127± 0.062	0.128± 0.049	0.136± 0.050	0.306± 0.101	0.361± 0.109	0.459± 0.123

VI. FIGURES

Figures 1 - 36 contain electron micrographs obtained from the right atrial myocardium of rats of various postnatal ages. All of the tissue was mordanted with tannic acid.

Figure 1. Well-mordanted adult cells in longitudinal section. Note: Abundance and degree of organization of the myofilaments. Banding pattern of dark A bands and light I bands, Z-lines transecting the I band, lighter H bands in the middle of the A bands. Branching of myofibrils is evident. Lumen of blood vessels (L) and endothelial cells with micropinocytotic vesicles, small unmyelinated axon adjacent to capillary (upper left). Intercellular junctions; tight junction (Tj), intercalated discs (id, and elsewhere), lateral cell-cell contacts. Rows of mitochondria (M) separating myofibrils. Sleeves of SR tubules (sr) partially surrounding the myofilaments. Caveolae are seen as dense black vesicles (small black arrowheads, upper left). Peripheral couplings (large white arrowheads) and coupling between SR and caveolae (small white arrowheads, lower right). x9,100.

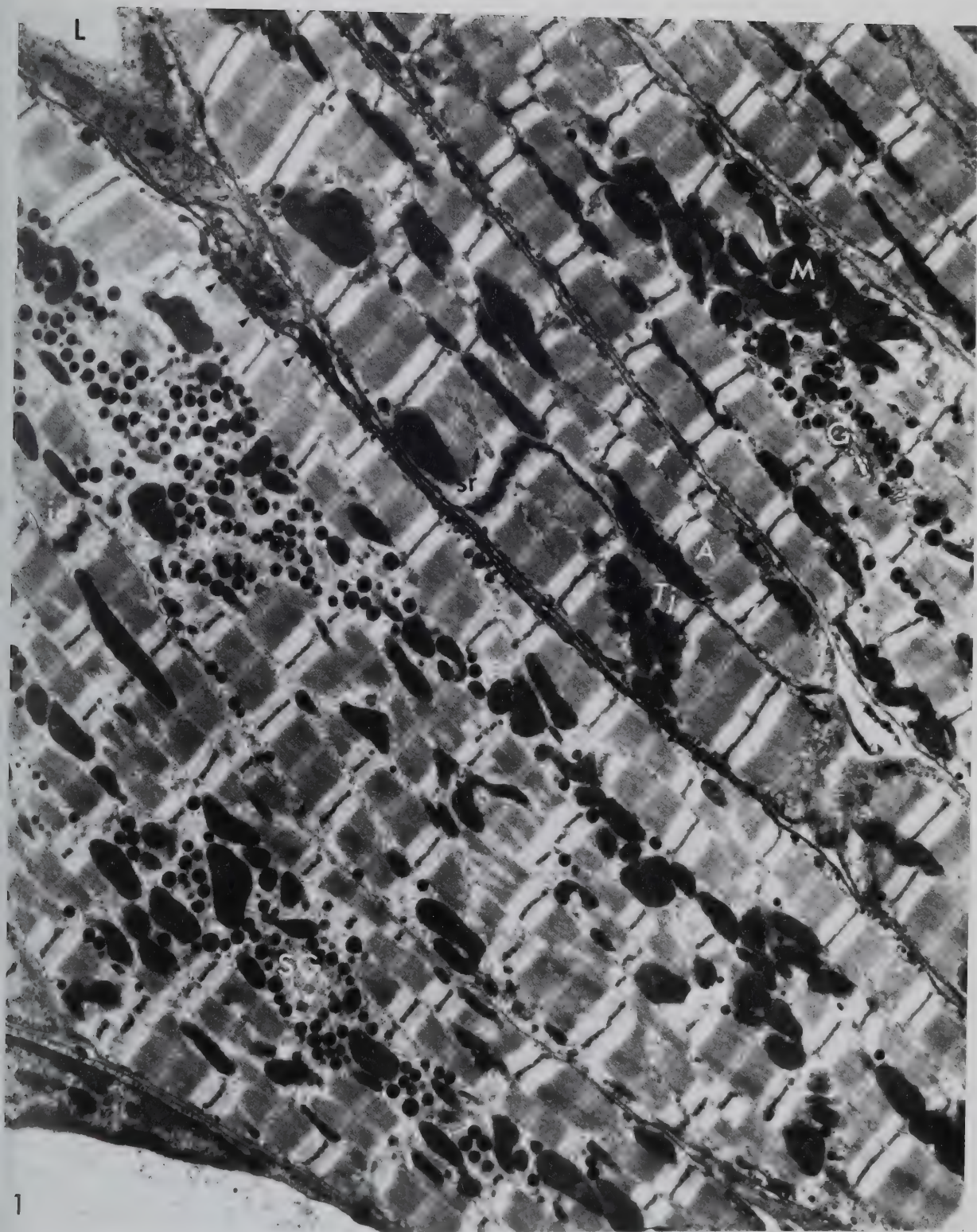


Figure 2. Adult cells in longitudinal section. Note:
Relatively poor infiltration of tannic acid. Large
central nucleus (N) with regular profile. Other
features similar to Figure 1. Caveolae (small
black arrowheads, centre left) more difficult to
visualize. x6,900



Figure 3. Adult cells, well-mordanted, oblique section.

A. Note: caveolar complexes (large white arrowheads) at sarcolemma and possibly mordanted tubules in interior regions (large black arrowheads) at Z-lines. x6,200.

B. Endocardial surface, Note: endothelial cells (en) and degree of development of underlying connective tissue. Small unmyelinated axon (a). Development of intercellular collagen (cf). Apparent difference between degree of myofibrillar development in cells directly below endocardial surface. x6,000

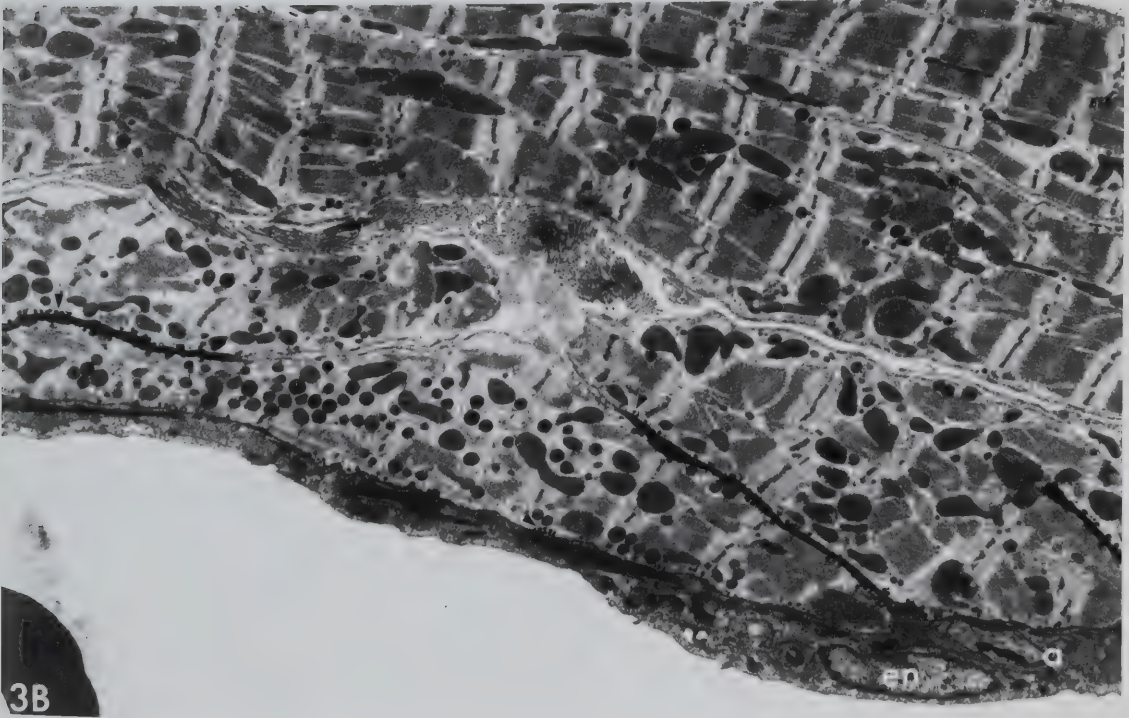
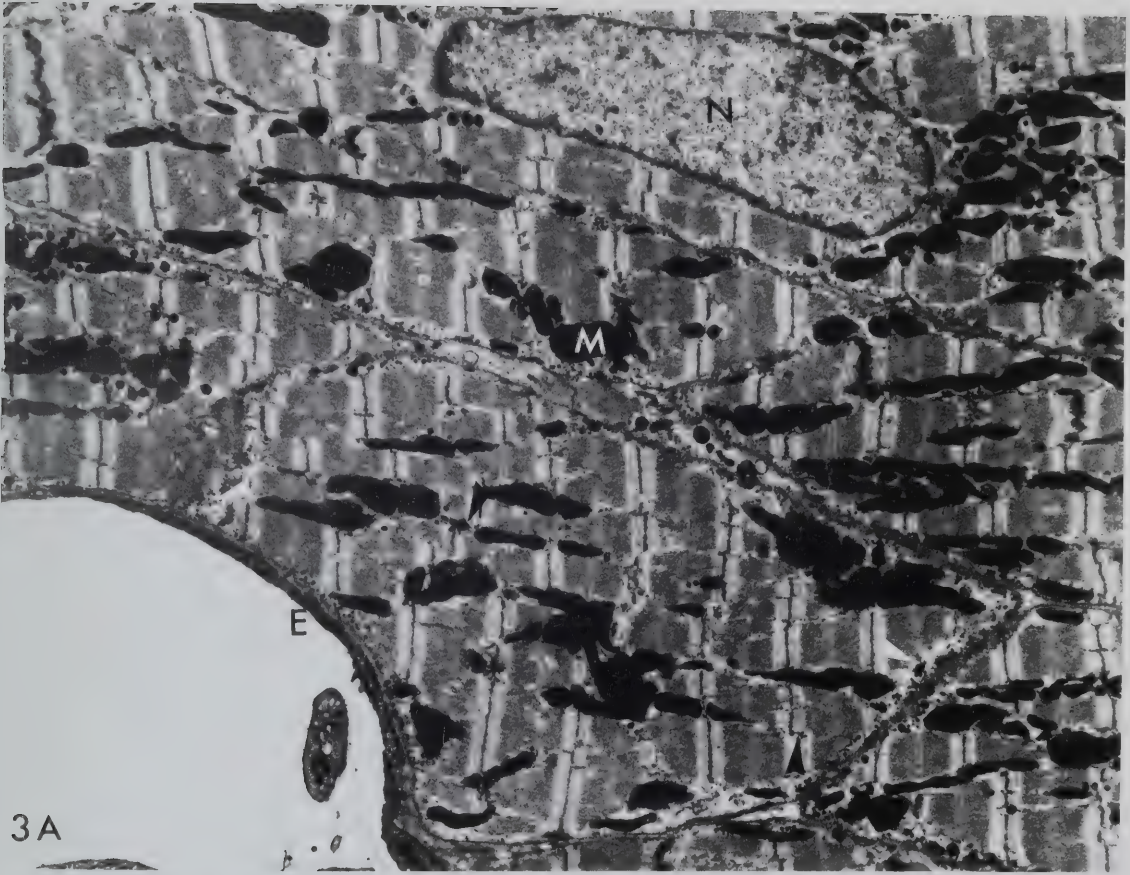


Figure 4. Trabecula from adult, oblique section. Note: endocardial surface on both sides of myocardial cells. Robust collagen fibrils (cf). Cell-cell junctions at lateral edges of cells (T), abundant caveolae at cell surfaces and invaginations to interior of cells (small black arrowheads, centre left, adjacent to endothelial surface). x9,300



Figure 5. Adult cells, oblique section. Note: Branching of myofibrils, aggregation of specific granules (SG), rows of mitochondria (M). Penetration properties of tannic acid limited to superficial areas. Caveolar complexes (c) at surface and deeper within the sarcoplasm. x14,000

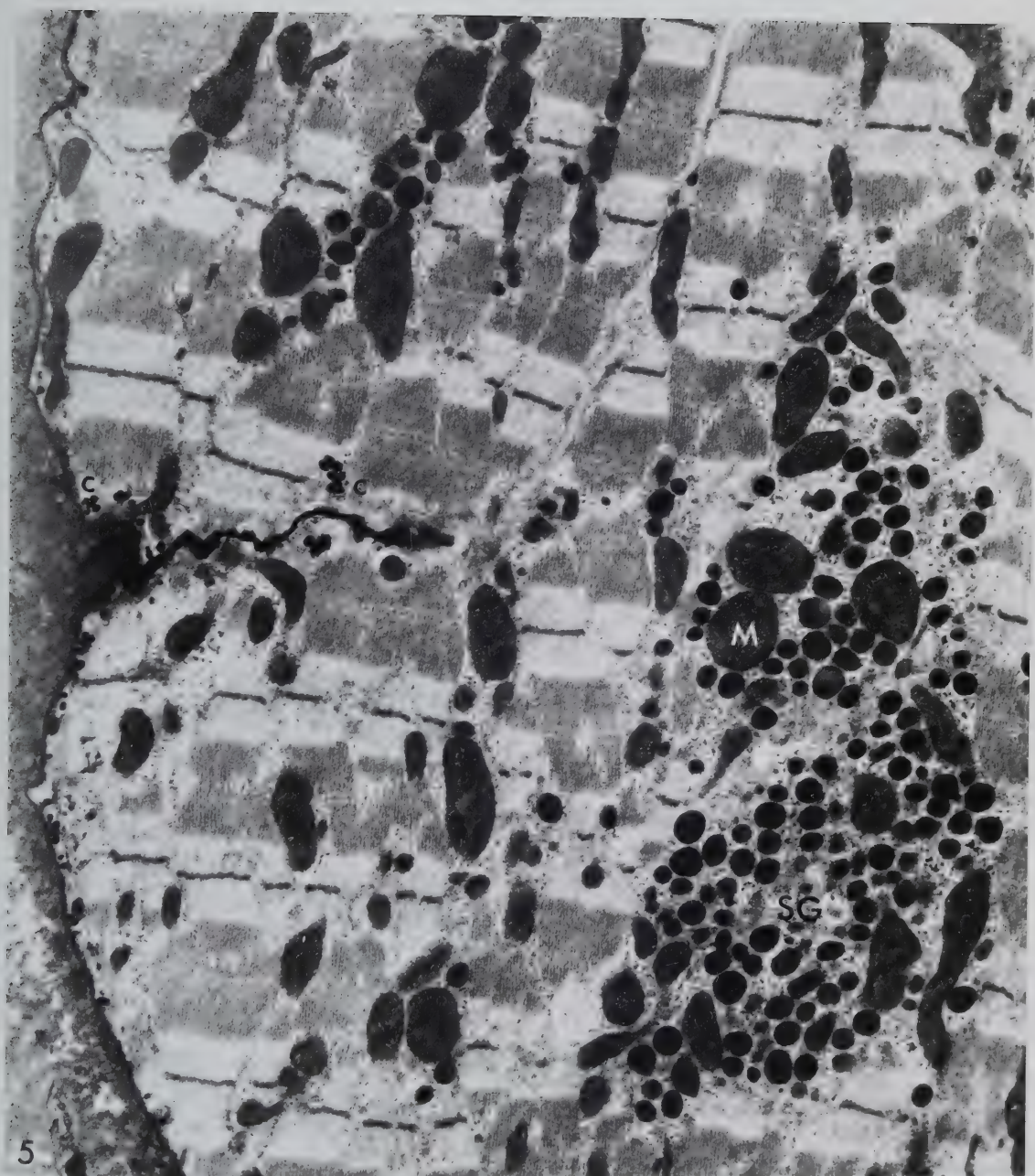


Figure 6. A. Adult cells, transverse section. Note: appearance of thick myofilaments (MF) as large round dots, thin filaments much smaller. Z-line in cross-section (z, centre right) much less distinct. Incomplete delineation of myofibrils by tubules of the sarcoplasmic reticulum (sr). Caveolae at cell surface and possibly in central regions (small black arrowheads, upper left). Peripheral couplings (large white arrowheads). x16,700

B. Adult Cells, oblique sections. Note: caveolar complexes and tubules in more central regions (small black arrowheads, centre). Internal coupling (large black arrow). Development of sarcoplasmic reticulum (sr). Association between SR and caveolae (large white arrowhead). x15,600

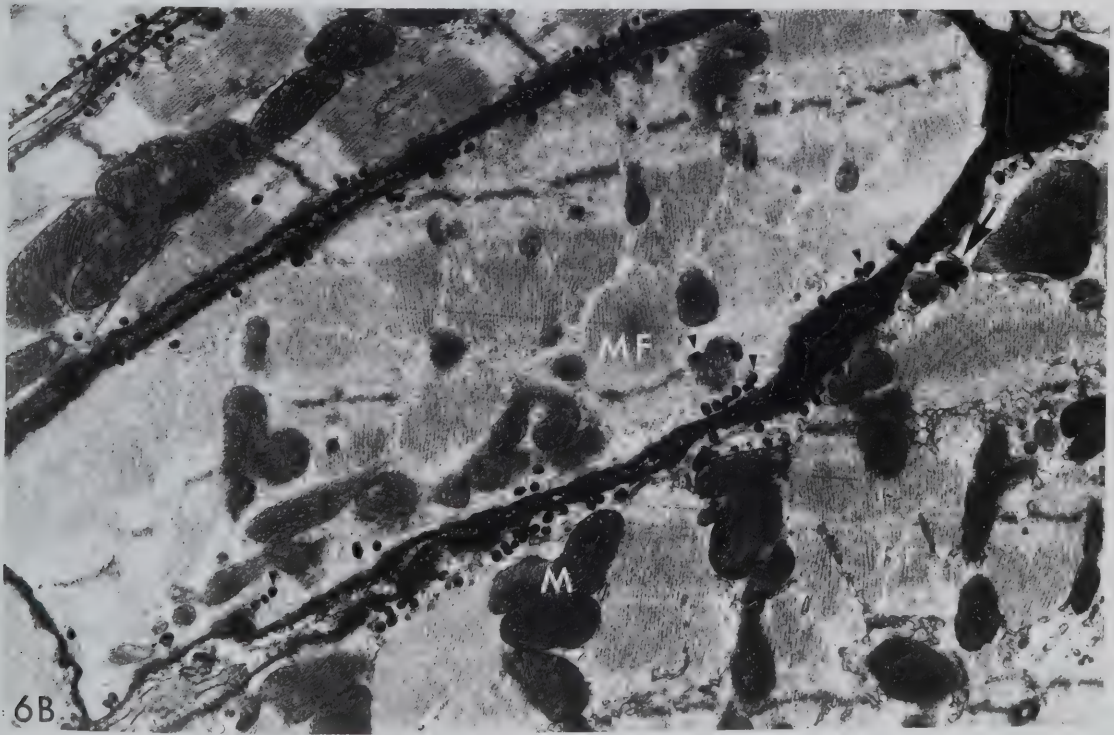
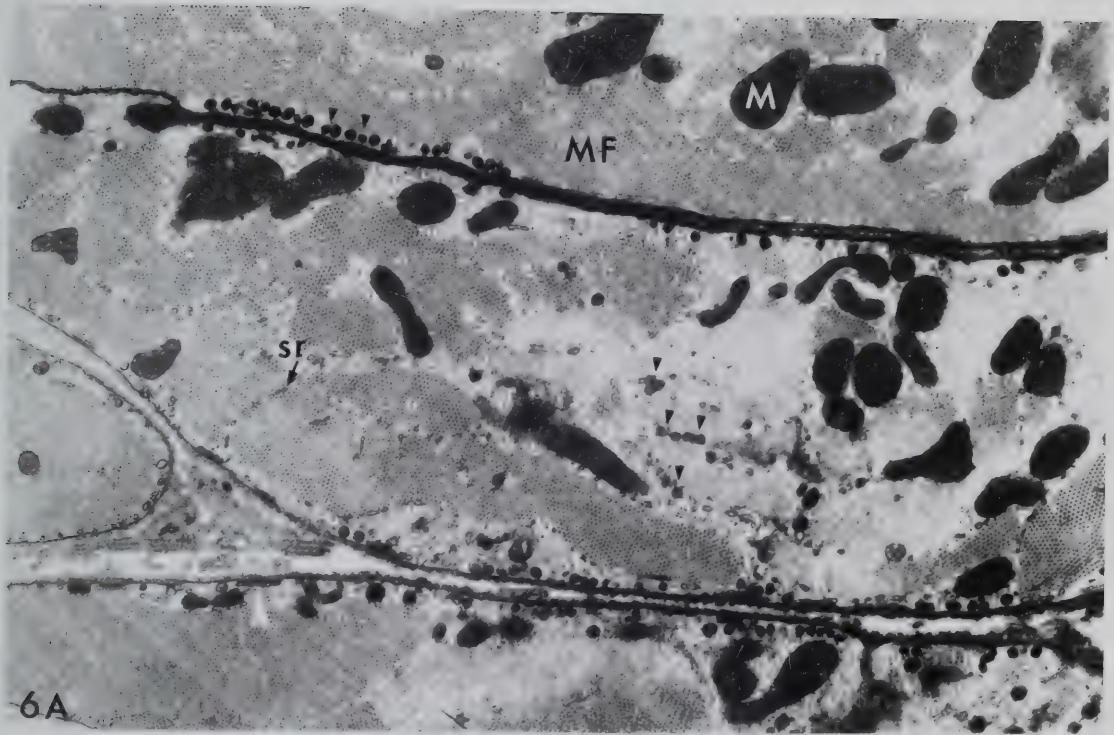


Figure 7. Adult Cells, well-mordanted.

A. Note: Caveolar complex (c) and relation to SR (small white arrowhead). Internal couplings (ic) at Z-lines. x19,800.

B. Note: T-tubule (T) and internal couplings with the SR (ic). Appearance of peripheral couplings with dense bridges in gap (large white arrowhead). x49,800

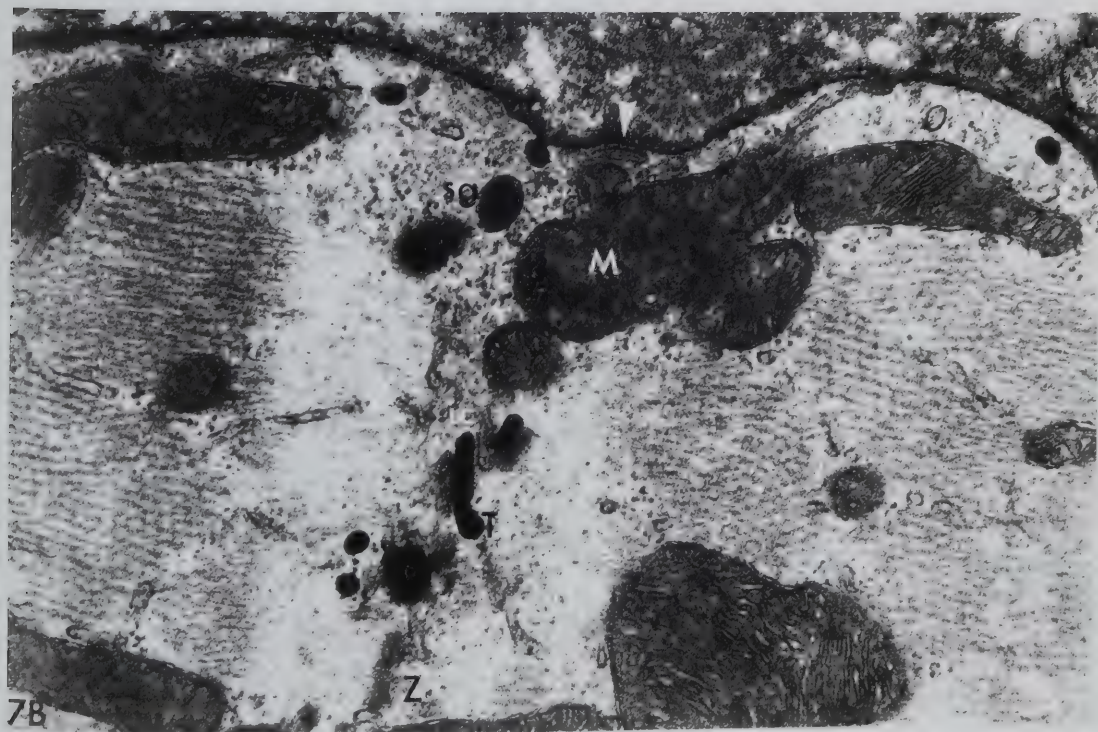
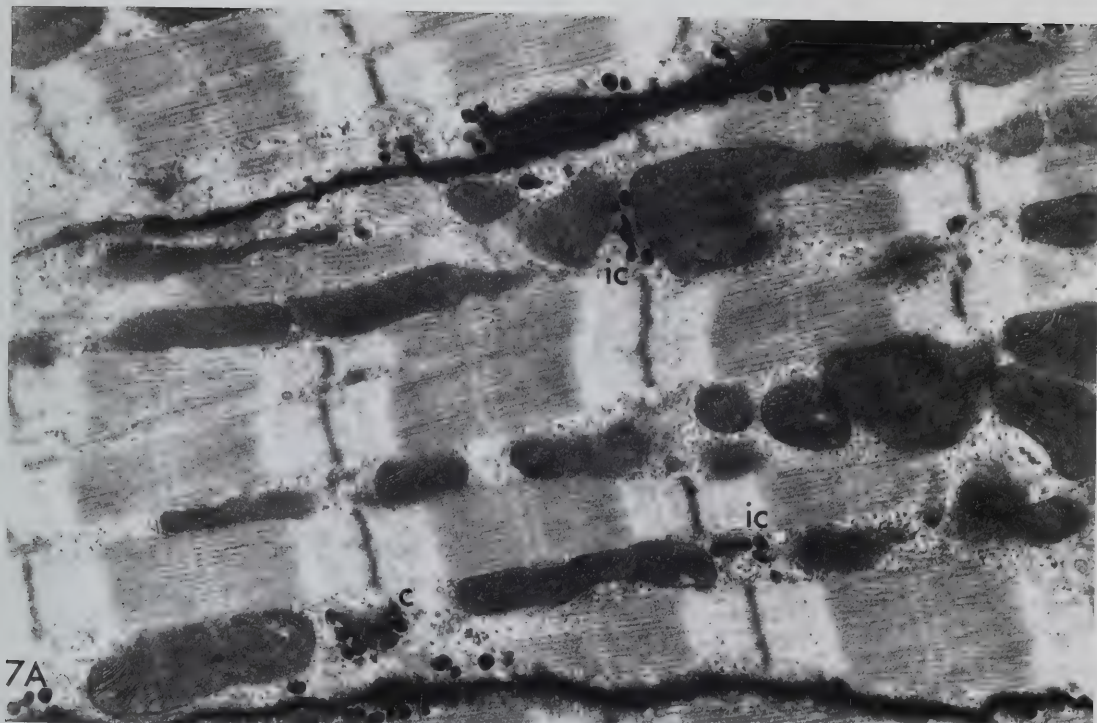


Figure 8. Adult Cells. A. Note: Caveolae, caveolar complexes (c) and their relation to sarcoplasmic reticulum (sr). x27,600.

B. Note convoluted T-tubule (T), continuity between adjacent caveolae (E). x62,400

C. Note: Endothelial cell (en) with micropinocytotic vesicles clearly in continuity with the ECS (small white arrowheads), less well infiltrated than caveolae. Caveolar complex (C) and relation to SR (large black arrowhead). x35,200.

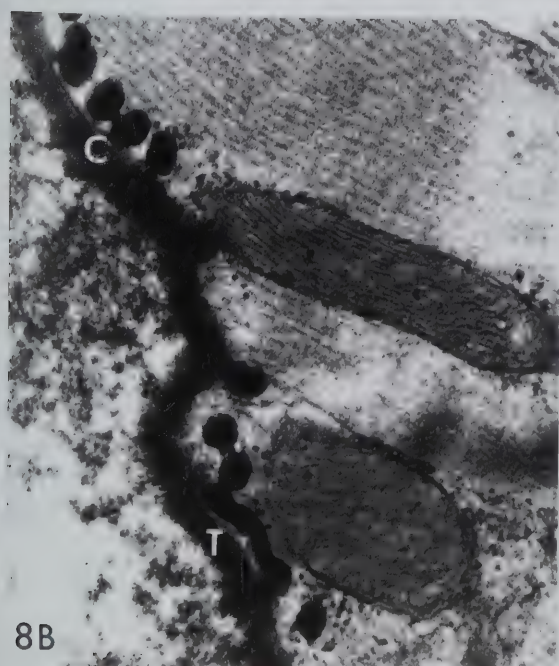


Figure 9. Neonatal cells, transverse section. Note: small size of cells (compare to Fig. 1). Large intercellular clefts (ecs). Frequency of fibroblasts (F). Scattered, small mitochondria (M) and specific granules. Irregular shaped nuclei (N). Relatively well-developed aggregations of myofilaments (MF) mainly towards cell periphery. Absence of SR sleeves around myofibrils and relative sparsity of caveolae (small black arrowhead, centre). x9,200

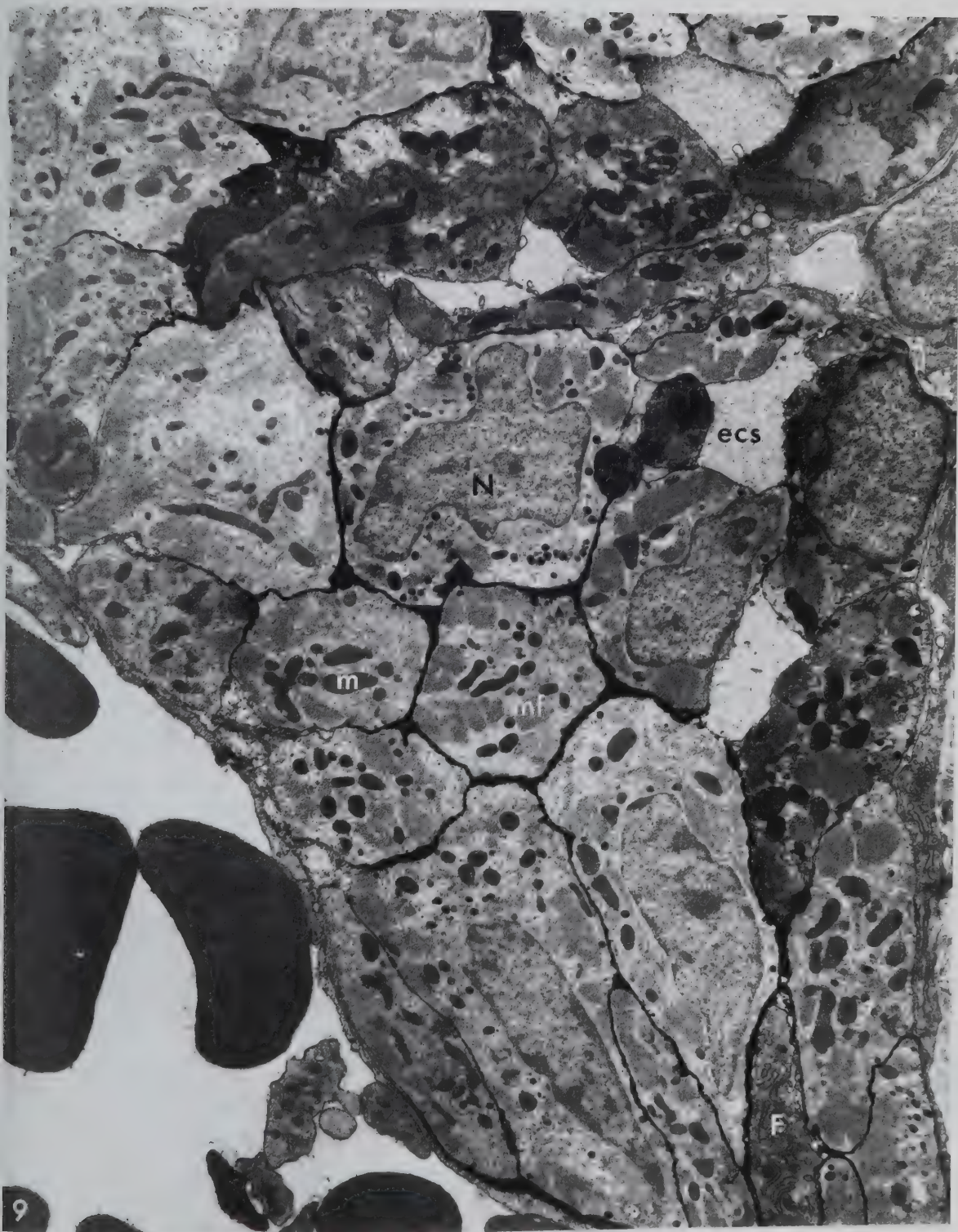


Figure 10. Neonatal cells, oblique section. Note: Sparsity of collagen at endocardial surface (en). Intercellular clefts (ecs). Immature appearance of cell-cell contacts. Degree of disorientation of myofilaments (MF) between adjacent cells and within cells. Dispersal of specific granules (sg) and mitochondria in central regions relatively devoid of contractile apparatus. x7,500

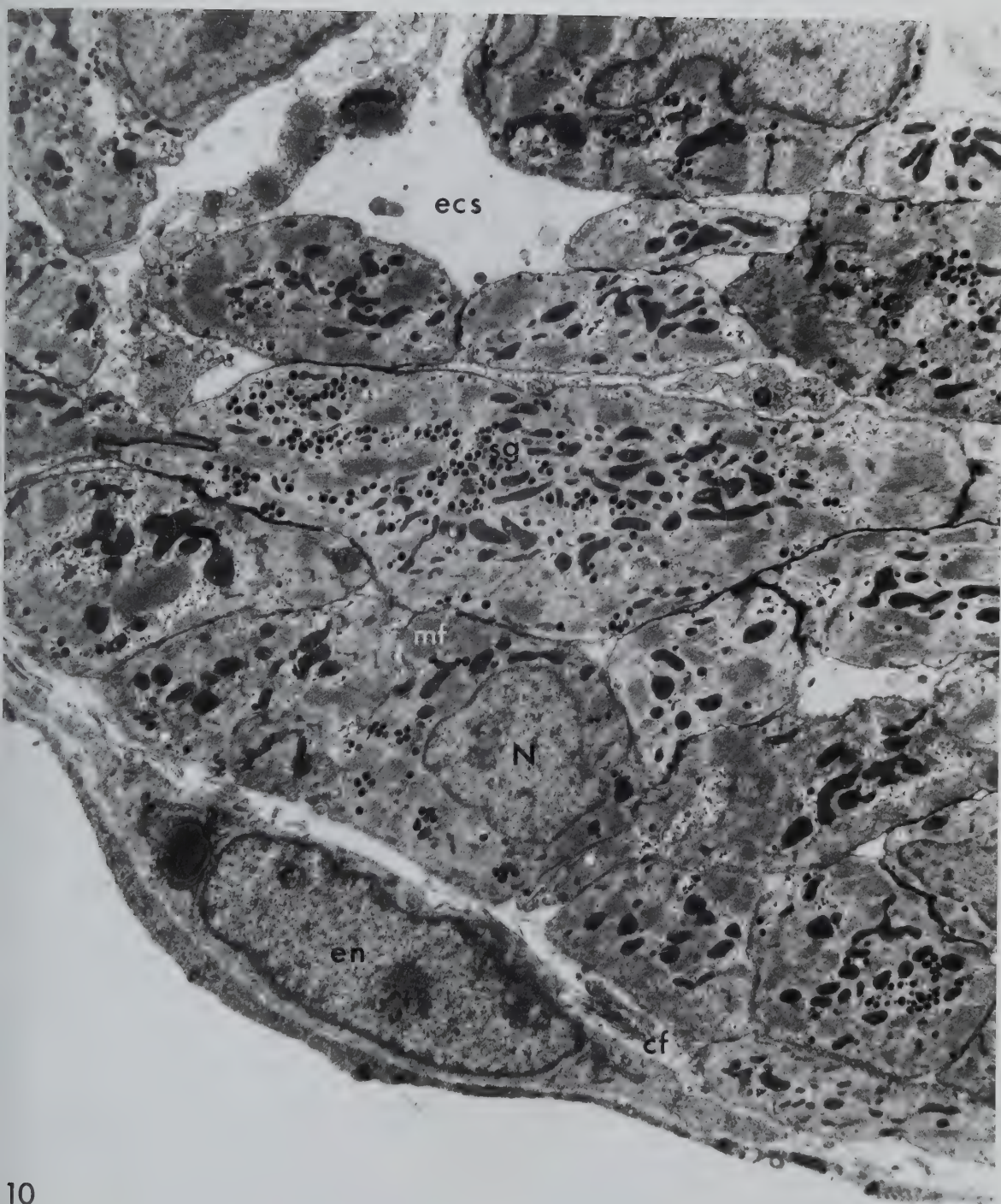


Figure 11. Neonatal cells, transverse section. This is a higher magnification of material in Figure 9. Note: Myofilaments (mf) appear less well oriented than at lower power. Infrequent caveolae (small black arrowheads, centre). Apparent invaginations into cell (small white arrowheads) which are more likely furrows or folds of the cell surface. Sparsity of the sarcoplasmic reticulum, most of which appears as granular endoplasmic reticulum (er). x16,500

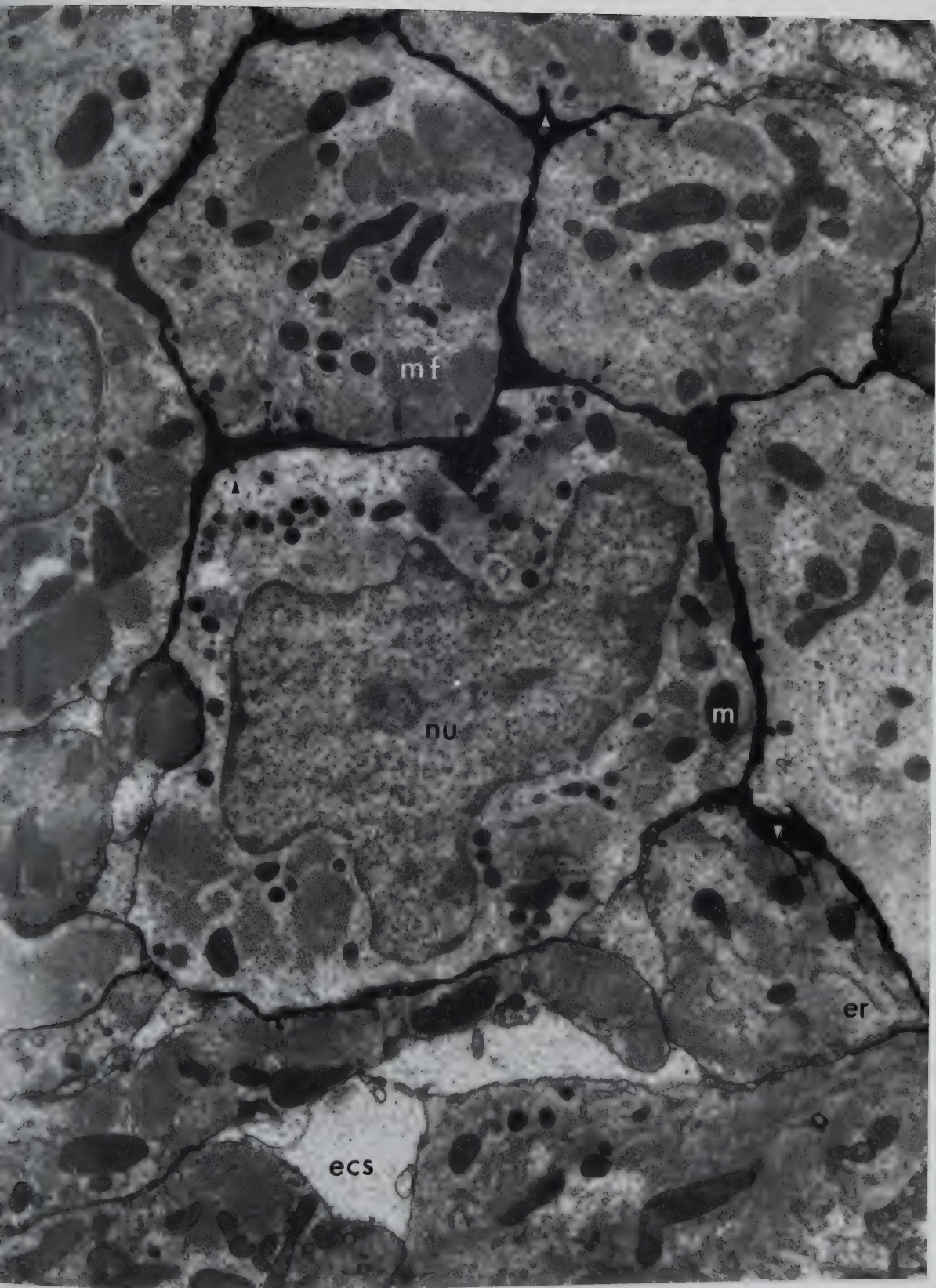


Figure 12. Neonatal cells, transverse section. Note:
Disorientation of filaments (mf). Immature,
thickened Z-lines (z). Poorly developed cell-cell
contacts (J). Well developed Golgi (G) and
associated clear vesicles and atrial specific
granules. Abundance of granular endoplasmic
reticulum (er). Occasional peripheral couplings
(large black arrowheads and elsewhere). Lipid
droplet (LD). x23,000

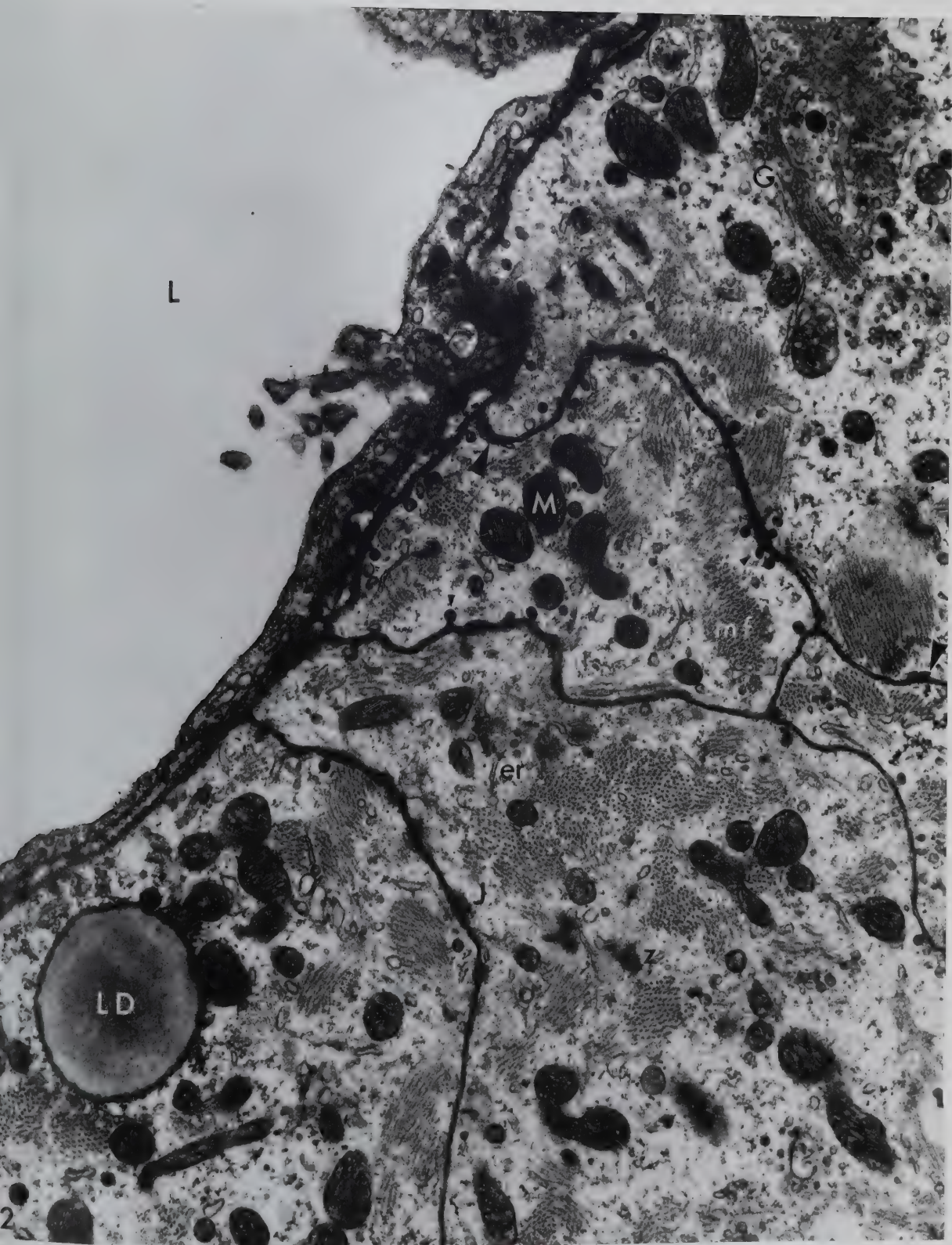


Figure 13 A and B. Neonatal trabecular tissue. Note: Lack of connective tissue underlying endothelial cells at luminal surfaces (L). Large intercellular clefts (ecs). Fibroblast activity (F). Immaturity of cell-cell contacts (id). A. x14,600. B. x10,000.

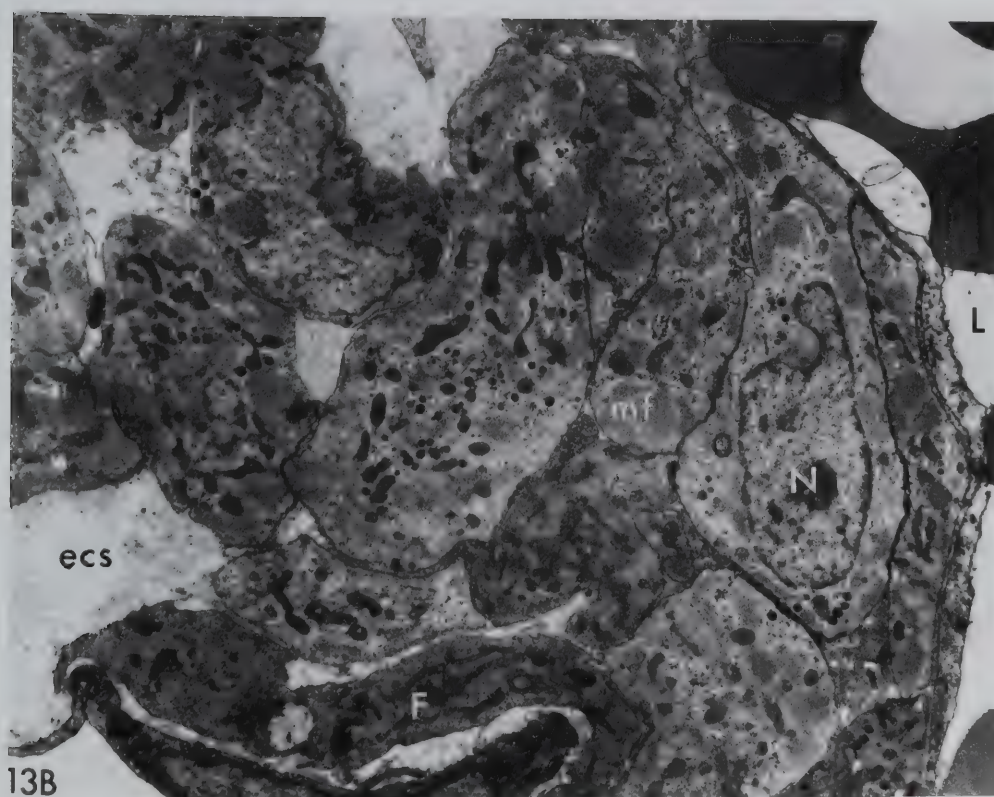
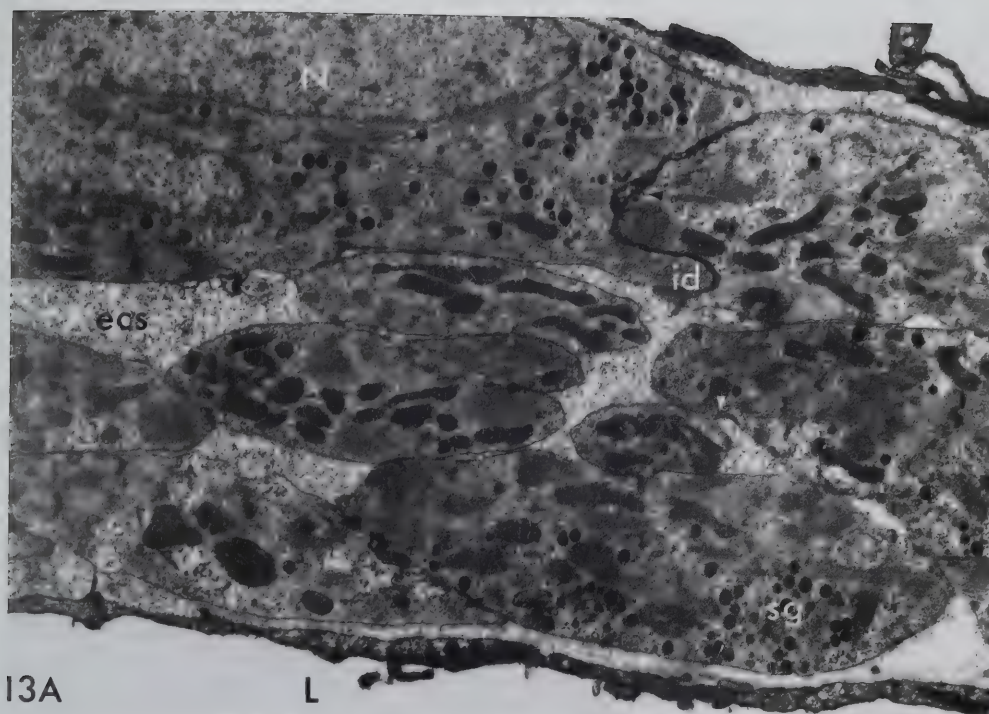


Figure 14. Seven day postnatal tissue, trabecular surface, transverse section. Note: Decrease in the size of extracellular clefts. Fibroblast activity (F). Increased abundance of myofilaments, organized in more central regions as well as peripherally. Appearance, distribution and organization of tubules of SR surrounding myofilaments (small white arrowheads, upper left, upper right, centre) as well as granular endoplasmic reticulum. Note: Increased frequency of peripheral couplings (large black arrowheads, centre) and caveolae (small black arrowheads). x21,000.

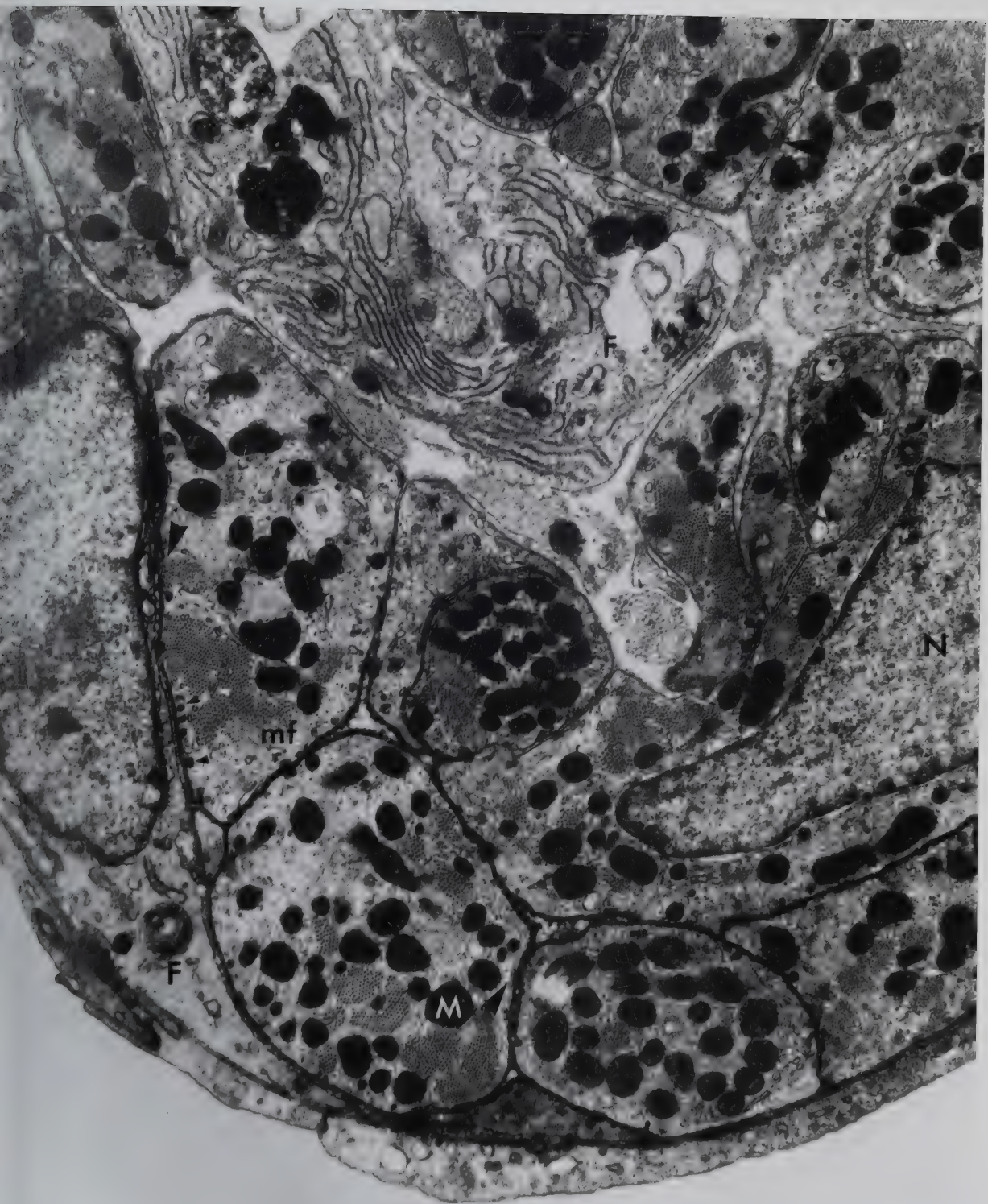


Figure 15. Seven day postnatal cells, longitudinal section. Note: large intercellular clefts (ecs) have not completely disappeared. Cell-cell contacts (id) still immature. Cells are still small compared to those of adult (eg. Figure 1). Myofilaments (mf) much more highly oriented, but myofibril-like units are of very small diameter. Mitochondria lining up into rows between contractile apparatus. There are still areas in most cells devoid of myofilaments. Occasional caveolar complexes (small black arrowheads, upper centre) and possible tubular invagination and internal coupling (star). x8,800.

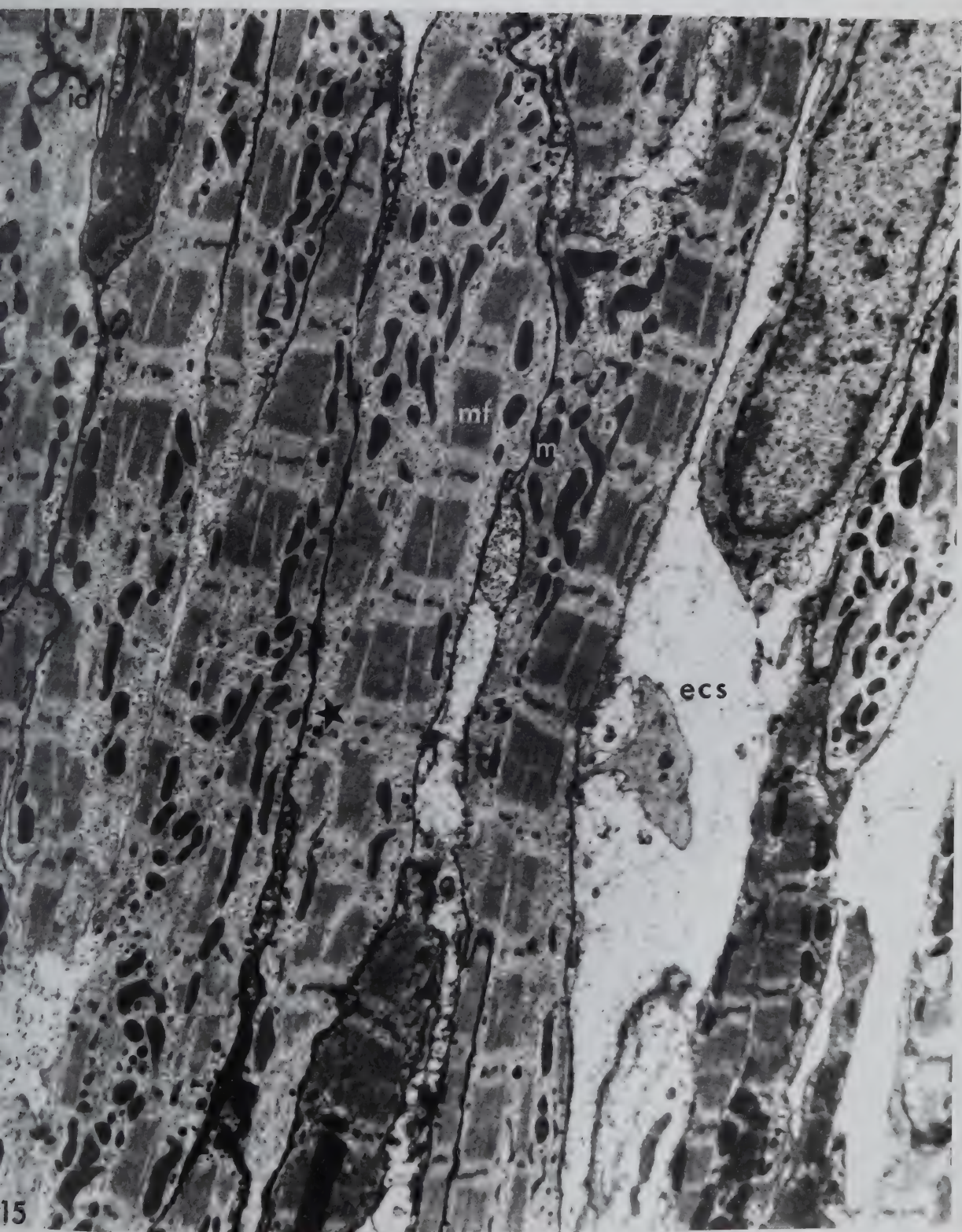


Figure 16. Seven day postnatal cells, transverse section.
Note: Immature appearance of capillary endothelial cells with thickened walls (L). Some nuclear profiles appear more rounded (N) but some are still irregular. High degree of myofilament organization (mf) and abundance of sarcoplasmic reticulum tubules (sr) surrounding myofibrils. Granular endoplasmic reticulum (large white arrowheads) still relatively abundant. Peripheral couplings (large black arrowheads) and caveolae (small black arrowheads). x13,100.

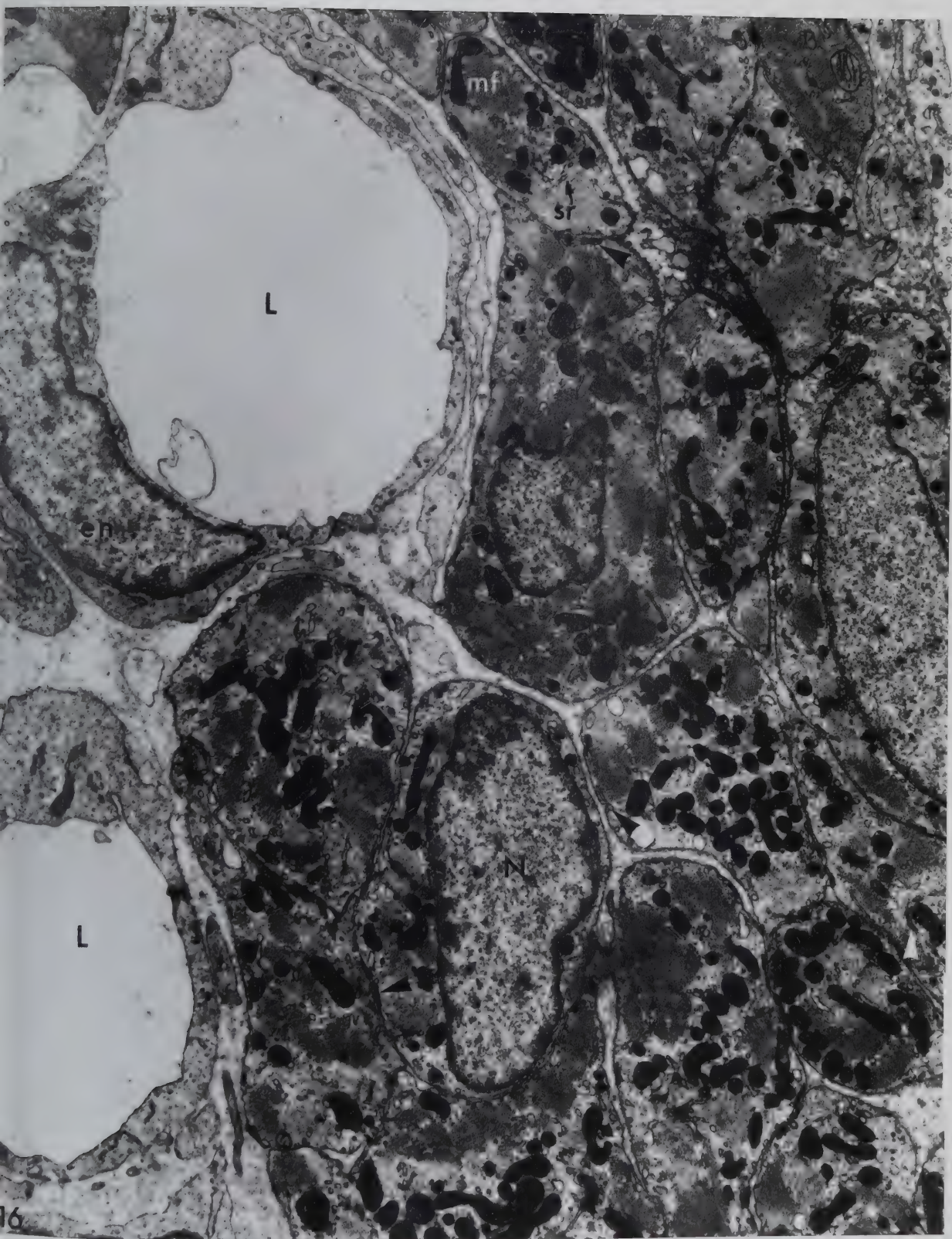


Figure 18. Seven day postnatal cells.

A. Transverse section. Note: at this higher magnification it is possible to see that while many of the tubules surrounding the myofilaments appear to be smooth, sarcoplasmic reticulum (sr), many are elements of granular ER with attached ribosomes. Peripheral couplings continuous with elements of SR which pass towards the central regions of the cell (large black arrowhead). x23,500

B. Epicardial surface (to right), lumen of blood vessel (to left). Note: High degree of fibroblast activity (F) elaborating the collagen fibrils (cf) at the epicardial surface. Small nerve fibre and associated Schwann cell (s). x10,500

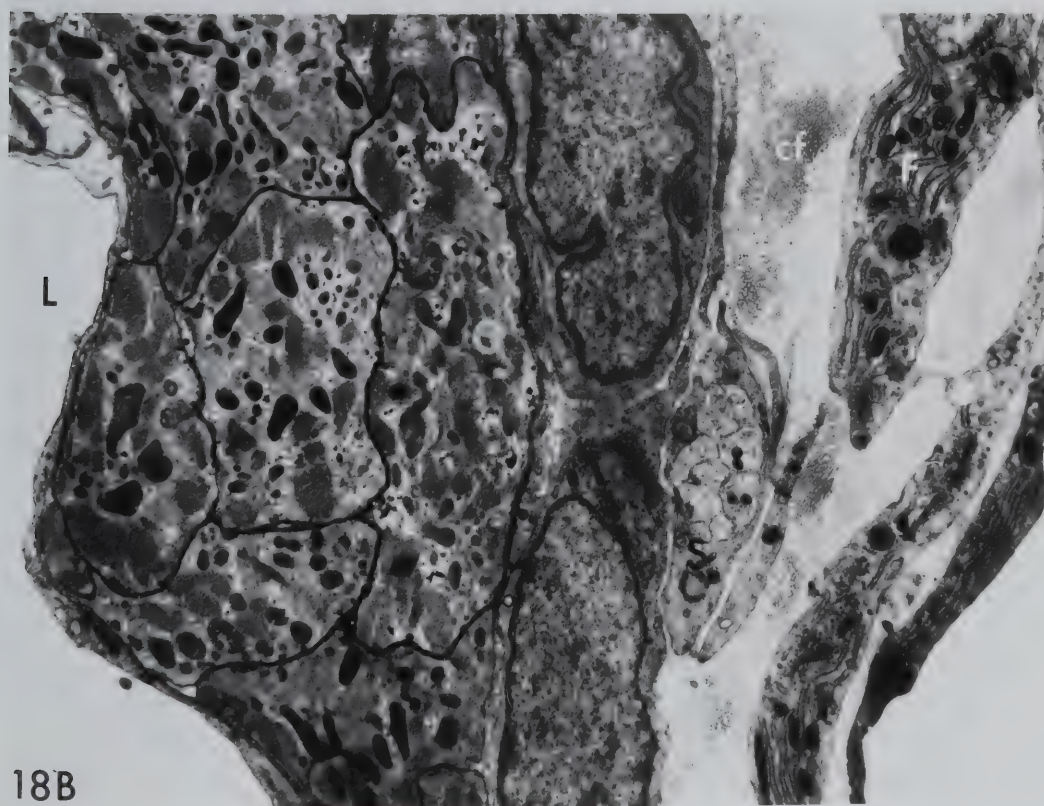
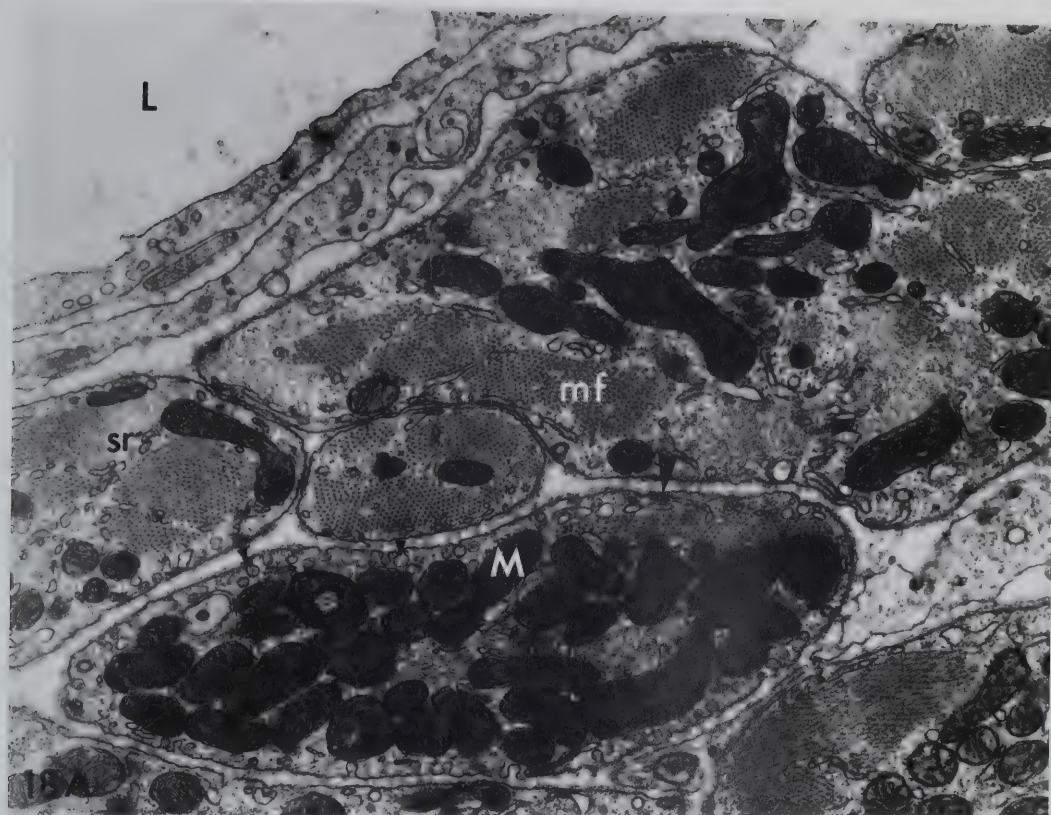


Figure 19. Fourteen day postnatal cells, trabecular area. Cells are still quite small, comparable in size to neonate (Figure 9) and seven day (Figure 15) cells. Intercellular clefts not as prominent. Active fibroblasts (F) still seen frequently. Many nuclei still have irregular profiles. Note: Increased abundance of myofilaments (mf) in central regions of cells and slightly larger diameters of myofibrillar units. Caveolae (small black arrowheads, centre and upper right) less visible in this material less well infiltrated with tannic acid. x9,700

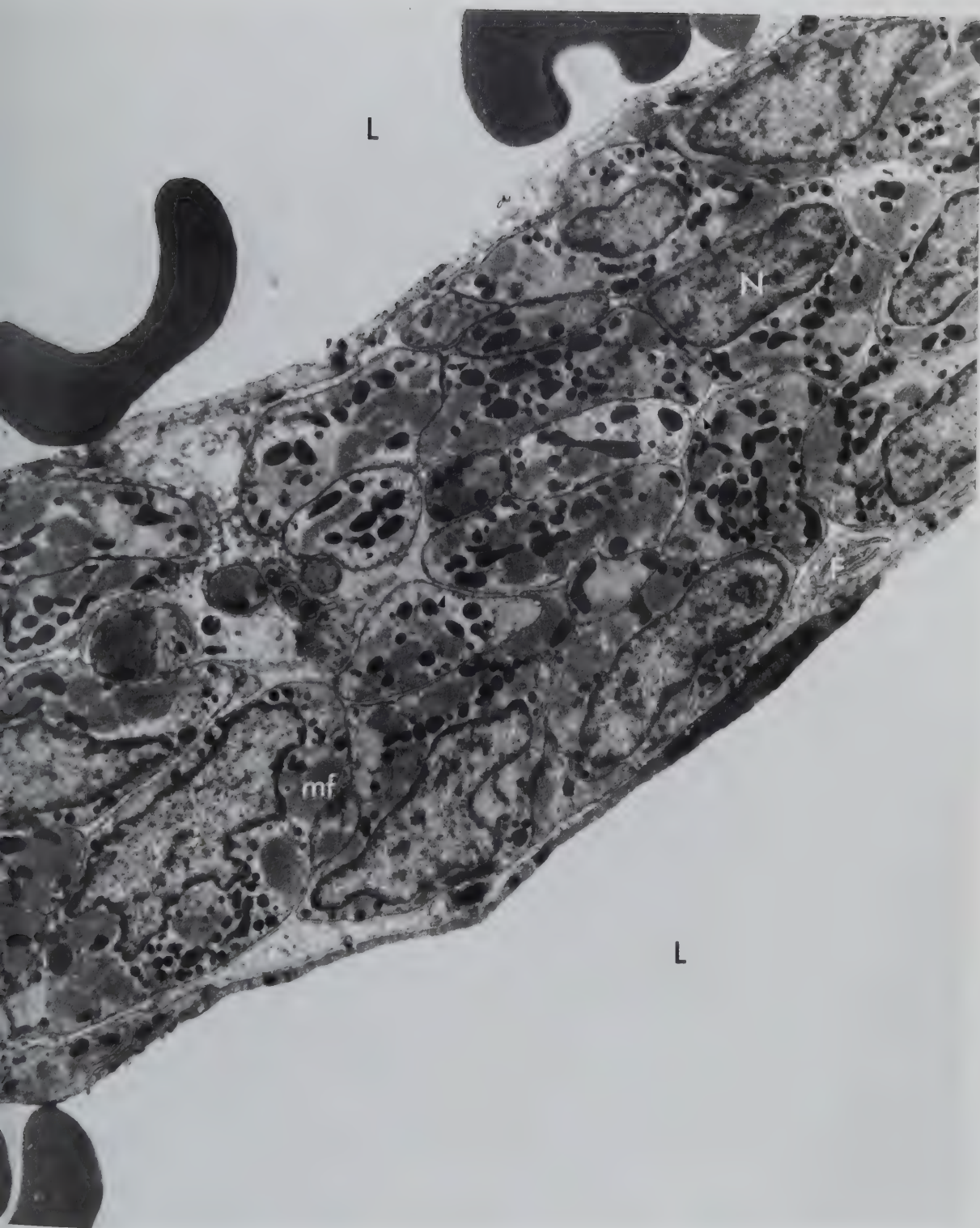


Figure 20. Fourteen day postnatal cells, oblique sections.

A. Note: Divergent orientation of myofilaments in adjacent cells. Some cells almost filled with myofilaments, others relatively more immature in appearance. x7,200

B. This is an area where the cells have very little development of myofibrils. Note: Cell-cell contacts becoming more mature (Jn). Caveolae (small black arrowheads). x7,000

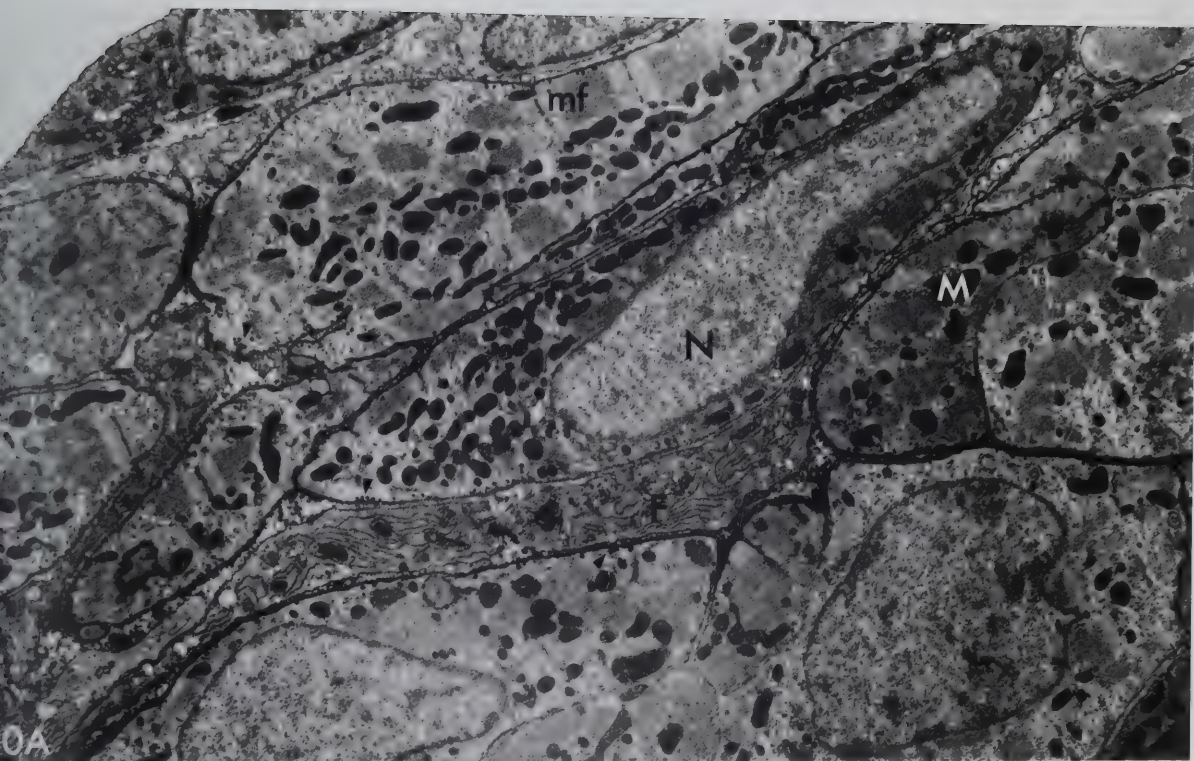


Figure 21. Fourteen day postnatal cells, transverse sections.

A. Note: Endothelial cells, encircling lumen (L) of blood vessels, still rather thick. Myofibrillar development well advanced in some cells. Granular endoplasmic reticulum (er) still abundant in some cells. x11,900.

B. Note: Degree of development of SR compared to cells seen in A. Specific granules (sg) becoming larger than those of neonatal and one week postnatal myocardial cells. Coated vesicle (white arrowhead, upper centre). Peripheral couplings (large black arrowheads) well-developed and slightly more abundant. x42,200

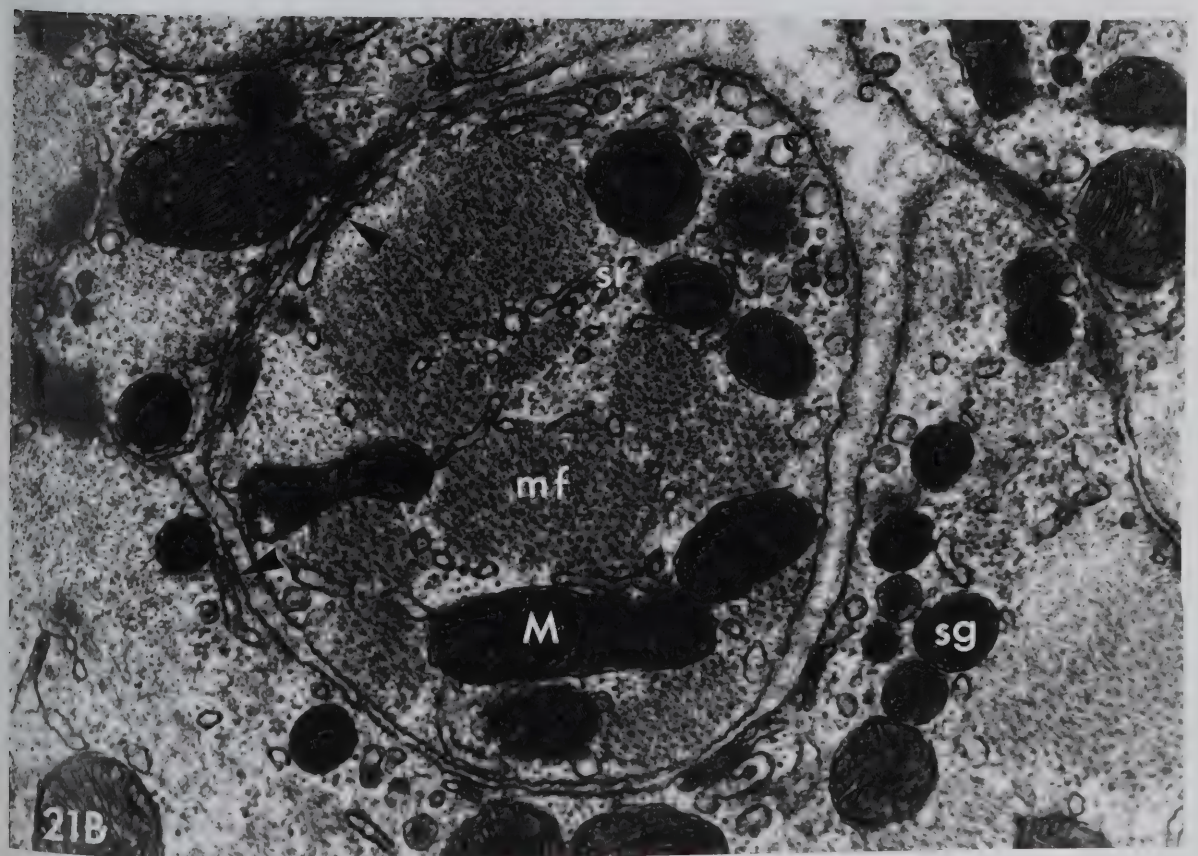
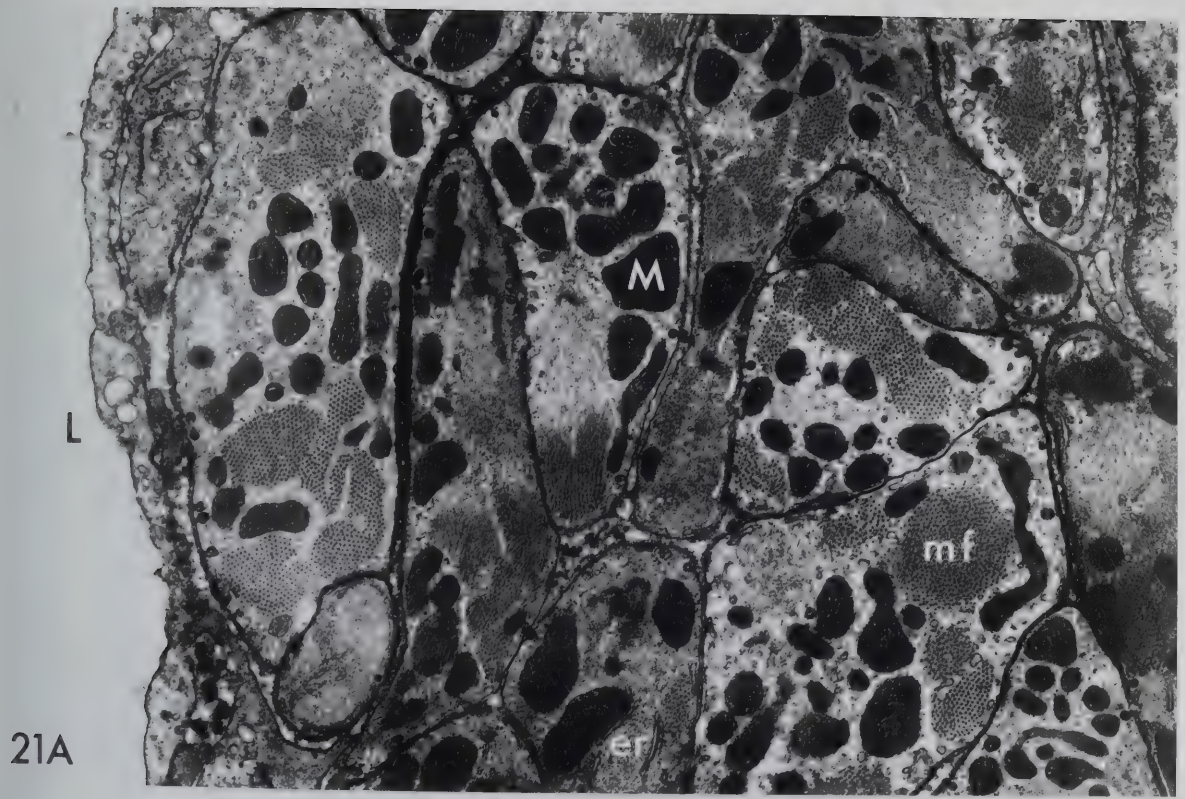


Figure 22. Fourteen day postnatal cells.

A. Transverse section. Area where myofilaments are extremely abundant, packing the cells. Note: cell at left where orientation of myofilaments is irregular. Peripheral couplings (large black arrowheads). Caveolae becoming slightly more abundant, tubular invaginations are seen more frequently. x16,700

B. Longitudinal section. Further evidence of caveolar development and tubule formation (small black arrowheads, lower left). x17,600

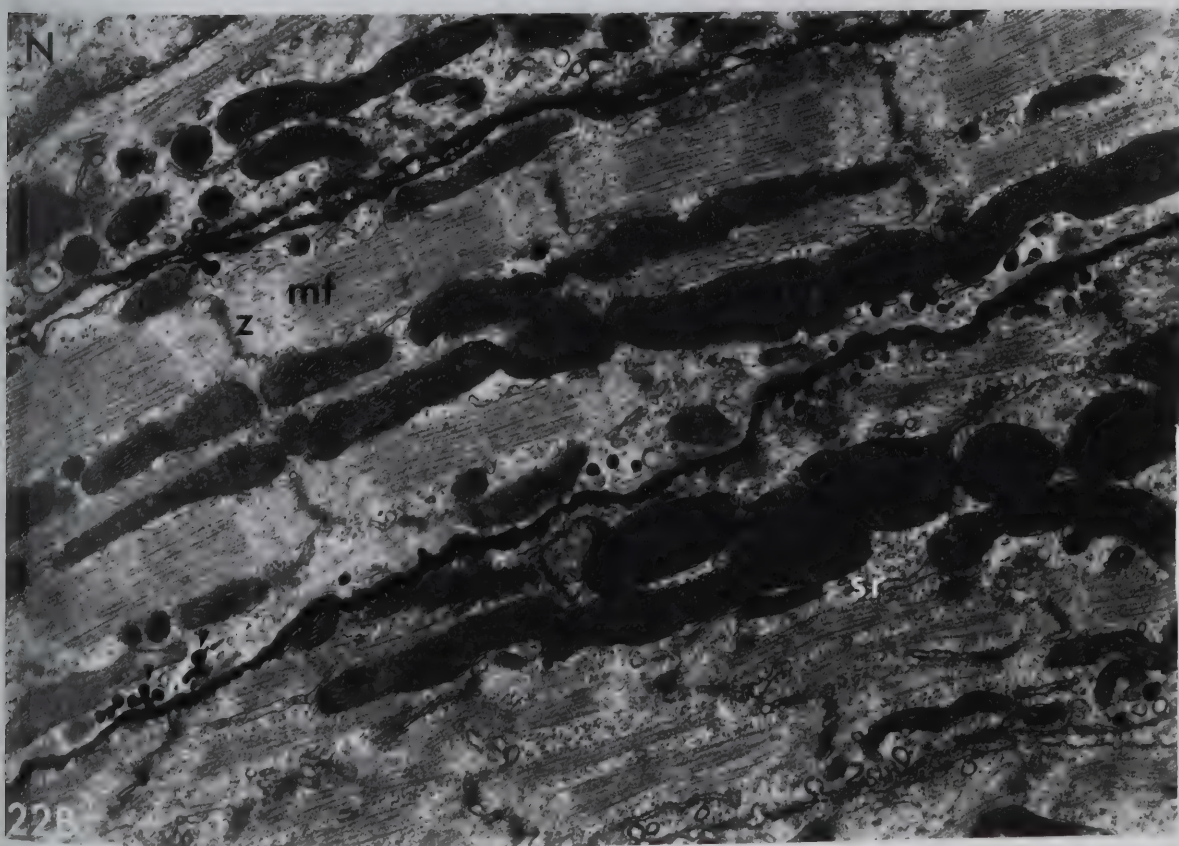
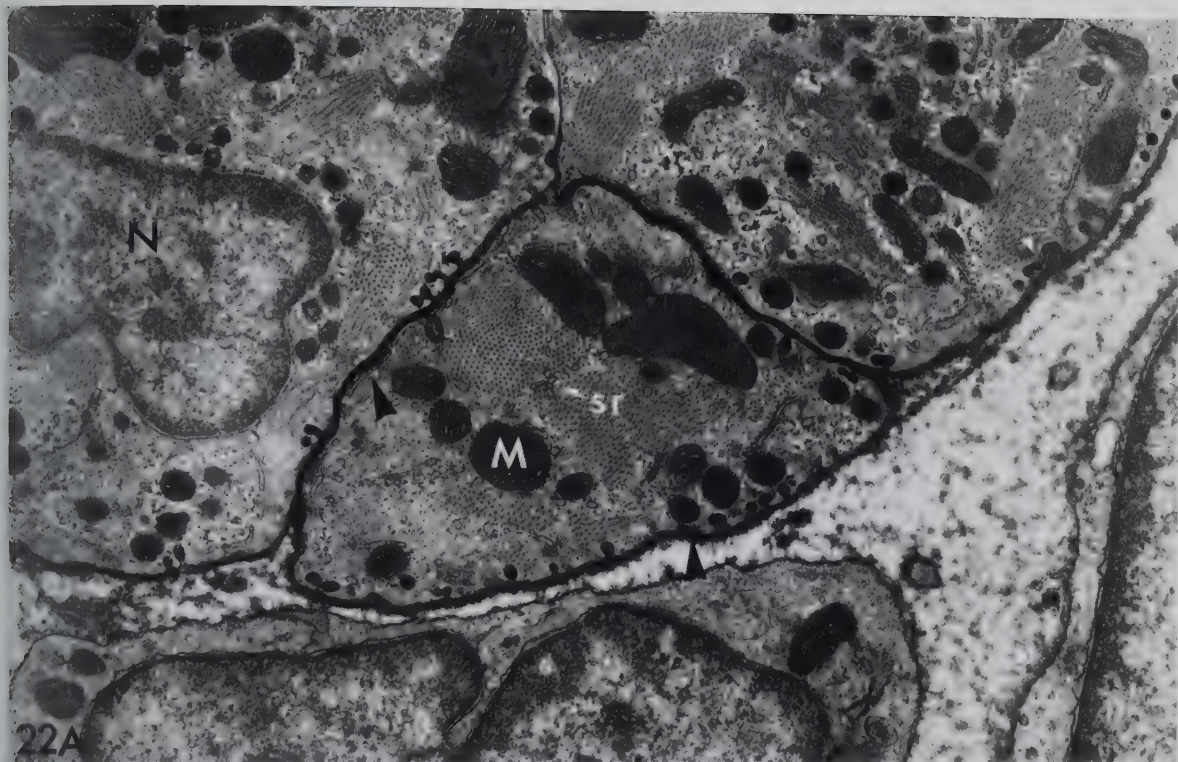


Figure 23. Sixteen day postnatal cells, oblique section. The endothelial cells at the endocardial surface (E) appear attenuated compared to the endothelial cells of the capillaries (L). Elastic fibrils (EF) as well as collagen are lying between the endocardial endothelium and the muscle cells. Myocardial cells are still not noticeably larger than earlier stages but intercellular clefts appear much reduced. Individual cells have a mature appearance, filled with myofibrillar protein. Mitochondria are generally pushed into the clefts between the myofibrils. Nuclei tend to have more regular outlines than those seen at earlier ages. Note: Tannic acid penetration superficially. Caveolae (black arrowheads) appear numerous when filled with tannic acid. x8,500

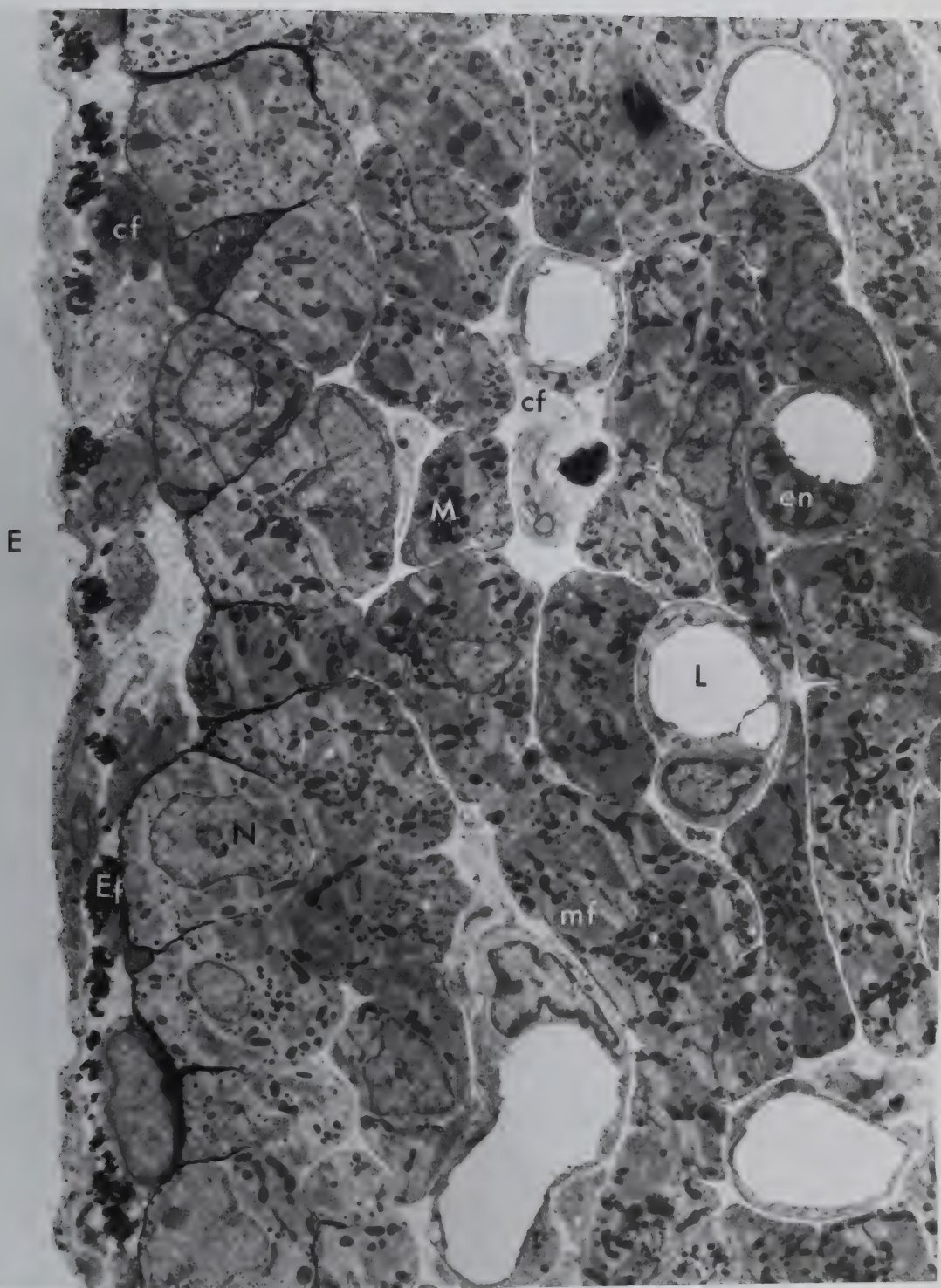


Figure 24. Sixteen day postnatal cells.

A. Oblique section. Note: myofibrillar (mF) development. Particularly note abundance of caveolae (small black arrowheads, centre and centre left). x12,600.

B. Transverse section. Sarcoplasm reticulum (SR) appears to be very well-developed around bundles of myofilaments. The bundles appear larger than those seen at earlier stages (Figure 21) incompleteness of sleeve of SR indicates branching of the myofibrils. Elements of granular endoplasmic reticulum are still relatively abundant (er). Note: caveolae (small black arrowheads, right and upper right). Particularly note abundance and large size of peripheral couplings (large black arrowheads). x53,900

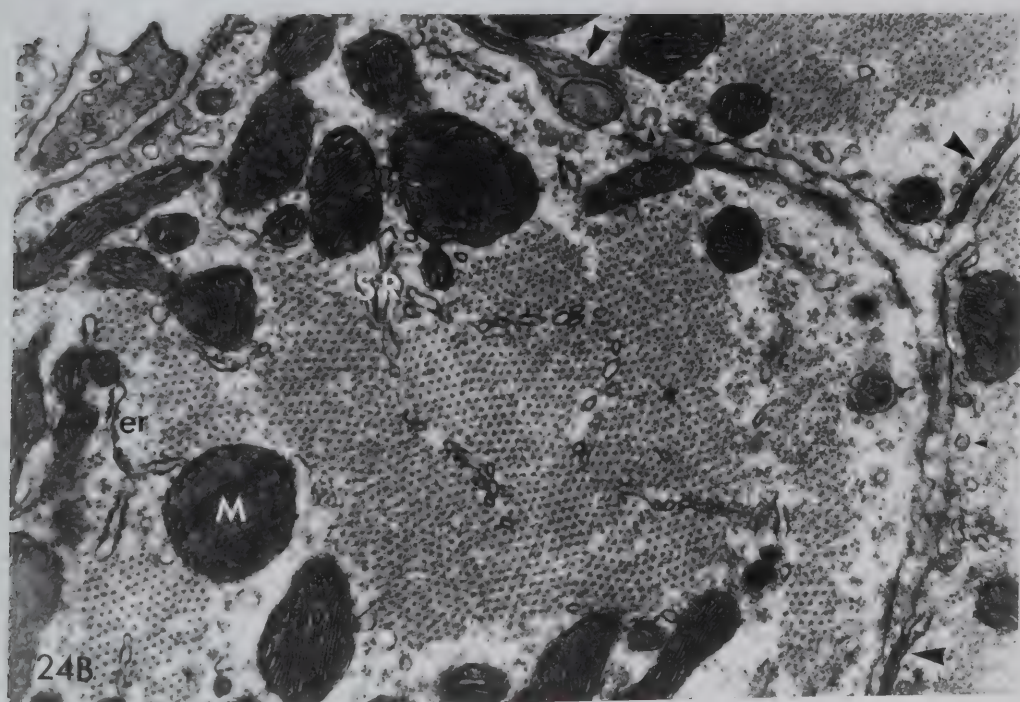
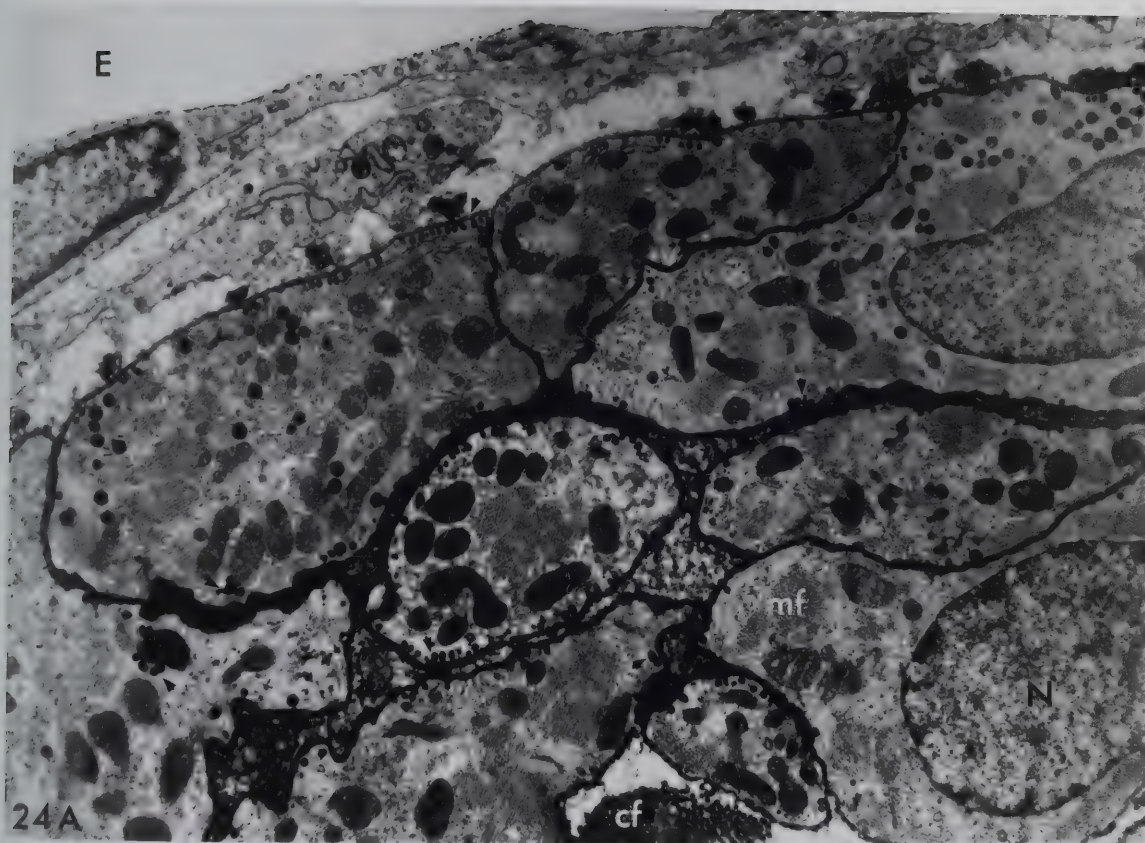


Figure 25 A and B. Sixteen day postnatal cells, oblique sections. Note: abundance and increasing complexity of sarcolemmal invaginations (small black arrowheads, centre and upper right). A. x20,300 B. x18,800

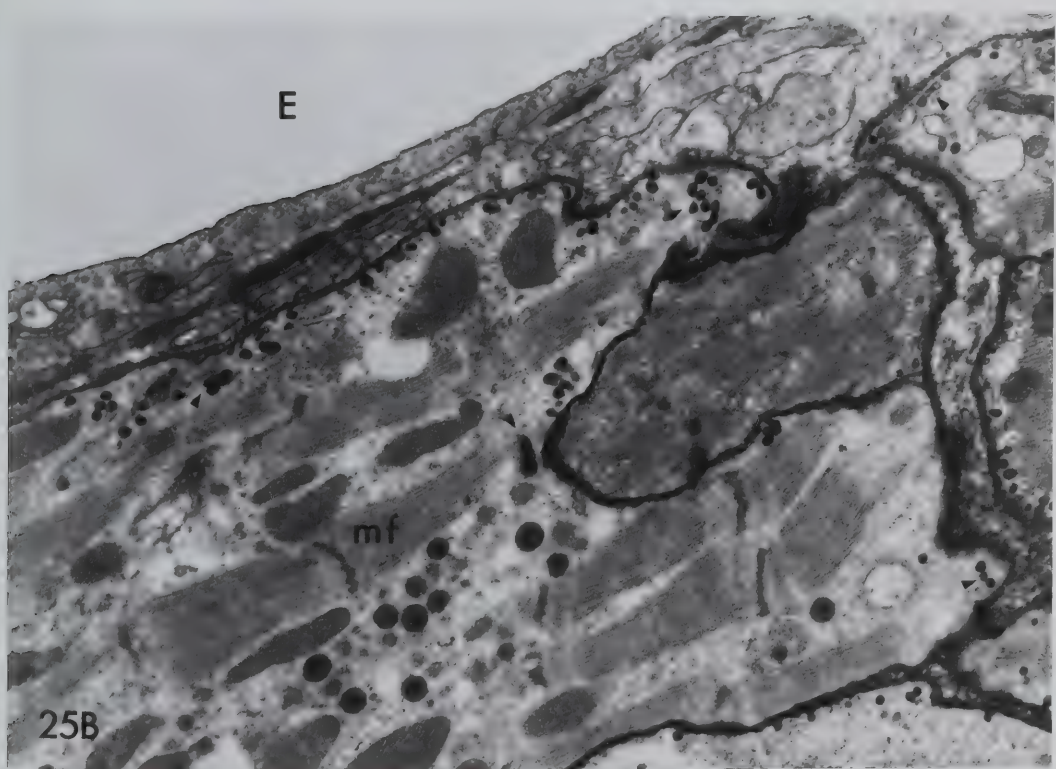
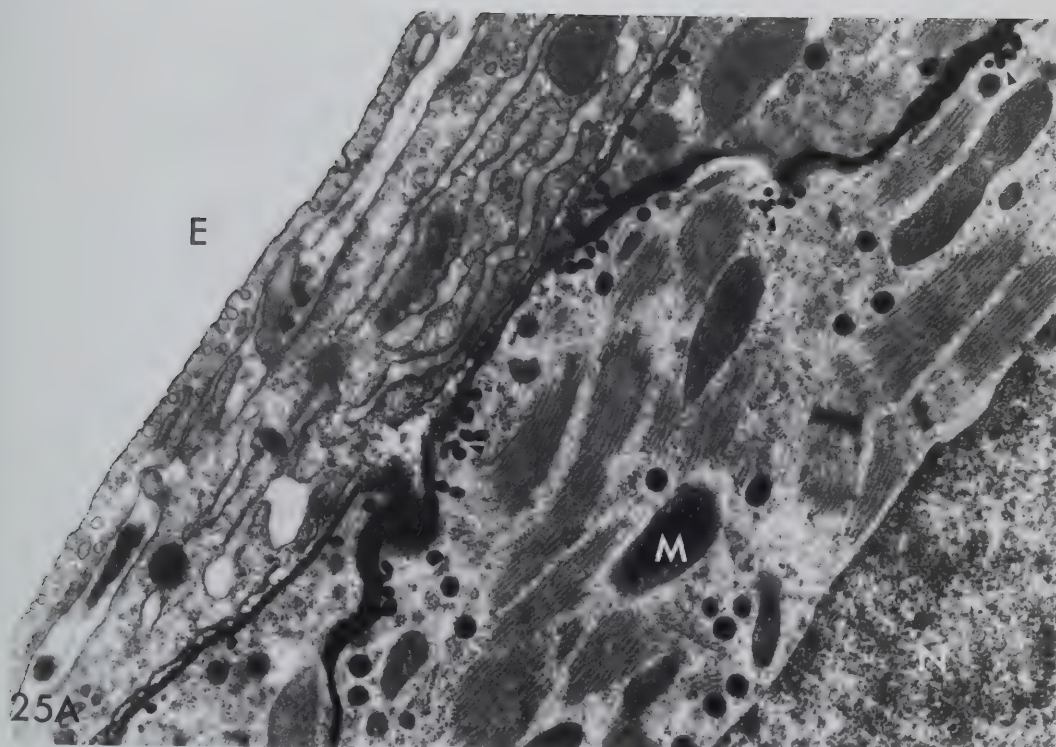


Figure 26. Sixteen day postnatal cells. A. T-tubules (TT) appear more frequently, invaginating towards Z-lines. x56,100.

B. T-tubules sometimes appear to branch x53,900.

C. Internal couplings are also more frequent, often at or near Z-lines. x19,500

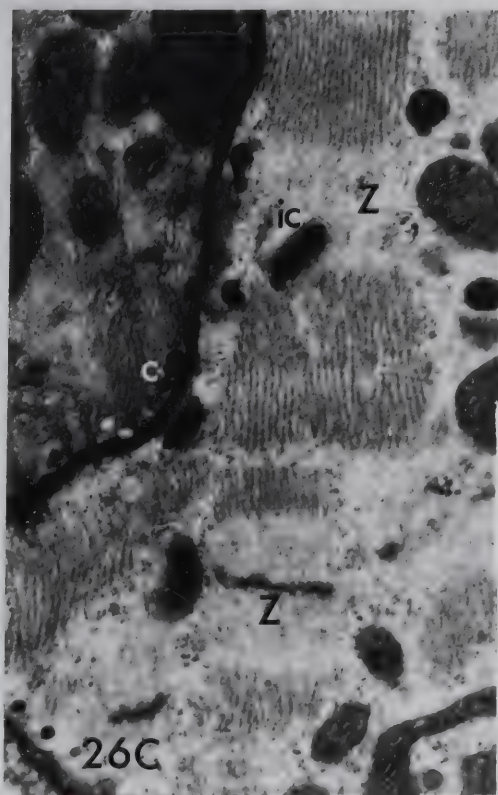
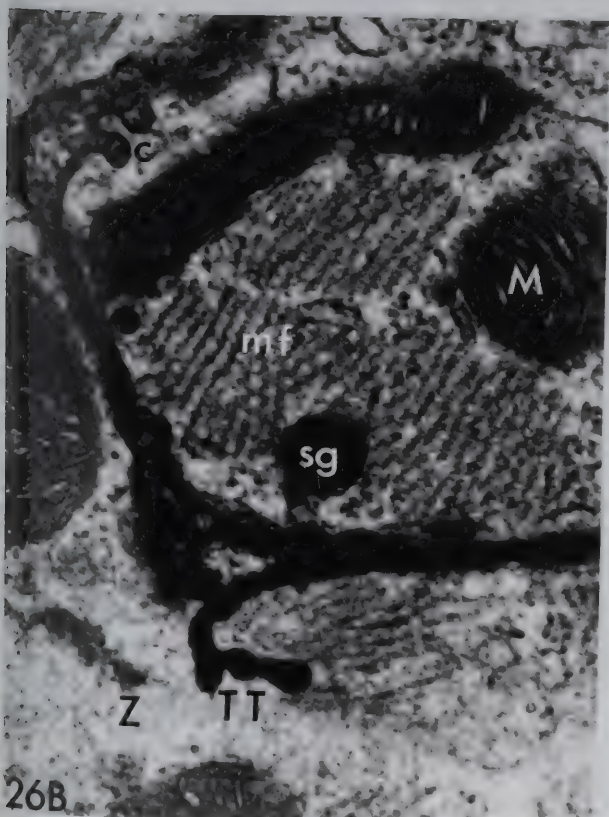
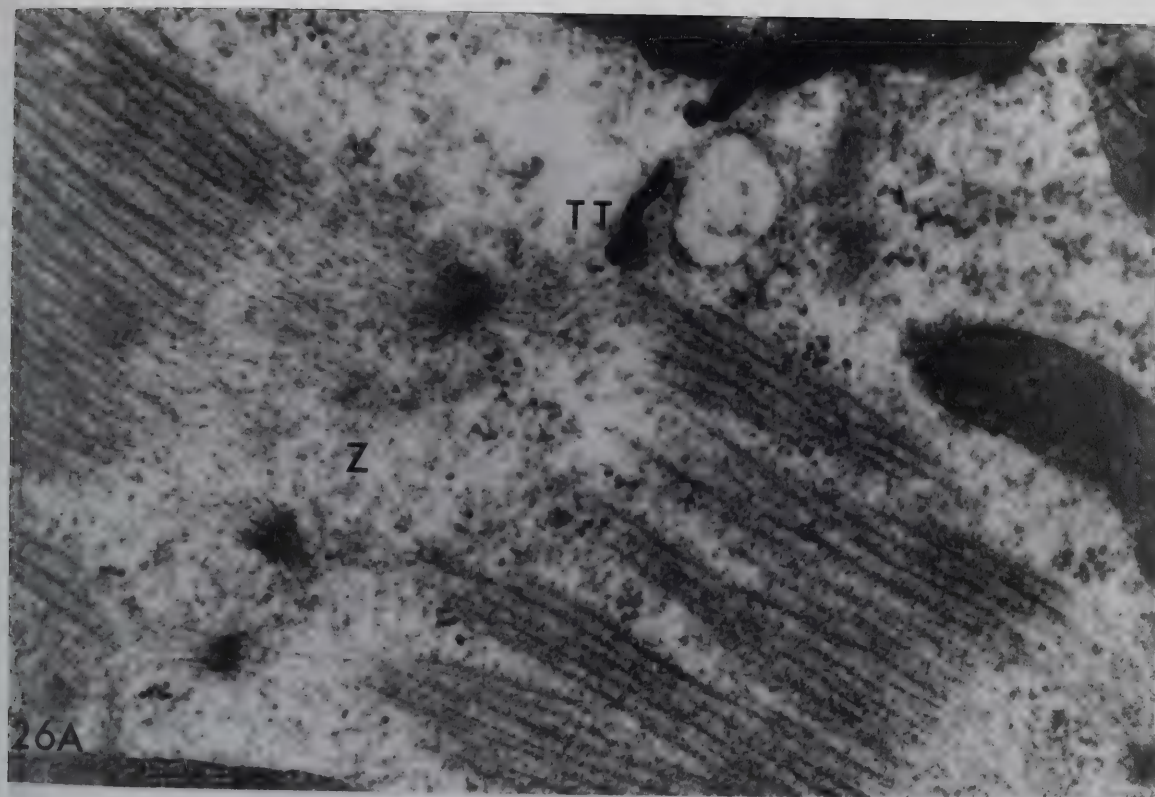


Figure 27. Eighteen day postnatal cells, longitudinal section. The individual cells are still relatively small but appear very mature. Intercellular clefts are very much reduced. Myofilaments appear to occupy most of the sarcoplasm and myofibrillar bundles are larger, tubular elements of SR are seen to be well-developed between the bundles of myofilaments. Sarcolemmal invaginations are very apparent. Note: caveolar complexes and tubular invaginations (small black arrowheads, centre right). x10,900



Figure 28. Eighteen day postnatal cells, oblique section. Endocardial endothelium (E) very much attenuated. Collagen fibrils (CF) of endomysium more robust. Fibroblasts (F) are still seen frequently. Note: abundance of caveolae (small black arrowheads, centre and upper left). x9,300



Figure 29. Eighteen day postnatal cells, transverse section.

A. At this magnification development of the SR is apparent. Note: Caveolae (small black arrowheads). Peripheral couplings (small white arrowheads) are particularly numerous. Granular endoplasmic reticulum (er) is still seen frequently, occasionally continuous with a peripheral coupling (centre of figure). x14,800

B. Similar to A. Note: Golgi apparatus (G) and associated specific granules. High degree of SR organization. Z-material in cross section (Z). Peripheral couplings (small white arrowheads). x17,900

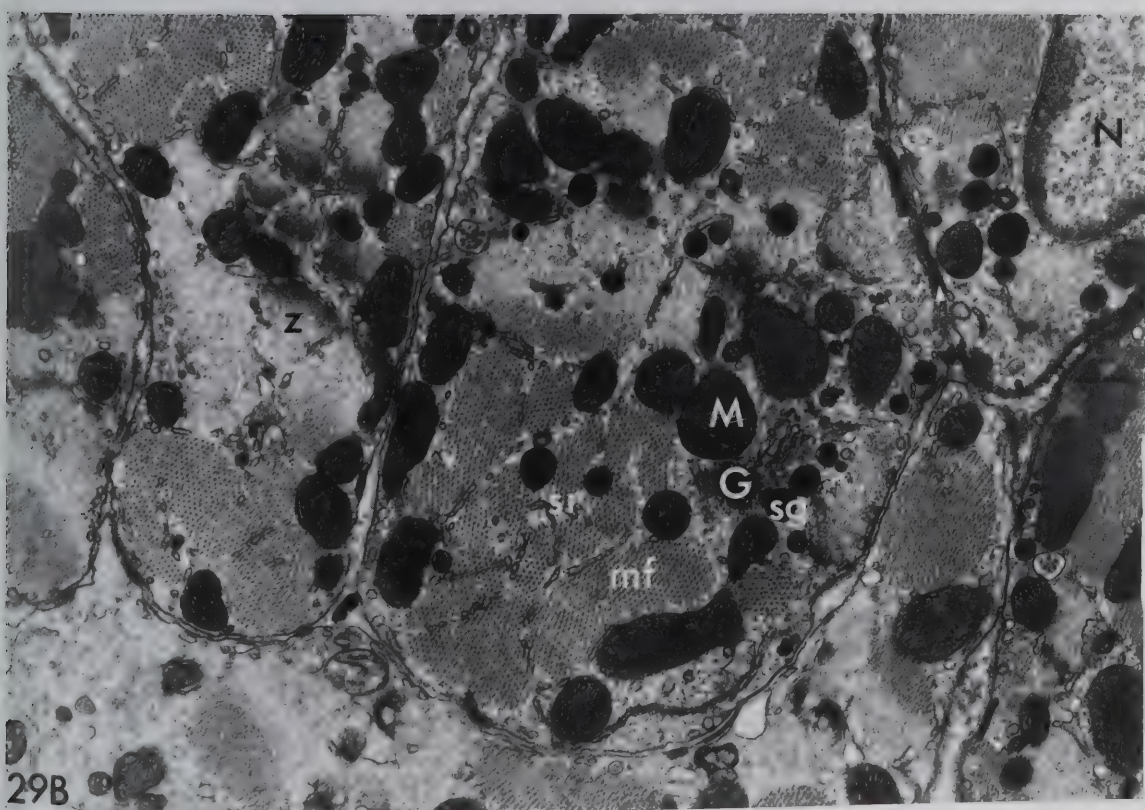
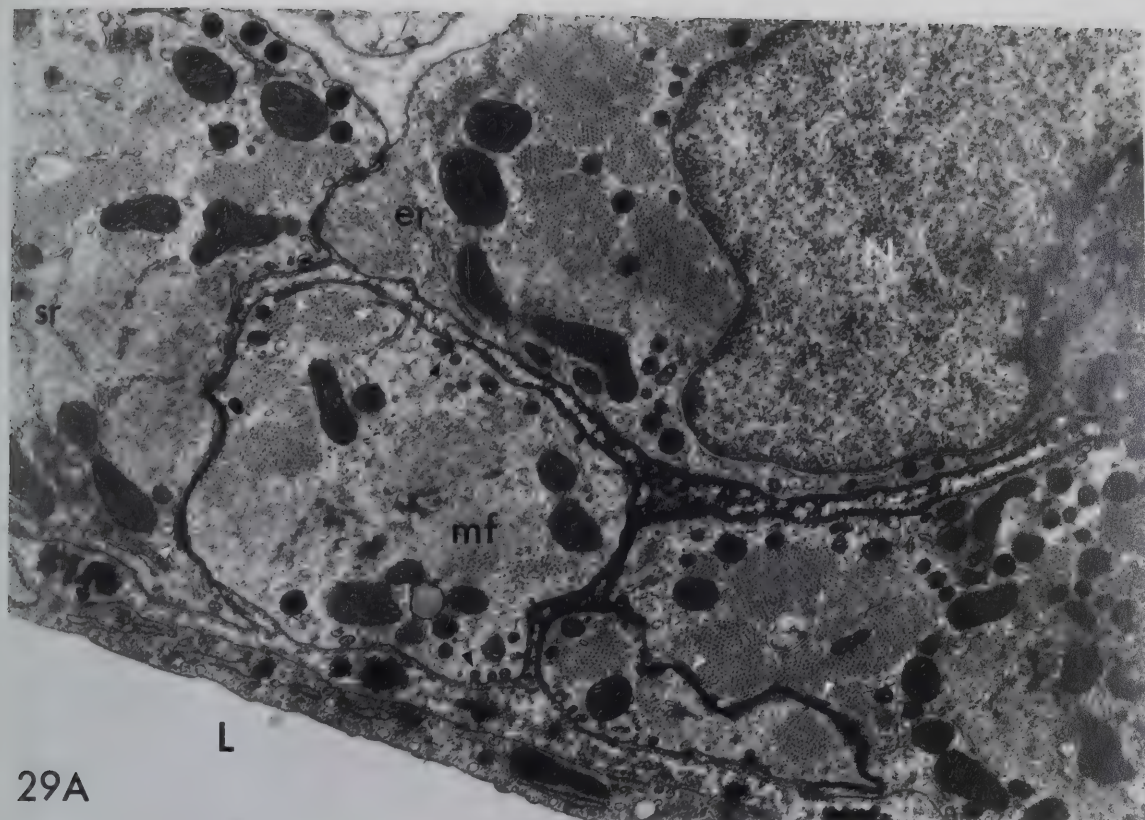


Figure 30. Eighteen day postnatal cells.

A. Oblique section. Some areas still retain a relatively immature appearance with a moderate amount of space between the cells and central areas of the cells relatively devoid of myofilaments. Note: Fibroblast activity (f) still seen. Capillary lumen (L) and thick capillary endothelial cells with micropinocytotic vesicles. Granular endoplasmic reticulum (er) abundant in some cells. Numerous caveolae (small black arrowheads). x8,400.

B. Cell with a mature appearance. Well developed and abundant myofibrils (mf) delineated by tubules of sarcoplasmic reticulum (sr). Abundance of caveolae. Note: Branching T-tubule (t) in interior of cell. x30,600

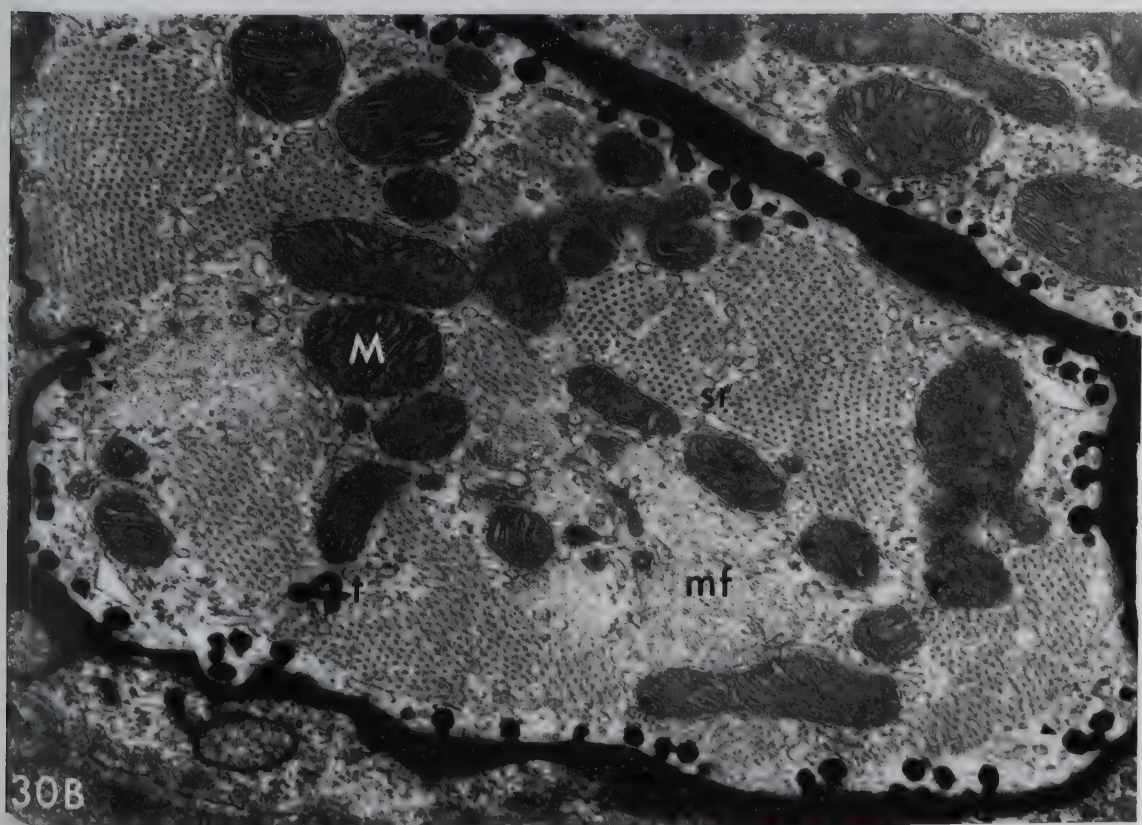
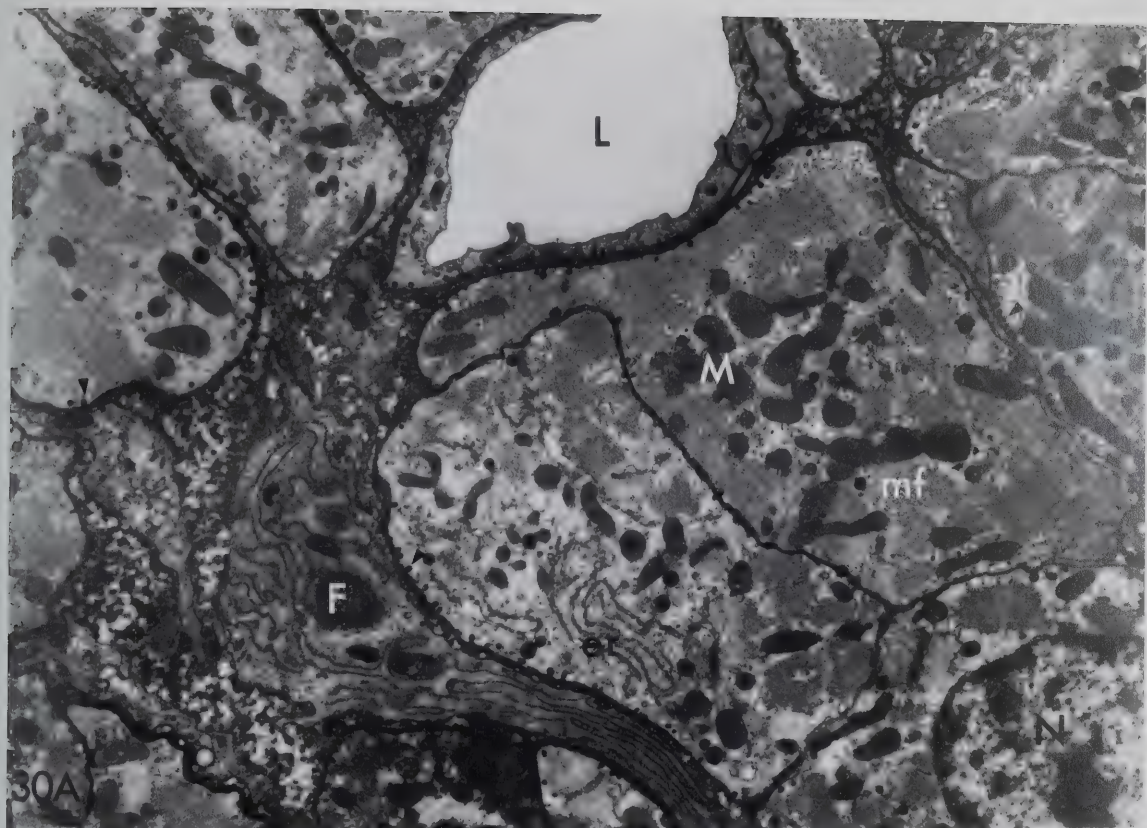


Figure 31 A and B. Eighteen day postnatal cells, oblique sections.

Note: abundant caveolae, convoluted T-tubules arising at Z-lines. Peripheral coupling at arrow.
A and B. x43,000

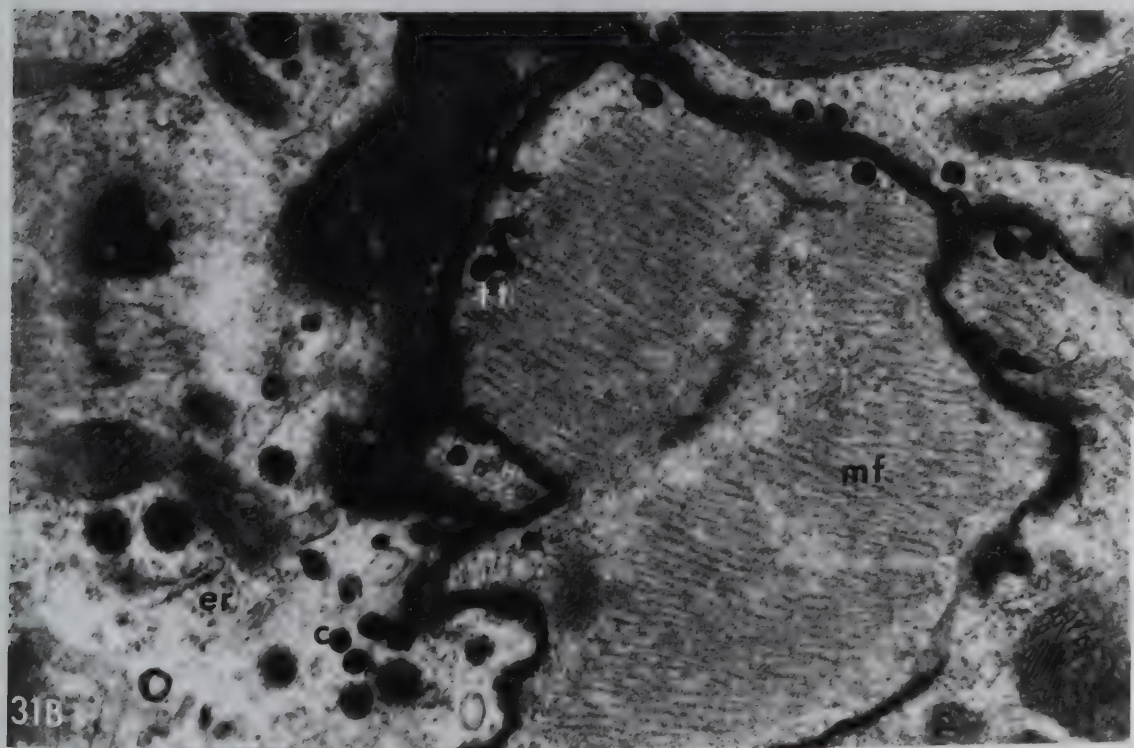
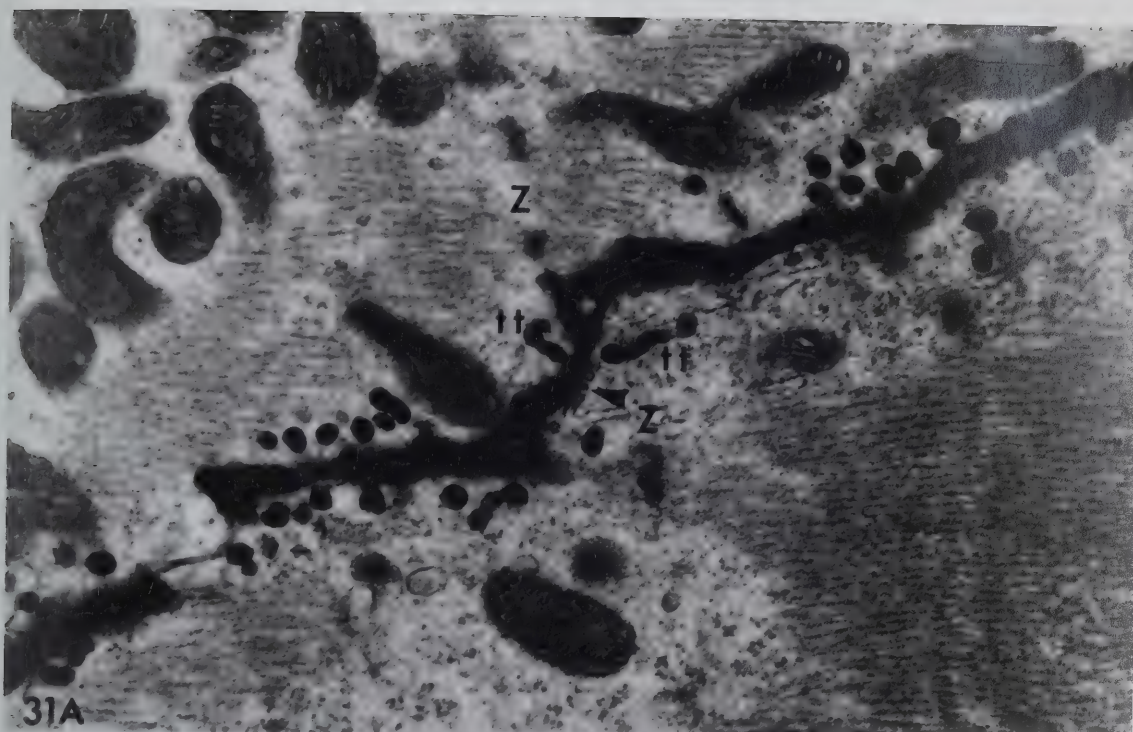


Figure 32. Eighteen day postnatal cells, oblique sections.

A. Note: T-tubule (T) appears to be giving rise to caveolae. Peripheral coupling (large black arrowhead) x43,400

B. Note: Caveolar clusters are becoming very complex (cc) and T-tubules are sometimes seen running parallel to sarcolemma (tt). x78,800

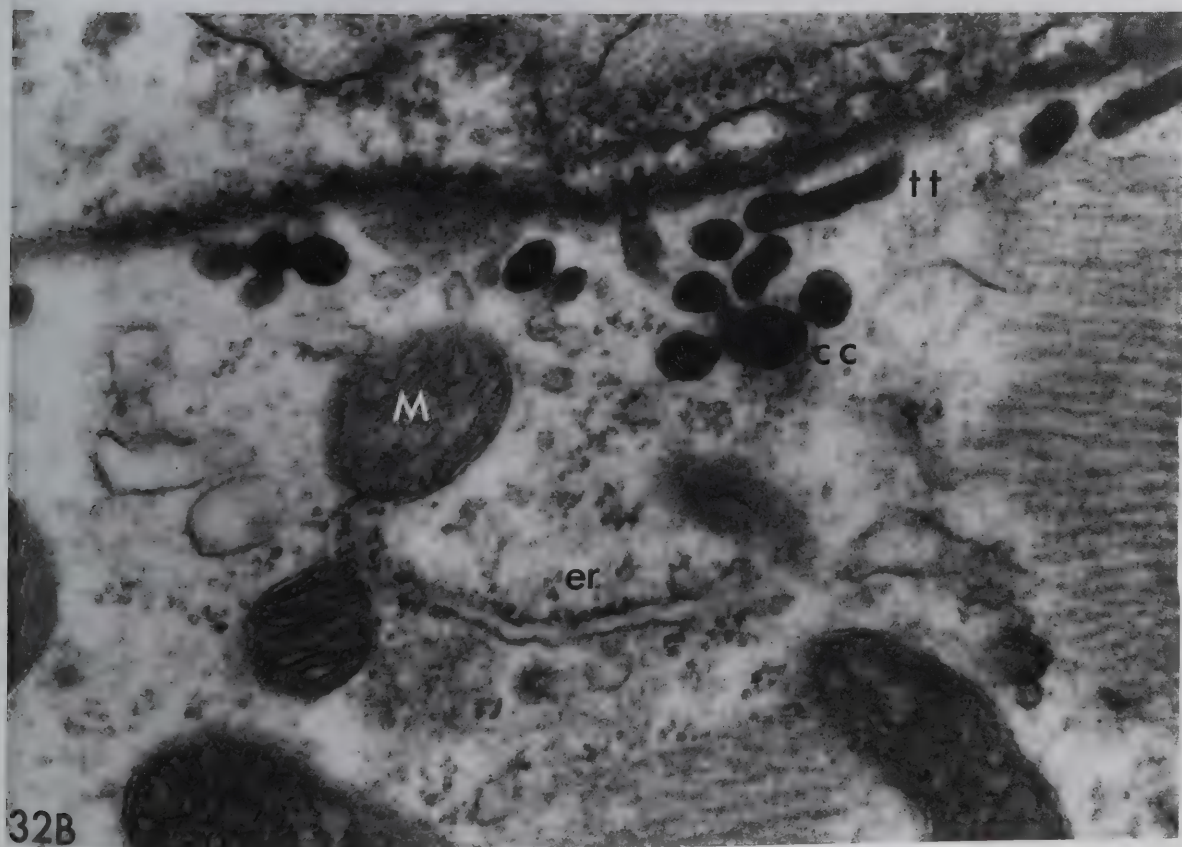
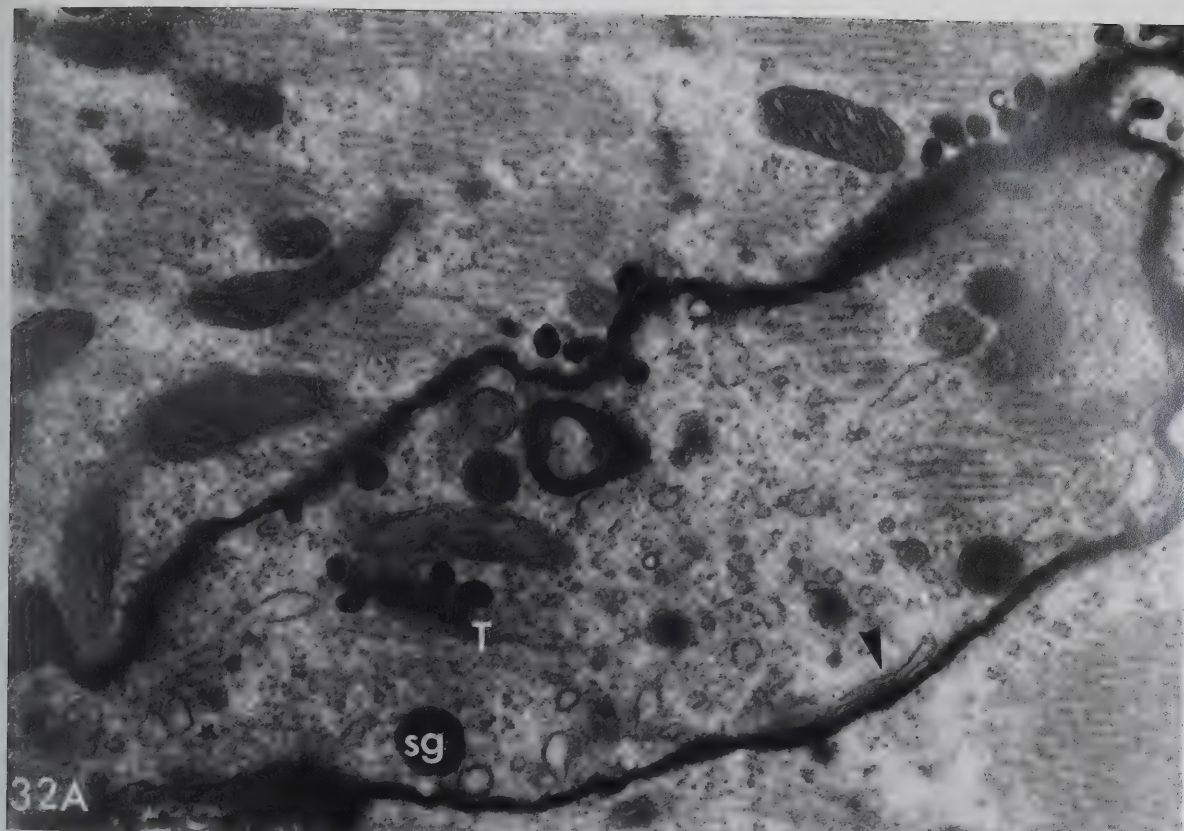


Figure 33. Twenty-one day postnatal cells, oblique sections. Cells seem slightly larger and intercellular clefts have all but disappeared. Capillary endothelial walls are still quite thick. Most of cells appear to be tightly packed with myofibrillar protein. The mitochondria are regularly arrayed, delineating the bundles of myofilaments. Sarcoplasmic reticulum cannot be distinguished at this low magnification. Fibroblasts are still active and the collagen fibrils of the endomysium are quite well developed in some areas. Most nuclear profiles appear to be quite regular in outline.

A. Note: collagen (cf) and elastic fibrils (ef) at endocardial surface (E) are particularly well developed. Aggregations of atrial granules are seen towards the central regions of some cells. x5,700

B. Note: fibroblasts (F) and robust connective tissue containing a larger blood vessel (top centre). Golgi bodies (G) are seen in the centre of several cells surrounded by specific granules. Cells in central region appear to have less abundant myofilaments. x4,400

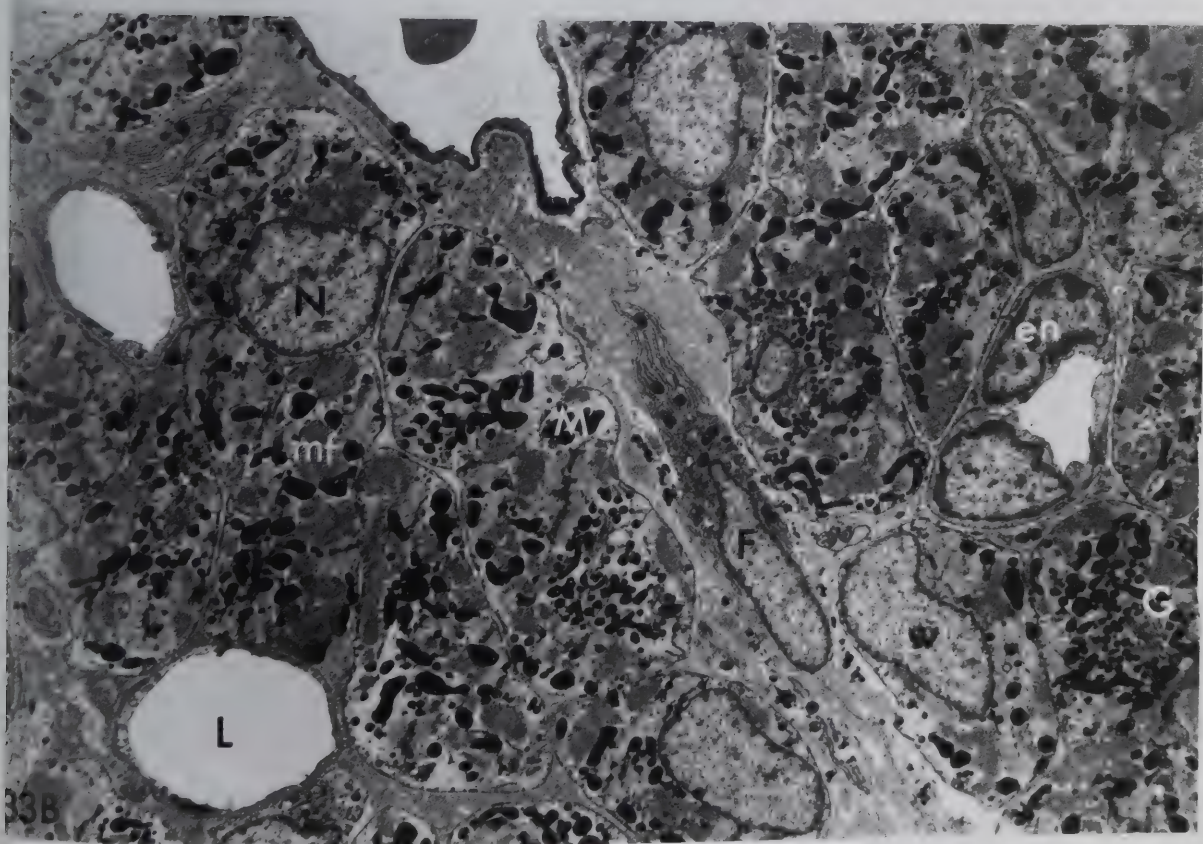


Figure 34. Twenty-one day postnatal cells, longitudinal section. Myofibrils seem of smaller diameter but fill the sarcoplasm and are clearly delineated by tubules of the SR and rows of mitochondria. The organization of the myofilaments is very regular. The sarcomeres are in register across the width of the cell. This was seen in some cells from eighteen day postnatal animals (Figure 27) but was not as regular as is seen here. Extracellular space is much reduced. x6,800

E

mf

M

N

L



Figure 35. Twenty-one day postnatal cells, transverse section. Degree of development of myofibrils and organization of the sarcoplasmic reticulum particularly well demonstrated. Peripheral couplings (pc) appear abundant and are quite large. Granular endoplasmic reticulum (er) is still relatively abundant. A. note apparent coupling between SR tubule and two caveolae (ic). Appearance of Z-disc in cross-section. x74,000

B. Note: possible T-tubule with vesicular expansion (T), this may just be a fold at the edge of the cell. x43,400

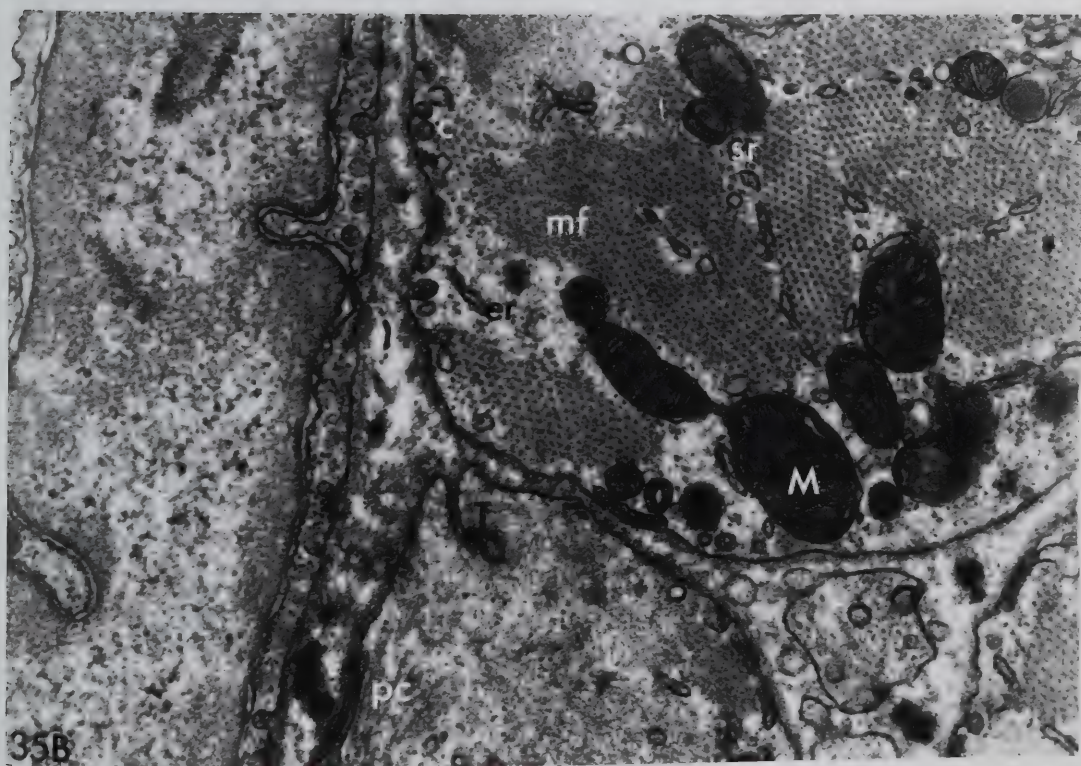
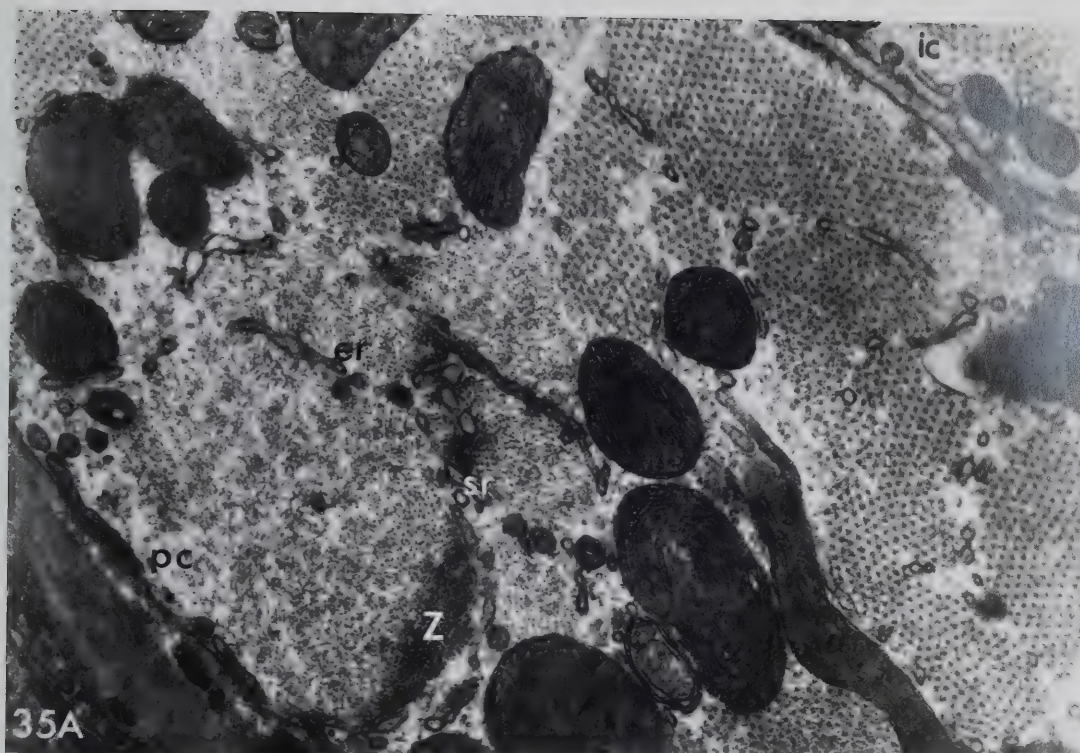


Figure 36. Twenty-one day postnatal cells.

A. Longitudinal section. Note: robust development of collagen fibrils (cf) and elastic fibres underlying the endothelial cell (E). Some of the myofibrils (MF) are becoming quite large in diameter. Cell-cell contacts are beginning to appear more like intercalated discs (In) Grazing section of sarcoplasmic reticulum (sr) showing a high degree of organization. Abundant caveolae forming clusters (cc), closely related to SR. Tubular invaginations and internal coupling (ic). x14,000

B. Note: T-tubule and well-developed dyad (ic) at a Z-line. x35,300

C. Note: Beaded shape of upper T-tubule and well-developed internal coupling (ic). The beaded shape gives the impression of a string of caveolae but may just be a convoluted tubule running in and out of the plane of section.

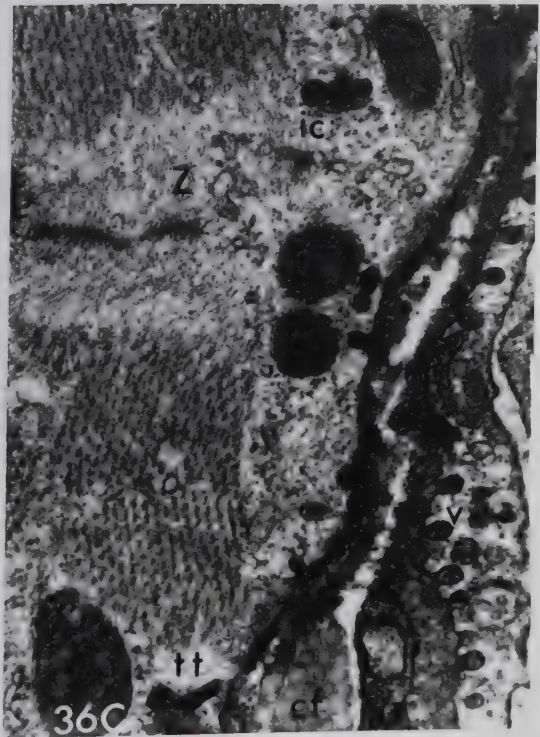
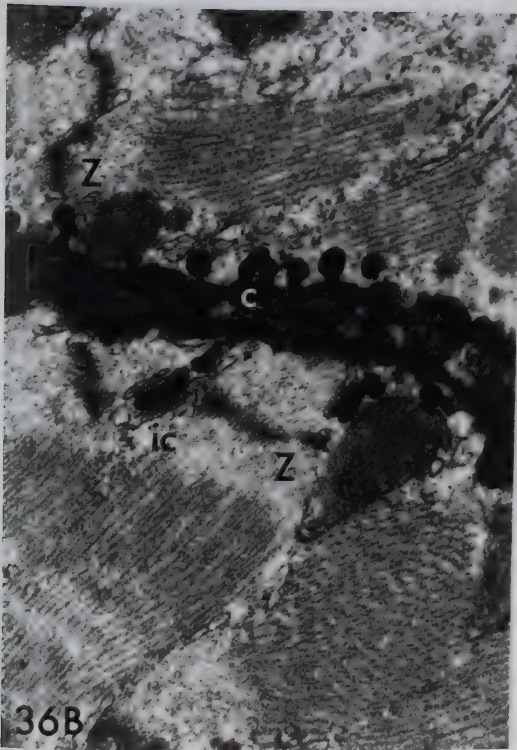
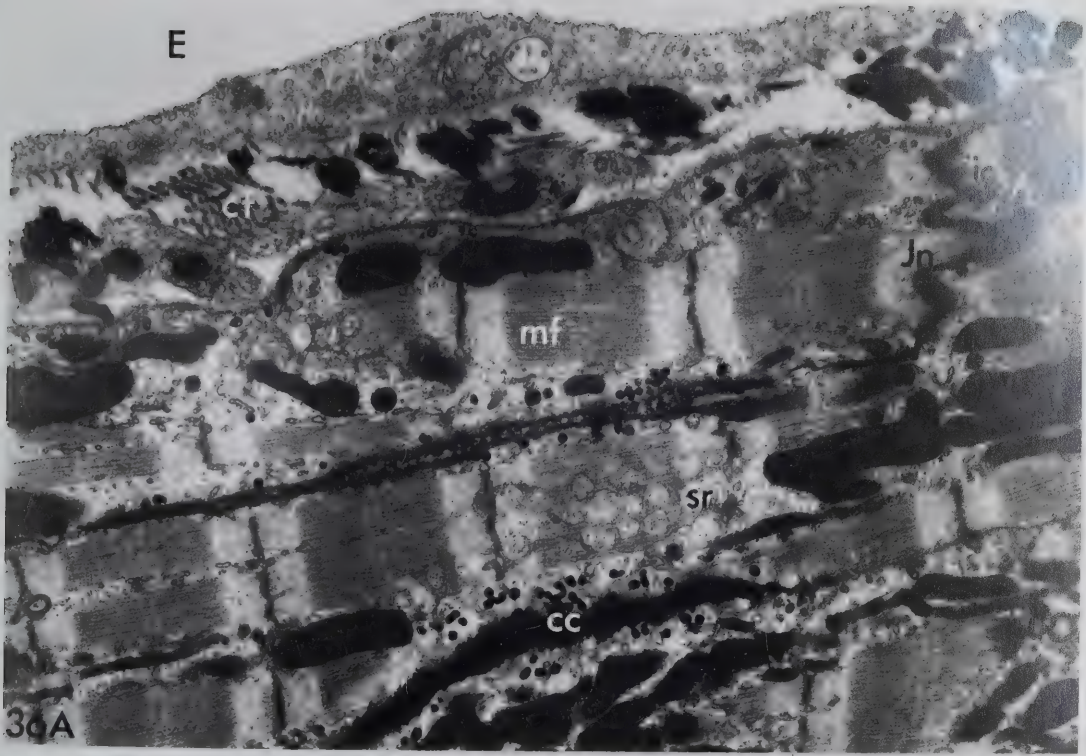


Figure 37. Diagram of a grid indicating location of the grid spaces used to obtain electron micrographs for stereology.

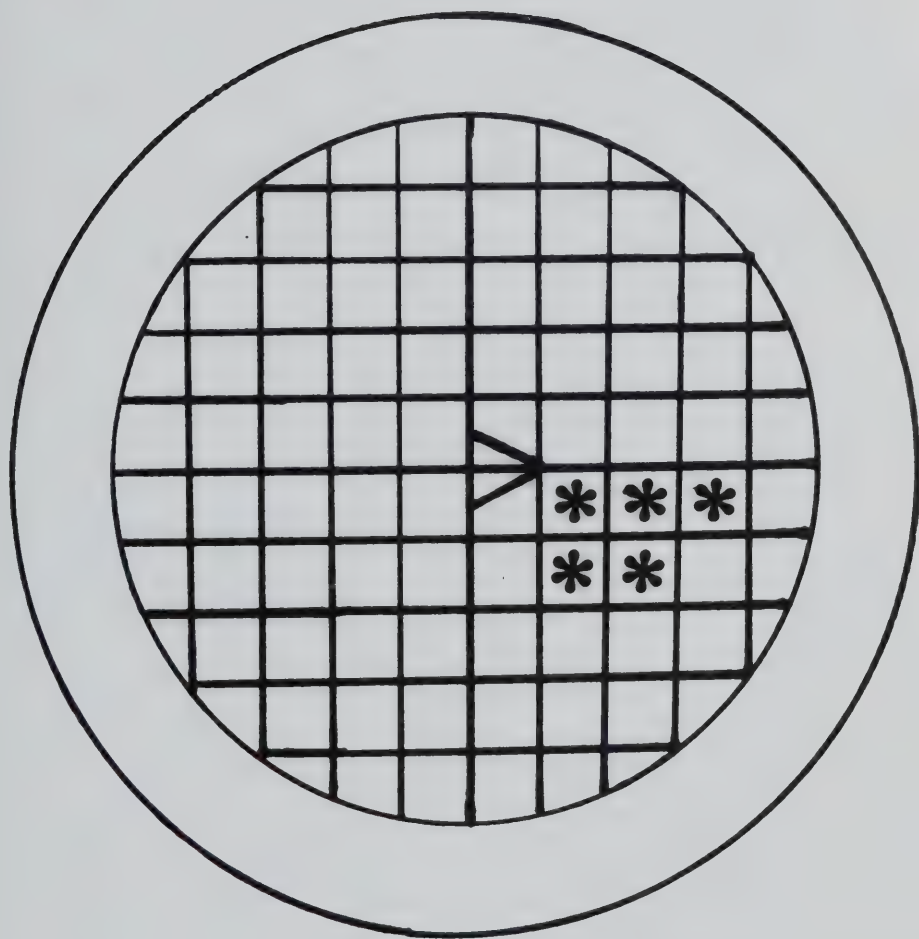


Figure 38. Plots of means and standard deviations of surface density (Sv) of caveolae and T-tubules (cav), peripheral couplings (pc) and internal couplings (ic) as a function of sarcolemmal surface for various postnatal ages. (*= $p < .01$, †= $p < .01$, ‡= $p < .01$).

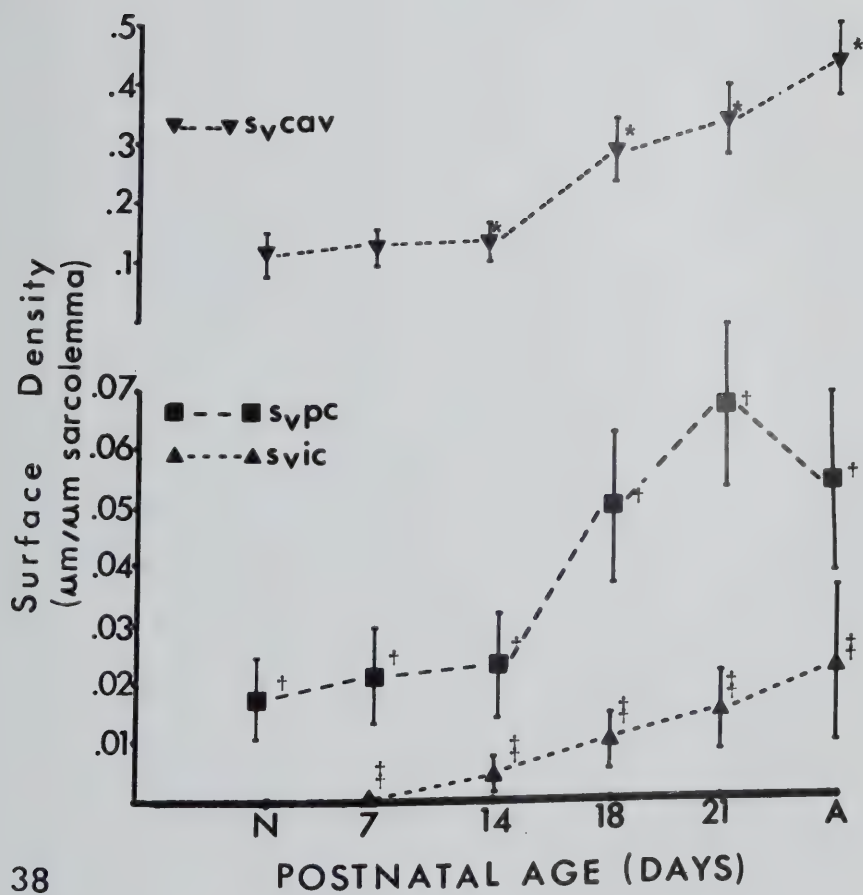


Figure 39. Plots of the means and standard deviations for the volume density of the myofibrillar protein (in % of cell area) and cell diameters (in μm .) as a function of postnatal age. Values were obtained from Table 3. (*= $p < .01$, **= $p < .01$, ‡= $p < .01$).

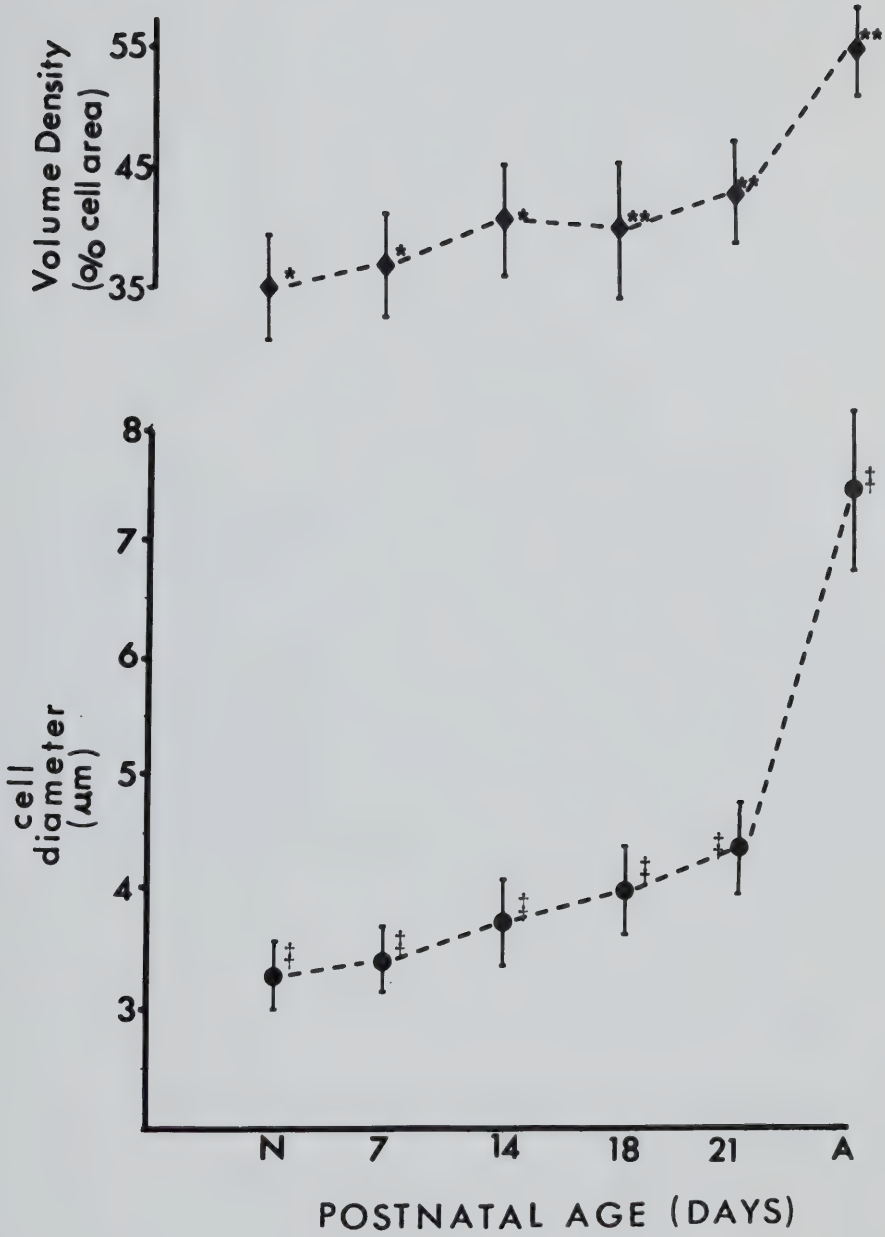


Figure 40. The MOP-3 digitizer manufactured by Carl Zeiss
Ltd.



156

BIBLIOGRAPHY

1. Adams, R. J., Schwartz, A. Comparative Mechanisms for Contraction of Cardiac and Skeletal Muscle. Chest 78 Suppl.1 123-139 (1980)
2. Adrian, R. H. Charge Movement in the Membrane of Striated Muscle. Ann. Rev. Biophys. Bioeng. 7 85-112 (1978)
3. Anderson, P. A. W., Manring, A., Sommer, J. R., Johnson, E. A. Cardiac Muscle: An Attempt to Relate Structure to Function. J. Mol. Cell. Cardiol. 8 123-143 (1976)
4. Anderson, R. H., Ho, S. W., Smith, A., Becker, A. E. The Internodal Atrial Myocardium. Anat. Record 201 75-82 (1981)
5. Anversa, P., Olivetti, G., Loud, A. V. Morphometric Study of Early Postnatal Development in the Left and Right Ventricular Myocardium of the Rat. I: Hypertrophy, Hyperplasia and Binucleation of Myocytes. Circ'n. Res. 46 495-502 (1980)
6. Anversa, P., Olivetti, G., Melissari, M., Loud, A. V. Stereological Measurement of Cellular and Subcellular Hypertrophy and Hyperplasia in the Papillary Muscle of the Adult Rat. J. Mol. Cell. Cardiol. 12 781-795 (1980)
7. Anversa, P., Vitali- Mazza, L., Loud, A. V. Morphometric and Autoradiographic Study of Developing Ventricular and Atrial Myocardium in Fetal Rats. Lab. Invest. 33 696-705 (1975)
8. Ashraf, M., Halverson, C. Structural Changes in the Freeze-fracture of the Sarcolemma of the Myocardium. Am. J. Pathol. 88 583-594 (1977)
9. Avanzino, G. L., Bianchi, D., Calligaro, A., Ermirio, R., Fisher, M. Morphological Aspects of the Crista Terminalis in the Rabbit Right Atrium. J. Physiol. 313 7P (1981)
10. Ayettey, A. S., Navaratnam, V. The T-tubule System in the Specialized and General Myocardium of the Rat. J. Anat.

127 125-140 (1978)

11. Bastian, J., Nakajima, S. Action Potential in the Transverse Tubules and its Role in the Activation of Skeletal Muscle. *J. Gen. Physiol.* 63 257-271 (1974)
12. Bers, D. M., Philipson, K. D., Langer, G. A. Cardiac Contractility and Sarcoplasmic Calcium Binding in Several Cardiac Muscle Preparations. *Am. J. Physiol.* 240 H576-H583 (1981)
13. Boland, R., Martonosi, A., Tillack, T. W. Developmental Changes in the Composition of Sarcoplasmic Reticulum. *J. Biol. Chem.* 249 612-623 (1974)
14. Bonilla, E. Staining of the Transverse Tubular System of Skeletal Muscle by Tannic Acid- Gluteraldehyde Fixation. *J. Ultrastruct. Res.* 58 162-165 (1977)
15. Bossen, E. H., Sommer, J. R., Waugh, R. A. Comparative Stereology of the Mouse and Finch Left Ventricle. *Tiss. Cell.* 10 773-784 (1978)
16. Bossen, E. H., Sommer, J. R., Waugh, R. A. Comparative Stereology of Mouse Atria. *Tiss. Cell.* 13 71-77 (1981)
17. Briarty, L. G. Stereology: Methods for Quantitative Light and Electronmicroscopy. *Sci. Prog., Oxf.* 62 1-32 (1975)
18. Brunschwig, J. P., Brandt, N., Caswell, A. H., Lukeman, D. S. Ultrastructural Observations of Isolated Intact and Fragmented Junctions of Skeletal Muscle by use of Tannic Acid Mordanting. *J. Cell Biol.* 93 533-542 (1982)
19. Cadwell, J. J. S., Caswell, A. H. Identification of a Constituent of the Junctional Feet Linking Terminal Cisternae to T-tubules in Skeletal Muscle. *J. Cell Biol.* 93 543-550 (1982)
20. Cantin, M., Tantu, C., Bullack, M., Yunge, L., Benchimol, S., Beuzeron, J. Ultrastructural Cytochemistry of Atrial Muscle Cells IX. Reactivity of Specific Granules in Cultured Cardiac Myocytes. *J. Mol. Cell Cardiol.* 12 1033-1051 (1980)

21. Cantin, M., Timm-Kennedy, M., El-Khatib, E., Huet, M., Yunge, L. Ultrastructural Cytochemistry of Atrial Muscle Cells VI. Comparative Study of Specific Granules in Right and Left Atrium of Various Animal Species. *Anat. Rec.* 193 55-70 (1979)
22. Caswell, A. H., Brandt, N. R. Ion-Induced Release of Calcium from Isolated Sarcoplasmic Reticulum. *J. Memb. Biol.* 58 21-33 (1981)
23. Caswell, A. H., Lau, Y. H., Garcia, M., Brunschwig, J-P. Recognition and Junction Formation by Isolated Transverse Tubules and Terminal Cisternae of Skeletal Muscle. *J. Biol. Chem.* 254 202-208 (1979)
24. Chacko, K. J. Observations on the Ultrastructure of the Developing Myocardium of Rat Embryos. *J. Morph.* 150 681-710 (1976)
25. Challice, C. E., Virágh, S. Origin and Differentiation of Cardiac Muscle Cells in the Mouse. *J. Ultrastruct. Res.* 42 1-24 (1973)
26. Challice, C. E., Virágh, S. The Architectural Development of the Early Mammalian Heart. *Tissue Cell* 6 447-462 (1973)
27. Challice, C. E., Virágh, S. (Eds.) *Ultrastructure of the Mammalian Heart.* Academic Press, N. Y. (1974)
28. Chapman, R. A. Excitation-Contraction Coupling in Cardiac Muscle. *Prog. Biophys. Med. Biol.* 35 1-52 (1979)
29. Claycomb, W. C. Cardiac Muscle Hypertrophy. Differentiation and Growth of the Heart Cell During Development. *Biochem. J.* 168 599-601 (1977)
30. Couttenye, M. M., DeClerck, N. M., Goethals, M. A., Brutsaert, D. L. Relaxation Properties of Mammalian Heart Muscle. *Circ'n. Res.* 48 352-356 (1981).
31. David, H., Meyer, R., Marx, I., Guski, H., Wenzelidis, K. Morphometric Characterization of Left Ventricular Cells of Male Rats During Postnatal Development. *J. Mol. Cell. Cardiol.* 11 631-638 (1979)

32. Devine, C. E., Somlyo, A. V., Somlyo, A. P. Sarcoplasmic Reticulum and Excitation-Contraction Coupling in Mammalian Smooth Muscles. *J. Cell. Biol.* 52 690-718 (1972)
33. Dhalla, N. S., Sulakhe, P. V., Lee, S. E., Singal, P. K., Varley, K. G., Yates, J. G. Subcellular Ca^{2+} Transport in Different Areas of Dog Heart. *Can. J. Physiol. Pharmacol.* 58 360-367 (1980)
34. Dulhunty, A. F., Franzini-Armstrong, C. The Relative Contributions of the Folds and Caveolae to the Surface Membrane of Frog Skeletal Muscle Fibers at Different Sarcomere Lengths. *J. Physiol.* 250 513-539 (1975)
35. Edge, M. B. Development of Apposed Sarcoplasmic Reticulum and the T-system and the Change in Orientation of Triads in Rat Skeletal Muscle. *Dev. Biol.* 23 634-650 (1970)
36. Eisenberg, B. R., Gilai, A. Structural Changes in Single Muscle Fibers After Stimulation at a Low Frequency. *J. Gen. Physiol.* 74 1-16 (1979)
37. Eisenberg, B. R., Eisenberg, R. S. The T-SR Junction in Contracting Single Skeletal Muscle Fibers. *J. Gen. Physiol.* 79 1-16 (1982)
38. Eisenberg, B. R., Kuda, A. M., Peter, J. B. Stereological Analysis of Mammalian Skeletal Muscle. Part 1, Soleus Muscle of the Adult Guinea Pig. *J. Cell Biol.* 60 732-754 (1974)
39. Elias, H., Hennig, A., Schwartz, D. E. Stereology: Applications to Biomedical Research. *Physiol. Rev.* 51 158-200 (1971)
40. Elias, H., Hyde, D. M. An Elementary Introduction to Stereology (Quantitative Microscopy). *Am. J. Anat.* 159 411-446 (1980)
41. Emberson, J. W., Challice, C. E. Studies on the Impulse Conducting Pathways in the Atrium of the Mammalian Heart. *Am. Ht. J.* 79 653-667 (1970)

42. Endo, M. Calcium Release from the Sarcoplasmic Reticulum. *Physiol. Rev.* 57 71-108 (1977)
43. Ezerman, E. B., Ishikawa, H. Differentiation of the Sarcoplasmic Reticulum and T-system in Developing Chick Skeletal Muscle *in vitro*. *J. Cell Biol.* 35 405-420 (1967)
44. Fabiato, A. Fluorescence and Differential Light Absorption Recordings with Calcium Probes and Potential Sensitive Dyes in Skinned Cardiac Cells. *Can. J. Physiol. Pharmacol.* 60 556-567 (1982)
45. Fabiato, A. Calcium Release in Skinned Cardiac Cells: Variations with Species, Tissues and Development. *Fed. Proc.* 41 2238-2244 (1982)
46. Fabiato, A., Fabiato, F. Calcium-Induced Release of Calcium from the Sarcoplasmic Reticulum of Skinned Cells from Adult Human, Dog, Cat, Rabbit, Rat and Frog Hearts and from Fetal and Newborn Rat Ventricles. *Ann. N.Y. Acad. Sci.* 307 491-522 (1978)
47. Fabiato, A., Fabiato, F. Use of Chlorotetracycline Fluorescence to Demonstrate Ca^{2+} -Induced Release of Ca^{2+} from the Sarcoplasmic Reticulum of Skinned Cardiac Cells. *Nature* 281 146-148 (1979)
48. Fabiato, A., Fabiato, F. Calcium and Cardiac Excitation-Contraction Coupling. *Ann. Rev. Physiol.* 41 473-484 (1979)
49. Fawcett, D. W., McNutt, N. S. The Ultrastructure of the Cat Myocardium: I. Ventricular Papillary Muscle. *J. Cell Biol.* 42 1-45 (1969)
50. Feldman, M. L., Navaratnam, J. Ultrastructural Changes in Atrial Myocardium of the Aging Rat. *J. Anat.* 133 7-17 (1981).
51. Forbes, M. S., Sperelakis, N. Myocardial Couplings: Their Structural Variations in the Mouse. *J. Ultrastruct. Res.* 58 50-69 (1977)
52. Forbes, M.S., Sperelakis, N. Ruthenium Red Staining of

Skeletal and Cardiac Muscles. Cell Tiss. Res. 200 367-382
(1979)

53. Forssmann, W. G., Girardier, L. A Study of the T-system in Rat Heart. J. Cell.Biol. 44 1-19 (1970).
54. Frank, G. B. The Current View of the Source of Trigger Calcium in Excitation-Contraction Coupling in Skeletal Muscle. Can. J. Physiol. Pharmacol. 60 427-439 (1982)
55. Frank, J. S. Beydler, S., Kreman, M., Rau, E. F. A Study of the Freeze-Fractured Sarcolemma in the Normal and Anoxic Rabbit Myocardium. Circ'n. Res. 47 131-143 (1980)
56. Frank, M., Albrecht, I., Sleater, W. W., Robinson, R. B. Stereological Measurements of Atrial Ultrastructures in the Guinea Pig. Experientia 31 578-580 (1975)
57. Franzini-Armstrong, C. Studies of the Triad I. Structure of the Junction in Frog Twitch Fibers. J. Cell. Biol. 47 488-49 (1970)
58. Franzini-Armstrong, C. Membrane Particles in Transmission at the Triad. Fed. Proc. 34 1382-1389 (1979)
59. Franzini-Armstrong, C. The Comparative Structure of Intracellular Junctions in Striated Muscle Fibers. Exc. Med. Int'l. Cong. 404 612-625 (1976)
60. Franzini-Armstrong, C. Structure of the Sarcoplasmic Reticulum. Fed.Proc. 39 2403-2409 (1980)
61. Franzini-Armstrong, C., Huisen, J. E., Reese, T. S., Somlyo, A..P., Somlyo, A. V. T-tubule Swelling in Hypertonic Solutions, a Freeze Substitution Study. J. Physiol. 283 133-140 (1978)
62. Franzini-Armstrong, C., Landmesser, L., Pilar, G. Size and Shape of Transverse Tubular Openings in Frog Twitch Muscle Fibers. J. Cell. Biol. 64 493-497 (1975)
63. Gabella, G. Inpocketings of the Cell Membrane (Caveolae) in Rat Myocardium. J. Ultrastruct. Res. 65 135-147 (1978)

64. Gerdes, A. M., Kasten, F. H. Morphometric Study of Endomyocardium and Epimyocardium of the Left Ventricle in Adult Dogs. *Am. J. Anat.* 159 389-394 (1980)
65. Gros, D., Challice, C. E. The Coating of Mouse Myocardial Cells. A Cytochemical Electronmicroscopical Study. *J. Histochem. Cytochem.* 23 727-744 (1975)
66. Haug, H. On the Proper Use of Point-Counting and Semi-automatic Procedures in Stereology. *Micr. Acta* 85 141-152 (1981)
67. Hibbs, R. G., Ferrans, V. J. An Ultrastructural and Histochemical Study of Rat Atrial Myocardium. *Am. J. Anat.* 124 251-280 (1969)
68. Hirakow, R. Ultrastructural Characteristics of Mammalian and Sauropsidan Heart. *Am. J. Cardiol.* 25 195-203 (1970)
69. Hirakow, R., Gotoh, T. A Quantitative Ultrastructural Study on the Developing Rat Heart. 33-79 *Dev. Physiol. Corr. Card. Muscle Vol.1* M.Leiberman, T.Sano (Eds.) Raven Press N.Y. (1975)
70. Hirakow, R., Gotoh, T., Watanabe, T. Quantitative Studies on the Ultrastructural Differentiation and Growth of Mammalian Cardiac Muscle Cells. I. The Atria and Ventricles of the Rat. *Acta Anat.* 108 144-152 (1980)
71. Hoerter, J. Mazet, F., Vassert, G. Perinatal Growth of the Rabbit Cardiac Cell: Possible Implications for the Mechanism of Relaxation. *J. Mol. Cell. Cardiol.* 13 725-740 (1981)
72. Ishikawa, H. Formation of Elaborate Networks of T-tubules in Cultured Skeletal Muscle with Special Reference to the T-system Formation. *J. Cell Biol.* 38 51-66 (1968)
73. Ishikawa, H., Yamada, S. Differentiation of the Sarcoplasmic Reticulum and T-system in Developing Mouse Cardiac Muscle. 21-35 *Dev. Physiol. Corr. Card. Muscle Vol.1* M.Leiberman, T.Sano (Eds.) Raven Press N.Y. (1975)
74. Janse, M. J., Anderson, R. H. Specialized Internodal

Pathways- Fact or fiction? Eur. J. Cardiol. 212 117-136 (1974)

75. Jorgensen, A. O., Shen, A. C-Y., Daly, P., MacLennan, D. H. Localization of Ca^{2+} and Mg^{2+} of the Sarcoplasmic Reticulum in Adult Rat Papillary Muscle. J. Cell Biol. 93 883-892 (1982)
76. Kaufman, M. H., Navaratnam, V. Early Differentiation of the Heart in Mouse Embryos. J. Anat. 133 235-246 (1981)
77. Kelly, A. M. Sarcoplasmic Reticulum and T-tubules in Differentiating Rat Skeletal Muscle. J. Cell Biol. 49 335-344 (1971)
78. Kelly, D. E., Kuda, A. M. Subunits of the Triadic Junction in Fast Skeletal Muscle as Revealed by Freeze Fracture. J. Ultrastruct. Res. 68 220-233 (1979)
79. Korecky, B. Michael, L. H. Regional Differences in Contractions of Mammalian Hearts. Rec. Adv. Stud. Card. Struct. Metab. 4 77-87 (1974)
80. Korecky, B., Rakusan, K. Normal and Hypertrophic Growth of the Rat Heart: Changes in Cell Dimensions and Numbers. Am. J. Physiol. 234 H123-H128 (1978)
81. Langer, G. A. The Role of Calcium in the Control of Myocardial Contractility. J. Mol. Cell. Cardiol. 12 231-239 (1980)
82. Lau, Y. M., Caswell, A. H., Brunschwig, J.-P., Baerwold, R. J. Lipid Analysis and Freeze-Fracture Studies of Sarcoplasmic Reticulum Subfractions of Skeletal Muscle. J. Biol. Chem. 254 540-546 (1979).
83. Leeson, T. S. Sarcotubules and Subsarcolemmal Caveolae and their Continuity with the Sarcolemma in Frog Striated Muscle. Am. J. Anat. 150 185-191 (1977)
84. Leeson, T. S. Sarcolemma, T-tubules and Subsarcolemmal Caveolae. Interrelationships and Continuity Demonstrated by Tannic Acid Mordanting. Can. J. Zool. 56 391-397 (1978a)

85. Leeson, T. S. The Transverse Tubule System of Rat Cardiac Muscle Fibers as Demonstrated by Tannic Acid Mordanting. *Can. J. Zool.* 56 1906-1966 (1978b)
86. Leeson, T. S. T-tubules, Couplings and Myofibrillar Arrangements in Rat Atrial Myocardium. *Acta Anat.* 108 374-388 (1980)
87. Leeson, T. S. Nonmyofibrillar Filamentous Material in Right Atrial Myocardial Cells of the Rat. *J. Mol. Cell Cardiol.* 12 , 267-284 (1980)
88. Legato, M. J. Ultrastructure of the Atrial, Ventricular and Purkinje Cell with Special Reference to the Genesis of Arrhythmias. *Circ'n.* 47 178-179 (1973)
89. Levin, K. R., Page, E. Quantitative Studies on Plasmalemmal Folds and Caveolae of Rabbit Ventricular Myocardial Cells. *Circ'n. Res.* 46 244-255 (1980)
90. Lorber, V., Bertaud, W. S. Cellular Surfaces of Amphibian Atrial Muscle. *J. Cell Sci.* 9 427-433 (1971)
91. Mall, G., Reinhard, H., Kayser, K., Rossner, J. A. An Effective Morphometric Method for Electronmicroscopic Studies on Papillary Muscles. *Virch. Arch. A* 379 219-228 (1978)
92. Marino, T. A., Biberstein, D., Nong Cook, P., Cook, L., Dwyer III, S. J. A Quantitative Morphological Analysis of Intraatrial Muscle Cells in the Ferret Heart. *Anat. Rec.* 201 31-42 (1981)
93. Nakata, K. Quantitative Analysis of Ultrastructural Changes in Developing Rat Cardiac Muscle During Normal Growth and During Acute Volume Load. *Jap. Circ'n. J.* 41 1238-1250 (1977)
94. Masson-Pevet, M., Bleeker, W. K., MacKaay, A. J. C., Bouman, L. N., Houtkooper, J. H. Sinus Node and Atrium Cells from the Rabbit Heart: A Quantitative Electronmicroscopic Description after Electrophysiological Localization. *J. Mol. Cell Cardiol.* 11 555-568 (1979)

95. Masson-Pevet, M., Gron, H., Besselsen, E. The Caveolae in Rabbit Sinus Node and Atrium. *Cell Tiss. Res.* 208 183-196 (1980)
96. Mayhew, T. M., Cope, G. H., Williams, M. A., Mahon, M., Cruze-Olive, L. M. Stereology: A Demonstration of some Basic Principles and applications. *J. Anat.* 123 264-295 (1977)
97. McNutt, N. S. Ultrastructure of the Myocardial Sarcolemma. *Circ'n. Res.* 37 1-13 (1975)
98. McNutt, N. S., Fawcett, D. W. The Ultrastructure of Cat Myocardium II. Atrial Muscle. *J. Cell Biol.* 42 46-67 (1969)
99. Meissner, G. McKinley, D. Permeability of Canine Cardiac Sarcoplasmic Reticulum Vesicles to K^+ , Na^+ , H^+ and Cl^- . *J. Biol. Chem.* 257 7704-7711 (1982)
100. Miyamoto, H., Racker, D. Mechanisms of Calcium Release from Skeletal Muscle Sarcoplasmic Reticulum. *J. Cell Biol.* 66 193-201 (1982)
101. Mizuhira, V., Futaesaku, Y. New Fixation for Biological Membranes using Tannic Acids. *Acta Histochem. Cytochem.* 5 233-234 (1972)
102. Mobley, B. A., Eisenberg, B. Size Components of Skeletal Muscle measured by Methods of Stereology. *J. Gen. Physiol.* 66 31-45 (1975)
103. Morgan, J. P., Blinks, J. R. Intracellular Ca^{2+} Transients in Cat Papillary Muscle. *Can. J. Physiol. Pharmacol.* 60 524-528 (1982)
104. Moses, R. L., Kasten, F. H. T-Tubes in Cultured Mammalian Myocardial Cells. *Cell Tiss. Res.* 203 173-180 (1979)
105. Myers, J. L. Fundamentals of Experimental Design. p. 73 Allyn and Bacon, Boston (1967)
106. Myklebust, R., Saetersdal, , T. S., Engedal, H.. The

T-tubule System in the Myocardium of the Sand Rat and Mouse as demonstrated by Horseradish Peroxidase. Cell Tiss. Res. 192 205-213 (1978)

107. Nakajima, S., Gilai, A., Radial Propagation of Muscle Action Potential along the Tubular System Examined by Potential Sensitive Dyes. J. Gen. Physiol. 6 751-762 (1980)
108. Nakata, K. Quantitative Analysis of Ultrastructural Changes in Developing Rat Cardiac Muscle During Normal Growth and During Acute Volume Load. Jap. Circ'n. J. 41 1238-1250 (1977)
109. Okita, , S. The Fine Structure of the Ventricular Muscle Cells of the Soft Shelled Turtle Heart (Amyda), with Special Reference to the Sarcoplasmic Reticulum. J. Electronmicr. 20 107-119 (1971)
110. Olivetti, G., Anversa, P., Loud, A. V. Morphometric Study of Early Postnatal Development in the Left and Right Ventricular Myocardium of the Rat II. Tissue Composition, Capillary Growth and Sarcoplasmic Alterations. Circ'n. Res. 46 503-512 (1980)
111. Page, E., Quantitative Ultrastructural Analysis in Cardiac Membrane Physiology. Am. J. Physiol. 235 C147-158 (1978)
112. Page, E. Buecker, J. L. Development of Dyadic Junctional Complexes between Sarcoplasmic Reticulum and Plasmalemma in Rabbit Left Ventricular Myocardial Cells: Morphometric Analysis. Circ'n. Res. 48 519-522 (1981)
113. Page, E., Earley, J., Power, B. Normal Growth of Ultrastructures in Rat Left Ventricular Myocardial Cells. Circ'n. Res. 34 (Sup. 2) 12-16 (1974)
114. Page, E., McCallister, L. B., Power, B. Stereological Measurement of Cardiac Ultrastructures Implicated in Excitation-Contraction Coupling. P.N.A.S. 68 1465-1466 (1971)
115. Page, E., Surdyk-Droske, M. Distribution, Surface Density and Membrane Area of Diadic Junctional Contacts between Plasma Membrane and Terminal Cisternae in Mammalian

Ventricle. Circ'n. Res. 45 260-267 (1979)

116. Pavlovich, E. R., Chervova, I.A. Morphometric Detection of Specialized Internodal Conducting Pathways of the Heart. Bull. Exp. Biol. Med. 92 1446-1449 (1982)
117. Rakusan, K., Raman, S., Layberry, R., Korecky, B. The Influence of Aging and Growth on the Postnatal Development of Cardiac Muscle in Rats. Circ'n. Res. 42 212-218 (1978)
118. Rayns, D. G., Simpson, F. O., Bertaud, W. S. T-tubule Apertures in Mammalian Myocardial Cells: Surface Array. Science 156 656-657 (1967)
119. Rayns, D. G., Devine, C. E., Sutherland, C. L. Freeze-Fracture Studies of Membrane Systems in Vertebrate Muscle. I. Striated Muscle. J. Ultrastruct. Res. 50 306-321 (1975)
120. Saetersdal, T., Ødegården, Rotevatn, S., , Engedal, H. Atrial Specific Granules of the Human Auricle in Embryogenesis. Tissue Culture and Hypertrophy. Cell Tiss. Res. 209 345-351 (1980)
121. Saetersdal, T., Rotevatn, S., Myklebust, , R., Ødegården Development of Specific Granules in Embryonic Cardiac Myocytes of the Human Auricular Wall. Anat. Embryol. 160 1-9 (1980)
122. Saito, A., Wang, C.-T., Fleischer, S. Membrane Asymmetry and Enhanced Ultrastructural Detail of Sarcoplasmic Reticulum Revealed with Use of Tannic Acid. J. Cell Biol. 79 601-616 (1978)
123. Scales, D. J. Aspects of the Mammalian Cardiac Sarcotubular System Revealed by Freeze-Fracture Electronmicroscopy. J. Mol. Cell. Cardiol. 13 373-380 (1981)
124. Scales, , D. J., Sabbadini, R. A. Microsomal T-system: A Stereological Analysis of Purified Microsomes Derived from Normal and Dystrophic Muscle. J. Cell Biol. 83 33-44 (1979)

125. Schiaffino, S., Margreth, A. Coordinated Development of the Sarcoplasmic Reticulum and T-system during Postnatal Differentiation of Rat Skeletal Muscle. *J. Cell Biol.* 41 855-875 (1969)
126. Schiaffino, S., Cantino, M., Sartore, S. T-system Formation in Cultured Rat Skeletal Muscle. *Tissue Cell* 9 437-446 (1977)
127. Sherf, L., James, T. N. Fine Structure of Cells and Their Histologic Organization Within Internodal Pathways of the Heart: Clinical and Electrocardiographic Implications. *Am. J. Cardiol* 44 345-369 (1979)
128. Sheridan, D.J. Postnatal Developmental Changes in the Electrophysiological Properties of Cat Right Ventricular Papillary Muscles. *Cardiovasc. Res.* 14 700-709 (1980)
129. Sheridan, D. J., Cullen, M. J., Tynan, M. J. Postnatal Ultrastructural Changes in the Cat Myocardium, a Morphometric Study. *Cardiovasc. Res.* 11 536-540 (1977)
130. Sheridan, D. J., Cullen, M. J., Tynan, M. J.. Qualitative and Quantitative Observations During Postnatal Development in the Cat Myocardium. *J. Mol. Cell. Cardiol.* 11 1173-1181 (1979)
131. Shibata, Y., Page, E. Freeze-Fracture Study of Dyadic Couplings in Rabbit Ventricular Myocardial Cells. *Fed. Proc.* 39 3003a (1980)
132. Siegel, S. Nonparametric Statistics for the Behavioral Sciences. McGraw-Hill, N. Y. (1956)
133. Simionescu, N., Simionescu, M. Galloylglucoses of Low Molecular Weight as Mordant in Electronmicroscopy 1. Procedure, and Evidence for Mordanting Effect. *J. Cell Biol.* 70 608-621 (1976a)
134. Simionescu, N., Simionescu, M. Galloylglucoses of Low Molecular Weight as Mordant in Electronmicroscopy 2. The Moiety and Functional Groups Possibly Involved in the Mordanting Effect. *J. Cell Biol.* 70 622-633 (1976b)

135. Simpson, F. O., Rayns, D. G. The Relationship between the T-tubule System and Other Tubules at the Z-disc Levels of Myocardial Cells in the Ferret. *Am. J. Anat.* 122 193-207 (1968)
136. Somlyo, A. V. Bridging Structures Spanning the Junctional Gap at the Triad of Skeletal Muscle. *J. Cell Biol.* 80 743-750 (1979)
137. Somlyo, A. P., Shuman, H., Somlyo, A. V. Composition of Sarcoplasmic Reticulum *in situ* by Electronprobe X-ray Microanalysis. *Nature* 268 556-558 (1977)
138. Sommer, J. R., Johnson, E. A. Comparative Ultrastructure of Cardiac Cell Membrane Specializations, a Review. *Am. J. Cardiol.* 25 184-194 (1970)
139. Sommer, J. R., Johnson, E. A. Ultrastructure of Cardiac Muscle, from the Handbook of Physiology, Vol. 1. The Heart. Berne, R. E., Sperelakis, N., Geiger, S. R. (Eds.), *Am. Physiol. Soc.* 113-186 (1979)
140. Sommer, J. R., Waugh, R. A. The Ultrastructure of the Mammalian Cardiac Muscle Cell - With Special Emphasis on the Tubular Membrane Systems. *Am. J. Pathol.* 82 192-232 (1976)
141. Smith, D. S., Aldrich, H. C. Membrane Systems of Freeze-Etched Striated Muscle. *Tissue Cell* 3 261-281 (1971)
142. Sperelakis, N., Forbes, M. S., Rubio, R. The Tubular Systems of Myocardial Cells: Ultrastructure and Possible Function. *Rec. Adv. Stud. Card. Struct. Metab.* 4 163-194 (1974)
143. Stephenson, E. W. Activation of Fast Skeletal Muscle: Contributions of Studies on Skinned Fibers. *Am. J. Physiol.* 240 C1-C19 (1981)
144. Tillack, T. W., Boland, R., Martonosi, A. The Ultrastructure of Developing Sarcoplasmic Reticulum. *J. Biol. Chem.* 249 624-633 (1974)

145. Underwood, E. E. Stereology or the Quantitative Evaluation of Microstructures. *J. Micr.* 89 pt 2 161-180 (1969)
146. Virágh, S., Challice, C. E.. Origin and Differentiation of Cardiac Muscle Cells in the Mouse. *J. Ultrastruct. Res.* 42 1-24 (1973)
147. Virágh, S., Challice, C. E. The Development of the Conduction System in the Mouse Embryo Heart 1. The First Embryonic Conduction Pathway. *Dev. Biol.* 56 382-396 (1977)
148. Virágh, S., Challice, C. E.. The Development of the Conduction System in the Mouse Embryo 3. The Development of the Mouse sinus Muscle and Sinoatrial Node. *Dev. Biol.* 80 28-45 (1980)]
149. Weibel, E. W. Stereological Principles for Morphometry in Electronmicroscopic Cytology. *Int'l. Rev. Cytol.* 26 235-303 (1969)
150. Weibel, E. A Stereological Method for Estimating Volume and Surface of Sarcoplasmic Reticulum. *J. Micr.* 95 pt.2 229-242 (1971)
151. Yunge, L., Ballak, M., Beuzeron, J., Lacasse, J., Cantin, M. Ultrastructural Cytochemistry of Atrial and Ventricular Cardiocytes of the Bullfrog (*Rana catesbeiana*). Relationship of Specific Granules with Reninlike Activity of the Myocardium. *Can. J. Physiol. Pharmacol.* 58 1463-1476 (1980)
152. Yunge, L., Benchimol, S., Cantin, M. Ultrastructural Cytochemistry of Atrial Muscle Cells III. Radioautographic Study of Synthesis and Migration of Glycoproteins. *J. Mol. Cell. Cardiol.* 11 375-388 (1979)
153. Yunge, , L., Benchimol, S., Cantin, M. Ultrastructural Cytochemistry of Atrial Muscle Cells VIII. Radioautographic Study of Synthesis and Migration of Proteins. *Cell Tiss. Res.* 207 1-11 (1980)
154. Zak, R. Development and Proliferative Capacity of Cardiac Muscle Cells. *Circ'n. Res.* 34 (Sup. 2) 17-26 (1974)

155. Flickinger, C. J., Brown, J. C., Kutchai, H. C.,
Ogilvie, J. W. Medical Cell Biology. W. B. Saunders Co.,
Philadelphia (1979)
156. Leeson, T. S., Leeson, C. R. Histology. W. B. Saunders Co.,
Philadelphia (1981)
157. Price, K. M., Littler, W. A., Cummins, P. Human Atrial and
Ventricular Myosin Light Chain Subunits in the Adult and
During Development. Biochem. J. 191 571-580 (1980)
158. Sartore, S., Gorza, L., Pierobon Bormioli, S.,
Dalla Libera, L., Schiaffino, S. Myosin Types and Fiber
Types in Cardiac Muscle. I. Ventricular Myocardium. J.
Cell Biol. 88 226-233 (1981)
159. Singh, S., White, F. C., Bloor, C. M. Myocardial Morphometric
Characteristics in Swine. Circ'n. Res. 49 434-441 (1981)
160. Doyle, D., Baumann, H. Turnover of the Plasma Membrane of
Mammalian Cells. Life Sci. 24 951-966 (1979)

APPENDIX 1

Raw data and calculations for morphometric measurements.

Table A1.1 Cell Area on Micrographs (mm²)

NEONATES	7 DAYS	14 DAYS	18 DAYS	21 DAYS	ADULT
15796.6	14482.2	14026.3	12066.8	18999.3	15870.4
16779.0	15951.7	15581.1	12974.7	19880.8	17894.5
15183.6	14089.1	19775.3	14516.9	18269.7	16747.0
17436.8	16104.1	15694.0	16518.9	17691.6	17567.1
16939.3	18287.6	16883.6	16488.4	15861.4	18353.1
16900.6	19780.0	13427.5	12031.7	20138.9	17382.2
13095.9	10026.9	19948.6	18256.7	16147.8	17871.7
17230.9	16898.2	15693.5	12033.5	17195.5	19036.5
15691.8	19972.4	15841.1	13967.1	17292.1	17820.2
12911.9	12361.0	17448.6	17639.7	16066.3	18502.6
15070.8	17668.9	15924.1	12490.6	10021.6	17832.1
13459.2	19951.8	6883.7	15744.8	15593.1	18368.9
14362.8	15812.9	13957.0	17356.6	16754.1	18150.6
15705.9	20214.1	14964.4	14041.1	20997.5	16239.8
13322.1	19362.5	17082.5	16914.6	18789.4	19234.1
17890.4	13767.1	15532.9	13894.9	13362.9	15902.5
17635.3	10286.7	9657.8	15119.0	17177.3	17220.2
17605.2	15670.0	9930.7	15042.7	15342.2	17607.0
17384.2	18342.0	12299.3	16636.5	20661.8	16863.2
17445.6	18246.0	14925.6	13453.0	13416.0	17122.3
18052.3	15436.4	16506.5	13936.4	16725.1	16756.8
12582.9	6223.0	10573.7	16798.2	14952.4	18368.8
18481.1	19451.8	13210.8	13366.5	18535.1	15012.2
18706.1	17806.5	16462.2	13391.8	12258.3	17014.8
14002.6	19586.9	17419.7	18647.0	19251.2	16665.2
12789.8	19731.2	16639.6	15642.9	19550.5	19209.3
17773.5	9264.6	16802.0	12863.0	16513.7	8923.3
17128.6	15018.2	13313.7	17518.1	15390.5	16325.5
15962.6	14930.2	18114.8	14732.2	13659.5	16545.4
18624.4	11795.7	12576.1	18082.9	17374.2	16968.7
14253.5	15718.3	17175.7	12384.1	15580.7	19108.6
17554.6	16436.2	11399.3	14654.1	20370.4	16595.6
9287.6	9247.5	11430.3	17714.1	17986.4	16651.2
17870.3	19620.8	16237.9	19173.2	19611.3	18582.4
18307.2	11772.3	9115.8	8104.3	19011.5	17869.6
11102.0	18212.1	14973.8	13084.4	14218.6	17372.1
16145.7	14364.8	11059.4	15656.2	18112.1	19345.8
9722.3	18378.0	16712.1	15748.9	20362.1	17656.8
9881.9	18006.1	18059.1	13302.9	15226.1	18672.8
16093.4	15843.3	19173.3	13401.8	19196.2	17964.9
16094.2	17848.4	20194.2	10365.5	16877.7	13347.3
19169.2	18851.8	15028.5	18434.9	18692.2	18209.3
17121.8	14685.7	11878.3	12392.6	19931.5	15014.2
19025.7	12769.7	18253.2	11843.7	21025.3	15214.0
18118.7	19500.5	11949.8	16321.5	16135.2	23151.6
8145.0	17991.8	17458.8	12945.9	20242.3	19356.0
15317.9	19736.7	8976.3	13058.1	18412.1	17484.1
17597.9	16259.4	14798.8	9929.7	11441.7	14717.5
16355.6	17825.6	14306.9	18175.3	21002.2	15404.8
19268.0	14551.4	14093.8	10878.9	20751.8	16711.6

Table A1.1 continued

NEONATES	7 DAYS	14 DAYS	18 DAYS	21 DAYS	ADULT
17940.1	10026.0	13741.6	10911.2	13281.4	14268.3
16591.8	18358.1	13827.9	15037.6	17700.3	11056.8
16842.9	17690.5	17973.6	16863.3	19904.1	12852.9
18911.6	13258.1	19464.8	14295.5	18140.1	19530.3
11341.6	6979.5	20096.3	8066.3	15800.4	14835.2
17258.0	18892.6	13116.9	9491.2	19009.2	18569.2
18473.8	10978.5	19576.1	8023.9	19625.1	17112.4
18443.0	12493.9	19347.3	14234.0	7845.7	18979.9
18564.6	16347.4	19231.9	15799.6	18454.6	17772.2
16971.6	15313.9	13436.8	14457.0	12178.7	12956.4
18444.1	11212.1	17370.5	19633.3	18551.9	15188.4
14315.3	14284.1	17574.0	20300.3	15018.5	16955.0
17603.0	15079.4	15236.5	21212.6	13930.3	15970.9
16221.1	18367.0	18155.8	19810.3	18034.2	18259.4
16277.5	15984.4	17151.7	14346.1	16459.1	19658.7
16543.2	12575.3	17060.4	20766.4	17109.2	17247.8
14626.2	19403.6	16285.5	20527.6	19573.7	16340.7
14999.7	9586.8	18060.9	19237.7	11709.4	14757.5
17511.5	15329.7	15585.2	19148.7	14467.3	17395.5
12614.3	17800.6	17734.3	17242.9	16925.3	17477.4
11827.0	18110.7	16987.7	16823.1	19980.2	14407.0
11959.0	17005.1	15990.2	19821.4	13555.2	18616.2
13865.1	15589.4	11916.9	11396.7	12583.0	15576.1
17524.0	12939.3	13157.1	17230.5	15902.9	11916.0
16989.5	14659.2	17613.8	16922.7	19700.8	17214.3
16275.1	15124.2	18154.1	13080.3	15605.9	18835.5
18251.8	13067.4	11501.3	17089.4	19623.5	20131.6
14489.2	13280.2	14170.3	17321.0	19442.9	15278.0
14902.1	15431.1	16293.2	16465.0	15468.9	17333.3
18657.1	14913.5	12257.3	19640.5	17314.5	17732.0
17620.6	12377.1	15929.7	11377.0	19365.5	18934.2
17963.5	19885.5	18388.5	15516.9	18488.0	18428.6
17931.7	17535.9	11052.2	19742.9	18245.4	16737.5
16154.9	16805.4	12118.9	9664.9	16345.1	17294.1
18684.2	14985.2	12434.8	17887.6	19343.7	17426.2
18598.0	14929.6	17028.9	16314.5	19156.7	18684.1
17443.0	18557.6	16687.8	10706.7	15318.3	18755.9
17495.0	19215.6	14364.3	18565.9	19832.5	18490.8
16481.6	16445.2	10856.6	18288.3	17550.4	13243.0
10959.3	19101.7	13069.9	11926.7	17787.5	14556.2
13680.6	15398.8	11461.9	16980.0	13127.0	18976.3
13183.1	15450.6	19740.8	13705.1	18221.3	17685.3
13429.9	16349.0	7763.6	14932.8	9703.5	16538.0
14977.2	9714.6	13325.7	20707.4	15877.2	13807.7
18702.3	13802.2	14342.1	15385.1	18366.7	16957.7
18417.6	20136.8	16428.1	10653.0	18703.5	15623.5
17138.8	17802.6	16574.5	20427.7	17736.0	18213.3
17411.6	17731.7	16305.6	12993.4	18012.1	18582.2
11445.3	20185.6	19157.2	11759.5	19003.1	10316.0
11885.8	15513.1	18841.5	17805.4	14727.1	12380.7

Table A1.2 Myofibrillar Area on Micrographs (mm²)

NEONATES	7 DAYS	14 DAYS	18 DAYS	21 DAYS	ADULT
4328.6	4901.0	7794.4	5254.3	7444.2	9757.4
5381.3	4171.2	5706.6	4762.5	9353.4	11867.3
6349.3	4007.1	9613.2	7661.3	6069.2	6325.0
5323.6	8055.4	4003.0	6626.3	7115.5	9780.7
6180.7	7012.5	7546.7	7150.5	8875.0	12198.9
7053.8	4905.2	4782.4	3045.5	7612.2	11451.0
3038.9	2650.0	7427.6	6691.7	6363.6	10721.5
6963.4	5351.2	6021.7	4694.9	6792.5	10857.3
8092.8	7131.8	5757.2	5721.9	4830.8	10056.8
4532.4	5816.9	5869.5	8692.8	5809.4	11226.8
5945.1	6353.8	4332.5	7284.5	5371.6	11091.2
7023.9	5659.4	3280.6	7161.7	6172.3	11004.9
7135.7	5313.6	6973.2	8289.9	5406.3	7643.7
4923.3	6545.4	5077.2	4962.1	7850.3	11092.3
2396.1	7544.4	4572.1	5677.8	7761.6	12538.9
5926.5	6713.4	6508.8	4927.2	4455.5	9136.8
7714.4	4689.8	4291.5	7609.2	5484.8	7680.0
6798.7	7451.2	5248.0	7039.3	5429.0	9583.9
5608.5	6139.0	5714.5	8501.3	14693.8	10217.0
5051.7	5483.6	8423.0	6462.4	4630.7	10455.0
7998.9	6235.3	6943.0	6936.0	6235.7	8136.0
4408.8	2761.4	6179.6	7132.5	4601.9	11044.1
5688.8	9924.0	7492.5	6125.5	6739.7	9103.6
7462.2	5844.6	7318.1	4539.4	4229.7	10845.9
4388.4	10463.9	7091.9	9236.7	7529.4	10952.0
3730.6	8168.0	7039.2	4959.0	7418.9	11283.3
4609.8	3124.6	7796.2	6840.6	6287.1	18160.8
4416.4	4422.3	5343.7	8034.2	5909.6	9166.6
4283.5	5498.2	9201.3	5612.4	5942.4	10584.2
5996.9	5400.6	6178.7	6185.3	8031.6	8792.3
3764.1	5477.2	8070.2	4650.4	10765.8	11364.6
8544.1	5587.8	5415.2	4661.0	8736.0	9882.3
1741.4	4303.4	5587.4	5201.8	9982.0	7407.8
6280.5	6060.2	4700.3	5932.8	10266.4	10115.6
4321.5	2848.1	4352.6	3191.7	9578.7	12353.5
3978.2	6355.3	5560.1	4137.0	6472.0	11352.4
5597.3	5924.2	5229.9	3666.7	7391.0	11566.5
3402.9	10154.8	7123.6	7365.4	10862.6	9933.0
3048.5	6176.2	8523.2	5569.6	7298.7	10133.3
3889.3	6055.5	10594.3	6551.9	8062.0	11046.6
4851.8	4434.1	8001.5	3024.0	6888.4	5599.4
5947.1	5229.2	5856.5	5107.8	6957.0	10539.6
7480.5	5227.9	6095.9	4866.3	8334.8	9035.8
8235.2	6074.2	6835.3	3555.1	9870.4	8510.4
6660.4	5221.1	5453.0	5305.7	8761.6	13967.3
4313.6	8629.0	8442.1	6020.6	6546.5	11523.7
4728.0	7560.7	3723.1	6724.0	9090.4	10027.2
6899.1	6329.3	5615.1	4026.6	3681.5	9057.0
6284.0	7872.3	6602.1	6585.4	7408.2	7773.4
4866.8	5580.8	6263.1	3297.3	8315.2	7740.0

Table A1.2 continued

NEONATES	7 DAYS	14 DAYS	18 DAYS	21 DAYS	ADULT
6364.9	5667.1	7640.9	3755.9	5540.8	8856.9
5238.8	4707.0	7136.9	5141.6	7652.4	6327.9
3067.1	3444.8	5000.9	6357.3	7652.7	7686.8
5104.2	6447.3	6827.0	6284.9	9265.5	10278.4
3485.4	2672.9	11046.0	2385.6	8919.9	9299.6
4215.7	5924.0	3717.0	3390.4	7323.7	10290.8
6606.8	6299.7	7489.1	2853.8	8639.8	9875.2
5710.9	4652.9	8499.0	7063.7	4460.6	10482.4
7943.6	5540.4	8020.3	8524.2	10776.5	11948.6
6288.1	4481.0	4912.4	5912.8	4711.9	6760.7
4922.9	4095.1	11223.1	11314.7	7494.2	9529.0
3448.3	5437.0	5412.4	5499.7	6887.5	7749.7
4399.6	4386.3	5800.8	11648.7	5300.1	7226.2
5127.5	5790.1	6609.9	10023.2	9424.7	9482.7
8463.1	4319.6	6227.1	6517.0	9958.6	9920.8
5940.3	4332.0	5815.9	9034.1	8147.7	6730.3
4652.6	9458.6	5564.6	10355.9	9515.1	10138.8
2986.9	3894.2	7863.9	7425.2	4958.5	7993.7
7753.0	6089.2	4023.3	6170.8	6450.5	9232.1
6564.6	9129.2	3559.5	4737.6	8684.6	11556.1
4968.8	5483.4	6171.9	8327.2	7541.7	8481.0
3758.4	5179.8	9048.4	5139.1	6815.1	9449.7
4374.4	7033.1	3539.6	3074.0	7358.1	9108.4
4762.1	6898.8	7093.9	4369.4	9416.0	7048.9
6890.7	7197.2	8348.6	7308.5	12176.6	10661.1
4950.0	5549.5	6801.9	8603.2	8523.6	7662.2
6608.4	4425.5	5497.9	6523.4	8175.5	10610.2
6451.8	6314.0	5381.6	5802.0	11128.0	7880.8
5300.7	4692.7	5083.0	5176.0	8162.8	10124.6
6578.8	6157.4	4615.9	7371.5	7687.0	11071.5
6730.9	6346.1	5231.1	4905.4	5660.6	7162.8
4967.7	6249.7	5495.8	5539.7	6636.5	10181.4
6217.3	8206.6	5902.2	9034.5	8053.8	9724.2
6698.8	6634.4	4564.8	4666.6	6898.3	9369.8
5218.2	7153.7	4512.0	7998.5	8110.7	11318.5
7079.0	4467.6	5519.4	6990.7	8246.8	10984.7
4015.8	8446.9	2736.8	4274.5	5345.9	8525.3
3971.6	4496.9	4653.1	7316.4	8269.8	10443.5
5120.1	7149.3	4870.8	6801.1	7011.0	8216.2
3864.6	6849.0	5351.3	5236.8	8332.7	7925.0
8264.6	5858.2	6424.8	7225.5	6371.2	7344.3
6896.2	8913.7	6342.4	6355.9	7720.8	8382.5
4374.2	5964.7	3589.3	7520.4	4254.6	7872.8
6020.5	5211.7	5069.2	9093.2	6185.4	5884.9
6399.7	6288.8	5263.9	6211.9	7414.3	8341.7
8113.6	8587.5	6534.5	6386.3	8579.7	9139.8
6319.2	7290.1	6896.4	5825.3	9645.3	11060.9
5676.7	6780.5	6257.1	5195.7	8518.7	10696.2
4259.1	6376.4	5761.0	5709.8	8874.8	7619.1
4485.8	4520.4	7507.7	9157.5	6072.9	7552.5

Table A1.3 Volume Density of Myofibrils (%cell volume)

NEONATES	7 DAYS	14 DAYS	18 DAYS	21 DAYS	ADULT
27.4	33.8	35.6	43.5	39.2	61.5
32.1	26.2	35.6	42.2	47.1	66.3
41.8	28.4	42.6	52.3	33.2	37.8
30.5	50.0	45.6	40.1	40.2	55.7
36.5	38.3	44.7	43.4	55.9	66.5
41.7	24.8	35.6	25.3	37.8	65.9
23.2	26.4	32.2	36.7	39.4	60.0
40.4	31.7	33.4	39.0	39.5	56.4
51.6	35.7	35.3	41.0	27.9	57.0
35.1	47.1	36.6	49.3	36.2	68.9
39.5	36.0	27.2	58.3	53.6	62.2
52.2	28.4	47.7	45.5	39.6	59.9
49.7	33.6	50.0	47.8	32.3	42.1
31.3	32.4	33.9	35.3	37.4	68.1
18.0	39.0	26.8	33.6	41.3	65.4
34.7	48.8	41.9	35.5	33.3	57.5
43.7	45.6	44.4	50.3	31.9	44.6
38.6	47.6	52.9	46.8	35.4	54.4
32.3	34.5	46.5	51.1	71.1	60.6
29.0	30.0	56.4	48.0	34.5	61.1
44.3	40.4	42.1	49.8	37.3	48.6
35.0	44.4	52.4	42.5	30.8	60.1
30.8	51.0	36.7	45.8	36.4	60.6
39.9	32.8	44.5	33.0	34.5	63.7
31.3	53.4	40.7	49.3	39.1	65.7
44.8	41.4	32.3	31.7	37.7	58.7
26.0	33.7	46.4	53.2	38.0	49.1
25.8	29.5	40.1	45.9	38.4	56.1
26.8	36.8	50.8	38.1	43.5	64.8
32.2	45.8	49.1	34.2	46.2	48.9
26.4	34.8	45.4	37.6	69.1	59.5
48.7	34.0	47.5	31.8	42.9	59.6
18.8	46.5	39.5	29.4	55.5	44.5
35.1	30.8	29.0	30.9	52.4	54.4
23.6	24.2	47.9	39.4	50.4	69.1
55.8	34.9	37.1	31.6	45.5	65.3
34.7	41.2	47.3	23.4	40.8	59.8
35.0	55.3	42.6	46.8	53.3	56.3
30.8	34.3	47.2	41.9	47.9	54.0
24.2	38.2	55.3	48.9	42.0	61.5
30.2	24.8	39.6	29.2	40.8	42.0
31.0	27.7	40.0	27.7	37.2	57.9
43.7	35.6	54.5	39.3	41.8	60.2
43.3	47.6	37.4	30.0	46.9	55.9
36.8	26.8	45.6	32.5	54.3	60.3
53.0	43.0	48.4	46.5	32.3	59.5
30.9	38.3	41.5	51.5	49.4	57.4
39.2	38.9	37.9	40.6	32.2	61.5
38.4	44.2	46.1	36.2	35.3	50.5
25.3	38.4	44.6	30.3	40.1	46.3

Table A1.3 continued

NEONATES	7 DAYS	14 DAYS	18 DAYS	21 DAYS	ADULT
35.5	56.5	55.6	34.4	41.7	62.1
30.9	25.6	51.6	34.1	43.2	57.2
18.2	19.5	45.8	37.7	38.5	58.9
27.0	48.6	45.1	44.0	51.2	52.6
30.7	38.3	35.0	29.6	56.5	62.7
24.4	31.4	28.3	35.7	38.5	55.4
35.8	57.4	18.3	35.6	44.0	57.7
31.0	37.2	41.9	49.6	56.9	55.2
42.8	33.9	41.7	53.9	58.4	67.2
37.1	29.3	16.8	40.9	38.7	52.2
26.7	36.5	58.8	57.6	40.4	50.5
24.1	38.1	30.8	27.1	45.9	45.7
25.0	29.1	38.1	54.9	38.0	45.3
31.6	31.5	36.4	50.6	52.3	51.9
52.0	27.0	34.3	45.4	60.5	39.0
35.9	34.5	34.1	43.5	47.6	62.1
31.8	48.7	34.2	50.5	48.6	54.2
19.9	39.6	43.5	38.6	42.3	53.6
44.3	39.7	28.8	32.2	45.0	58.9
52.0	51.3	28.1	27.5	51.3	66.1
42.0	30.3	38.3	49.0	37.8	50.8
31.4	30.5	56.6	25.9	50.3	58.5
31.6	45.1	29.7	26.8	58.5	59.2
27.2	53.3	53.9	25.4	59.2	61.9
40.6	49.1	47.4	43.2	61.8	67.7
30.4	36.7	37.5	66.8	54.8	40.7
36.2	33.9	47.8	38.2	41.7	52.7
44.5	47.5	38.0	33.5	57.2	51.6
35.6	30.4	31.7	31.4	52.7	58.4
34.7	41.3	37.7	37.5	44.4	62.4
38.2	51.3	32.8	43.1	29.2	37.8
27.7	31.4	29.9	35.7	35.9	55.2
34.7	46.8	53.4	45.7	44.1	58.1
41.4	39.5	36.8	48.3	42.2	54.2
27.9	47.7	36.3	44.7	41.9	65.0
38.1	29.9	32.4	42.8	43.1	58.8
23.0	45.5	16.4	40.0	34.9	45.5
27.7	23.4	32.4	39.4	41.7	56.5
31.1	43.5	44.9	37.2	40.0	62.0
35.3	35.9	40.9	43.9	46.9	54.4
60.6	38.0	56.0	42.5	48.5	38.7
52.3	57.7	32.1	46.4	42.4	47.4
32.6	36.5	46.2	50.4	43.8	47.6
40.2	53.7	38.0	43.9	39.0	42.6
34.2	45.6	36.7	40.4	40.4	49.2
44.1	42.6	39.8	60.0	45.9	58.5
36.9	40.9	41.6	28.5	54.4	60.7
32.6	38.2	38.4	40.0	47.3	57.7
37.2	31.6	30.1	48.5	46.7	73.9
37.7	29.1	39.9	51.4	41.2	61.0

Table A1.4 Cell Diameters (μm)

NEONATES	7 DAYS	14 DAYS	18 DAYS	21 DAYS	ADULT
3.08	3.03	3.02	3.94	4.06	8.11
2.87	3.37	4.42	3.72	5.99	7.94
3.11	2.61	3.66	2.60	4.88	6.66
2.62	2.94	5.23	3.13	4.51	6.78
3.41	4.49	3.74	3.41	4.32	6.03
3.48	3.45	1.48	3.59	5.47	7.08
2.67	3.47	2.93	4.09	4.75	8.82
3.94	3.35	3.91	3.76	3.95	8.17
3.04	3.26	3.76	3.54	5.34	7.59
3.39	3.67	3.29	3.83	4.12	7.06
2.35	3.05	4.42	5.69	4.73	9.94
3.19	3.62	4.40	5.64	5.44	6.89
3.61	3.18	4.23	4.37	5.66	7.97
2.52	4.09	3.21	4.68	5.34	8.61
2.92	3.31	3.31	4.70	4.30	8.40
3.04	2.72	3.23	4.24	5.27	6.28
4.13	2.96	3.60	3.30	5.08	6.60
3.77	3.18	2.19	3.87	4.34	6.84
2.77	3.76	3.67	4.22	5.38	6.57
2.58	2.96	2.73	3.37	7.36	8.50
3.82	3.51	3.26	5.02	3.28	6.78
3.63	3.46	4.41	4.32	3.76	5.88
4.22	3.23	3.99	4.35	5.05	6.31
3.86	4.03	5.19	3.76	5.50	6.75
3.49	3.27	3.54	3.46	4.13	7.19
2.65	2.74	4.12	3.44	4.37	6.94
2.44	2.92	3.32	3.90	4.99	14.32
2.37	3.37	3.17	4.16	4.35	7.52
2.73	3.84	3.06	3.13	5.15	6.16
3.55	3.31	3.54	4.47	4.74	7.06
2.56	3.13	3.49	4.55	4.04	6.64
4.18	3.59	4.25	4.24	3.45	7.38
3.61	3.61	3.97	4.34	5.03	6.78
2.94	2.98	4.06	4.85	4.91	11.86
3.11	2.48	3.13	3.88	3.73	7.83
2.37	3.97	5.18	4.58	4.43	5.85
3.21	2.59	4.93	4.32	4.72	7.42
3.99	3.62	3.36	4.51	4.09	6.73
3.32	2.78	4.17	4.18	5.19	8.26
3.51	2.98	2.80	5.37	5.60	7.17
3.56	3.26	4.28	4.45	4.39	6.97
3.41	2.69	4.48	3.64	4.22	6.33
3.39	2.96	3.49	3.42	4.66	6.73
3.88	2.80	4.06	3.42	4.30	6.23
3.58	4.19	3.47	4.03	4.15	8.06
3.88	3.49	4.48	3.97	5.06	9.46
3.52	3.64	3.61	4.53	3.88	5.72
3.23	3.55	4.30	3.80	3.90	7.40
3.21	3.17	3.94	4.21	4.34	6.34
3.97	3.15	4.14	3.99	3.94	7.18

Table A1.4 continued

NEONATES	7 DAYS	14 DAYS	18 DAYS	21 DAYS	ADULT
4.25	2.78	2.69	3.66	4.56	7.16
4.41	3.49	3.92	3.64	3.69	7.60
5.08	3.68	2.91	4.33	4.83	7.00
2.69	2.56	3.05	4.69	3.05	7.01
3.47	3.74	4.70	2.44	4.30	7.95
2.49	2.44	3.55	5.33	3.16	7.45
2.99	3.03	3.89	4.77	3.69	9.89
2.91	3.01	3.10	4.73	5.00	10.33
3.19	4.42	4.72	0.67	3.21	7.33
4.06	3.36	5.06	4.41	4.05	8.93
2.75	3.66	4.15	4.01	4.64	7.70
4.36	3.42	5.08	3.77	3.11	5.50
2.89	3.98	2.93	4.32	3.60	11.74
2.97	3.83	3.40	4.34	3.50	7.00
3.76	2.52	4.51	3.20	3.77	5.41
2.73	3.62	4.10	3.58	3.97	4.47
2.75	2.82	3.78	3.97	3.36	6.90
3.90	3.06	4.12	4.60	3.13	6.53
2.75	2.78	4.12	2.73	3.75	9.95
3.27	2.80	3.13	3.99	3.45	5.90
2.43	4.07	3.02	3.46	3.69	6.47
3.46	2.78	3.06	4.80	3.88	7.16
2.90	3.12	2.70	2.91	3.86	6.50
3.00	2.91	4.42	5.29	3.82	8.63
3.46	2.57	3.23	3.03	4.31	6.72
2.31	3.68	3.59	4.34	4.74	7.41
2.78	4.11	3.77	5.03	3.93	6.43
3.40	3.71	4.02	3.01	3.86	6.82
3.02	2.20	4.44	3.13	4.34	7.57
2.77	4.02	4.40	5.60	4.48	8.27
3.04	2.84	3.00	3.61	4.59	6.47
3.28	3.90	3.73	3.21	4.79	8.46
2.78	4.08	3.63	3.80	3.74	6.87
3.04	4.54	3.33	4.69	4.33	7.37
3.69	2.65	3.33	4.67	4.28	7.16
4.17	3.73	5.01	4.55	4.89	7.16
3.26	4.43	3.43	4.06	3.74	5.35
2.98	4.30	4.24	3.98	3.95	6.56
3.63	2.78	4.54	3.57	3.56	8.45
3.97	4.17	3.87	4.96	4.32	9.04
3.08	3.91	3.71	3.70	4.13	7.85
3.32	3.73	4.84	3.57	4.35	7.03
4.03	3.59	3.32	2.72	4.50	6.87
3.56	3.35	2.74	3.84	3.78	6.08
3.65	3.59	3.91	4.47	4.22	5.23
3.63	3.63	3.80	3.96	4.52	7.24
2.69	4.72	3.56	4.65	6.31	8.87
2.63	3.50	2.63	4.14	4.90	7.36
2.96	3.22	2.70	4.28	3.93	16.71999
3.54	4.10	3.76	3.90	4.81	7.39

Table A1.5 Boundary Trace of Sarcolemma (mm)

NEONATES	7 DAYS	14 DAYS	18 DAYS	21 DAYS	ADULT
1030.2	1110.7	734.7	1141.8	682.6	991.5
438.7	1045.2	506.5	547.9	452.2	557.2
1263.8	473.2	586.1	1269.6	826.8	848.6
618.0	1146.4	409.9	1316.8	1037.3	623.5
458.5	1369.8	432.5	1288.3	644.9	346.0
696.8	983.6	1051.9	868.1	374.6	537.8
878.4	675.2	974.6	1128.4	570.3	300.1
669.0	892.6	695.1	843.9	992.1	771.4
1045.8	1678.8	1279.9	947.7	874.3	654.1
1031.6	1055.4	1401.1	1029.8	835.8	385.1
841.0	881.9	585.5	335.2	712.0	488.2
452.3	1075.7	338.9	683.0	835.6	514.9
946.5	733.5	856.2	561.2	1177.3	313.4
729.8	857.1	889.7	528.2	611.1	221.1
850.9	1393.8	569.9	1069.9	1025.8	314.6
804.6	344.7	1542.0	617.3	935.3	699.0
386.9	658.2	864.8	1094.5	1160.6	705.7
309.7	821.7	194.1	548.9	600.7	617.4
457.7	845.0	1625.1	934.1	716.0	750.7
1261.5	720.5	989.4	1070.5	864.3	631.2
803.0	1042.1	1413.6	744.8	899.9	381.3
726.0	265.9	677.6	1171.6	470.5	658.0
936.1	1152.0	917.8	703.2	970.1	871.1
1061.1	1015.4	1292.8	619.0	715.4	738.9
1107.4	983.8	480.5	893.7	404.4	809.4
887.1	1214.5	1030.4	794.5	860.2	272.0
960.7	701.1	848.8	1119.4	566.2	452.9
898.9	918.6	1080.0	1317.9	630.1	791.5
997.1	926.9	927.4	746.2	767.3	1240.3
1724.4	734.8	925.7	1103.0	477.1	541.8
241.0	1211.6	511.0	1776.3	510.4	711.9
1479.0	787.4	988.2	485.6	389.1	487.5
435.0	628.1	785.5	561.1	509.9	379.7
1154.9	1824.6	1175.7	647.1	1057.1	241.4
95.0	498.2	382.2	491.3	843.9	537.9
1215.5	611.3	753.9	372.8	257.3	353.3
1660.2	902.3	494.5	480.9	676.5	240.7
825.6	1264.5	840.5	590.5	504.2	467.3
674.4	506.9	586.1	708.2	826.3	388.1
664.5	606.9	463.5	902.5	766.6	840.6
1231.8	735.8	825.6	533.7	705.3	567.5
634.8	764.5	533.9	478.7	1024.3	541.2
1033.5	684.7	800.6	1022.7	791.8	434.1
899.4	985.0	1084.2	632.4	610.4	598.9
1312.6	847.5	591.6	972.3	593.6	426.3
510.2	1011.6	824.9	639.5	336.1	255.7
936.0	733.2	770.4	928.5	431.3	508.1
1280.0	1278.0	607.5	628.2	116.5	539.9
1183.4	1257.6	984.6	603.9	728.4	398.5
780.3	930.2	808.9	646.4	403.8	276.3

Table A1.5 continued

NEONATES	7 DAYS	14 DAYS	18 DAYS	21 DAYS	ADULT
819.7	602.7	55.6	82.6	46.5	03.3
1213.8	783.4	913.3	744.3	788.2	726.0
933.6	733.5	919.9	710.3	1031.1	549.9
791.8	783.4	162.7	437.0	970.6	413.9
757.4	368.7	484.8	458.3	631.7	932.9
940.3	694.7	175.2	674.9	413.7	494.4
1185.3	751.8	49.5	344.1	696.1	673.3
1199.7	531.5	1210.8	967.6	393.8	380.5
1433.7	698.0	712.2	376.5	329.2	506.0
1309.2	1185.6	845.0	216.4	441.4	542.0
1197.8	492.5	669.6	359.7	439.3	823.4
953.9	1256.3	275.0	458.8	765.2	336.3
1109.9	649.9	341.9	433.0	905.6	535.2
802.0	1131.4	183.3	365.6	471.3	475.6
1524.2	1142.1	551.4	592.6	770.1	467.9
713.8	1368.3	708.5	1059.4	491.9	423.2
951.3	1197.2	1624.4	233.9	981.7	688.6
857.8	941.6	489.4	1004.0	795.0	534.6
1664.1	1133.4	1016.3	527.9	346.1	704.1
1032.1	1322.6	996.8	571.0	541.2	655.0
754.7	953.9	958.0	714.9	606.5	482.9
967.6	731.4	669.0	556.9	491.5	205.0
776.0	669.3	843.8	210.1	618.1	763.9
1201.0	836.2	829.2	517.7	442.4	187.4
1054.7	827.9	764.2	163.2	552.5	484.5
2073.1	767.9	812.4	813.7	747.8	247.7
939.2	681.2	723.8	830.1	531.3	842.3
1144.2	1261.5	792.0	455.4	264.9	707.6
749.9	567.5	756.6	1022.3	1149.4	781.9
1239.4	918.1	901.7	386.5	1308.2	514.5
892.5	955.6	1103.9	910.5	580.9	104.3
523.8	916.7	1249.7	1108.7	460.4	757.8
265.2	1432.7	537.0	513.8	1058.3	348.2
436.1	1392.5	679.5	893.8	701.5	588.2
310.6	902.5	1060.7	983.8	998.4	868.8
878.1	769.1	1055.7	596.8	699.0	445.8
977.7	1144.9	536.2	329.5	580.4	669.3
902.3	900.4	940.0	841.6	783.8	638.9
1048.1	1288.0	501.1	1084.4	747.4	385.9
660.7	1451.5	316.4	763.5	1133.7	635.9
711.7	647.4	464.4	767.9	590.4	508.7
966.4	342.7	556.3	803.1	697.6	638.0
1136.4	1046.8	375.0	726.5	734.7	549.1
658.3	355.8	791.6	926.0	380.1	315.8
722.9	622.9	1094.6	563.9	1101.3	837.5
1540.9	1010.7	1161.8	557.7	902.6	569.7
1038.3	881.0	843.0	1141.6	1038.4	513.2
869.5	660.1	863.2	801.0	1068.8	1069.4
1213.0	765.7	397.9	827.6	421.5	623.1
828.8	1331.7	1152.0	1042.5	743.3	598.8

Table A1.6 Boundary Trace of Caveolae and T-tubules (mm)

NEONATES	7 DAYS	14 DAYS	18 DAYS	21 DAYS	ADULT
154.1	189.1	41.6	287.8	216.9	363.1
74.4	231.3	118.0	140.5	256.9	188.9
199.5	72.1	100.2	348.1	304.2	430.7
137.2	119.7	87.1	347.8	297.6	264.1
94.2	147.5	10.8	241.2	295.9	195.5
126.3	149.4	144.2	268.4	99.3	263.6
130.6	56.0	82.6	314.3	138.3	125.9
113.4	147.0	11.1	258.7	360.0	308.6
78.8	239.3	235.8	215.2	311.0	352.6
127.0	110.0	130.1	166.5	278.4	109.8
96.0	146.0	157.6	140.2	206.6	168.5
86.6	232.6	46.5	253.6	364.5	213.3
187.4	77.5	127.3	94.8	162.9	81.5
28.1	154.5	134.3	121.8	232.5	187.3
123.2	119.4	69.6	313.5	267.7	110.1
153.3	66.2	168.3	204.2	231.1	231.3
74.0	150.4	176.7	294.4	191.0	293.7
52.5	98.6	39.1	334.9	262.1	206.8
124.2	170.8	144.3	268.0	166.8	232.6
131.6	179.8	82.9	259.1	172.8	262.2
108.8	168.0	266.9	294.4	228.4	149.9
77.2	53.5	117.3	424.4	203.5	400.9
187.4	135.2	183.0	165.6	164.0	451.8
124.8	107.7	306.4	291.4	199.6	267.4
155.2	126.7	43.8	183.3	125.4	436.3
86.1	150.3	128.0	181.4	446.7	81.1
81.9	134.4	84.5	276.3	218.0	261.8
105.0	129.7	130.3	404.8	216.0	339.4
94.1	88.0	65.6	137.1	236.7	648.5
187.5	86.6	93.2	142.4	281.8	134.9
70.3	365.1	112.1	645.0	155.9	230.8
131.8	154.6	169.5	201.6	166.0	258.1
42.5	80.9	91.0	232.7	255.3	242.7
126.1	132.5	84.2	149.0	699.7	79.6
20.7	42.0	35.0	106.3	262.8	225.1
44.0	77.4	108.2	128.2	105.9	166.8
102.8	136.0	80.6	49.2	274.9	189.9
36.7	101.1	78.2	128.4	296.0	221.7
39.3	40.6	64.1	195.5	264.7	178.7
40.2	85.2	35.0	269.5	311.7	462.1
112.9	128.5	93.9	180.3	233.0	155.8
139.5	82.9	83.6	83.8	297.7	212.8
94.7	73.8	58.8	276.3	308.0	175.2
168.5	159.7	122.2	206.8	226.9	180.8
265.3	92.0	74.8	227.4	275.6	304.5
59.7	67.1	132.0	288.1	111.3	123.7
167.5	59.1	44.9	399.0	172.4	210.5
169.1	151.6	78.3	254.3	65.5	110.4
102.9	112.7	111.6	226.9	180.4	100.6
111.9	89.4	123.6	330.5	154.2	115.8

Table A1.6 continued

NEONATES	7 DAYS	14 DAYS	18 DAYS	21 DAYS	ADULT
105.2	116.0	105.5	244.6	213.0	363.5
122.6	75.5	78.9	322.4	204.2	292.6
169.9	89.7	201.6	270.2	354.3	237.1
93.4	119.1	84.3	203.2	436.3	217.4
108.9	32.5	145.8	216.7	219.1	467.9
84.4	70.1	22.6	236.3	149.1	241.4
121.5	91.0	10.1	148.7	201.7	359.6
227.6	45.2	104.0	188.9	235.7	157.1
141.9	140.4	159.1	113.0	76.2	170.7
129.7	80.0	104.3	123.5	205.5	212.9
73.6	57.8	45.6	118.8	159.0	245.8
119.4	128.8	50.3	106.9	350.2	139.6
54.1	109.9	92.0	129.8	330.1	230.1
96.2	93.6	23.8	117.2	191.9	249.7
204.3	115.0	53.8	265.5	310.1	211.5
119.7	68.0	84.4	329.8	175.6	87.9
96.1	102.5	168.1	107.3	311.0	335.8
118.6	108.2	89.0	270.1	192.6	256.7
143.0	105.0	118.5	182.9	134.4	278.8
89.7	111.1	61.6	121.0	184.2	351.2
77.8	108.1	75.0	268.6	239.7	279.4
104.0	92.8	74.6	233.9	146.0	101.0
65.5	56.1	77.9	60.4	188.6	327.1
107.8	119.4	77.8	149.6	225.9	61.3
127.4	89.8	71.7	55.0	186.1	291.9
141.8	34.8	83.9	274.7	280.2	144.9
86.2	108.3	89.4	276.6	248.8	340.0
158.0	126.5	165.7	242.9	153.9	354.0
66.6	40.8	237.4	340.4	384.0	346.6
68.8	95.7	149.5	108.6	392.5	349.9
68.2	67.6	152.4	366.1	241.4	55.8
130.0	127.3	122.0	395.8	230.6	512.4
79.2	205.4	51.4	198.5	293.4	219.2
97.4	206.4	99.3	161.2	305.4	293.0
11.1	188.9	147.2	197.2	273.8	443.5
118.3	73.6	136.6	166.5	462.9	232.2
129.8	119.2	91.3	104.8	167.2	288.6
121.5	58.6	137.3	192.9	214.8	277.8
57.8	109.3	92.3	128.9	275.5	234.1
51.1	126.3	49.7	109.3	272.5	220.1
39.0	68.5	72.3	106.9	196.5	260.4
91.8	87.7	103.2	259.3	186.4	396.3
97.7	126.2	43.7	161.5	208.6	299.5
87.6	42.5	69.0	237.8	189.6	153.3
124.0	73.6	85.2	158.3	198.2	364.6
108.4	86.3	69.6	146.9	272.1	380.9
60.4	146.0	118.6	239.7	335.1	230.5
49.3	82.0	123.8	113.5	346.3	332.3
48.7	98.1	107.2	205.6	88.8	444.8
59.2	101.	144.4	277.8	189.0	241.9

Table A1.7 Surface Density of Cav+T ($\mu\text{m}^2/\mu\text{m}^2$)

NEONATES	7 DAYS	14 DAYS	18 DAYS	21 DAYS	ADULT
.150	.170	.056	.252	.318	.366
.170	.221	.233	.256	.568	.339
.158	.221	.182	.274	.368	.508
.222	.104	.216	.264	.287	.424
.206	.108	.136	.187	.459	.565
.181	.152	.136	.309	.265	.490
.149	.083	.085	.278	.243	.420
.169	.165	.174	.306	.363	.400
.075	.143	.184	.227	.356	.539
.123	.104	.093	.162	.333	.285
.114	.166	.269	.418	.290	.345
.192	.216	.137	.371	.436	.414
.198	.106	.149	.169	.138	.260
.038	.180	.160	.231	.381	.847
.145	.086	.122	.296	.261	.350
.191	.192	.169	.331	.247	.331
.239	.229	.204	.269	.165	.416
.169	.120	.214	.610	.436	.335
.271	.202	.089	.287	.233	.310
.104	.249	.084	.242	.200	.415
.136	.161	.189	.395	.254	.393
.106	.201	.173	.362	.433	.609
.200	.117	.145	.236	.169	.518
.118	.106	.160	.471	.279	.362
.140	.129	.091	.205	.310	.539
.097	.124	.124	.228	.519	.298
.085	.192	.100	.247	.385	.578
.117	.141	.121	.307	.343	.429
.094	.095	.071	.184	.309	.523
.109	.118	.101	.129	.591	.249
.292	.301	.219	.363	.305	.324
.089	.196	.172	.415	.427	.529
.098	.129	.116	.415	.501	.639
.109	.073	.072	.230	.662	.330
.218	.084	.092	.216	.311	.419
.036	.127	.136	.344	.412	.472
.062	.151	.163	.102	.406	.789
.045	.080	.093	.218	.587	.474
.058	.080	.109	.276	.320	.459
.060	.140	.076	.299	.407	.550
.092	.175	.114	.338	.330	.275
.220	.108	.157	.175	.291	.393
.092	.108	.073	.270	.389	.404
.187	.162	.113	.327	.372	.302
.202	.106	.126	.234	.464	.714
.117	.066	.160	.451	.331	.484
.178	.081	.058	.430	.400	.414
.132	.119	.129	.405	.562	.205
.087	.090	.113	.376	.248	.252
.143	.096	.153	.511	.382	.419

Table A1.7 continued

NEONATES	7 DAYS	14 DAYS	18 DAYS	21 DAYS	ADULT
.128	.193	.124	.358	.477	.453
.101	.096	.082	.433	.259	.403
.182	.122	.204	.380	.343	.431
.118	.152	.177	.465	.450	.525
.144	.088	.147	.473	.346	.502
.089	.101	.129	.350	.360	.488
.103	.121	.204	.432	.290	.534
.190	.085	.085	.195	.599	.413
.099	.201	.223	.300	.232	.337
.099	.068	.123	.571	.466	.471
.061	.117	.068	.330	.362	.299
.125	.103	.205	.233	.458	.415
.049	.169	.109	.300	.364	.430
.120	.083	.130	.321	.407	.525
.134	.101	.098	.448	.403	.452
.168	.050	.119	.311	.357	.208
.101	.086	.104	.459	.317	.488
.138	.115	.194	.269	.243	.480
.086	.093	.117	.347	.388	.396
.087	.084	.068	.212	.340	.536
.103	.113	.078	.378	.395	.579
.108	.127	.112	.420	.297	.491
.084	.084	.092	.288	.305	.428
.090	.143	.123	.289	.511	.327
.121	.109	.094	.337	.337	.603
.068	.045	.103	.338	.375	.585
.092	.159	.123	.333	.468	.404
.138	.100	.209	.533	.581	.500
.089	.072	.314	.333	.334	.443
.055	.105	.166	.281	.300	.679
.076	.089	.138	.402	.416	.535
.248	.139	.098	.357	.501	.676
.299	.143	.096	.386	.277	.630
.223	.118	.146	.180	.435	.498
.036	.209	.139	.200	.274	.511
.135	.096	.129	.279	.662	.521
.133	.104	.170	.318	.288	.431
.335	.065	.146	.229	.274	.435
.055	.085	.184	.119	.369	.607
.077	.087	.157	.143	.240	.346
.055	.106	.156	.139	.333	.512
.095	.256	.186	.323	.267	.621
.086	.121	.117	.222	.283	.545
.133	.119	.087	.257	.498	.485
.172	.118	.078	.281	.180	.435
.070	.085	.060	.263	.302	.669
.058	.166	.141	.210	.323	.449
.057	.124	.143	.142	.324	.311
.040	.128	.269	.248	.211	.714
.071	.076	.129	.266	.254	.404

Table A1.8 Boundary Trace of Peripheral Couplings (mm)

NEONATES	7 DAYS	14 DAYS	18 DAYS	21 DAYS	ADULT
10.76	22.43	31.52	4.38	89.95	74.86
2.81	27.57	15.57	25.62	49.57	29.24
6.57	37.90	9.95	42.67	43.86	0.81
1.95	14.57	14.90	26.29	87.67	46.71
4.86	39.57	16.81	59.86	59.62	24.48
13.43	13.33	7.10	15.86	32.52	43.33
4.52	2.90	26.33	79.19	24.10	28.24
8.05	24.57	21.67	56.95	35.00	31.33
4.86	32.29	15.48	32.00	69.62	31.76
9.62	31.43	26.57	46.43	43.43	46.71
7.05	25.62	5.33	8.90	47.48	20.24
5.19	23.10	13.67	19.52	44.67	40.05
5.71	8.62	11.81	2.05	59.00	10.62
6.10	29.38	20.57	19.71	28.86	17.95
3.19	29.86	20.86	19.90	24.00	13.67
3.43	21.67	2.90	19.62	29.86	18.10
18.57	32.52	0.0	5.19	3.90	26.33
17.33	29.43	4.38	13.29	64.86	24.52
24.62	27.90	26.33	10.57	34.10	27.38
14.90	46.19	54.00	13.71	35.10	12.95
4.05	14.90	5.48	28.62	56.95	15.14
14.10	17.24	7.05	63.76	38.86	18.76
11.33	8.67	4.71	42.43	40.71	33.48
9.71	21.81	18.71	54.90	69.76	40.10
16.67	4.38	21.81	24.57	52.00	0.0
6.05	0.0	39.29	42.43	62.81	27.43
20.05	4.71	35.81	108.29	44.05	34.48
26.95	26.48	10.95	43.67	40.24	26.19
4.76	22.67	32.43	39.81	44.00	32.00
39.29	20.14	29.48	78.10	50.14	22.00
2.48	19.05	16.76	33.71	39.10	18.81
39.90	20.24	6.52	31.43	20.48	24.57
25.95	7.57	12.95	51.76	16.24	28.62
15.05	24.00	24.62	32.81	73.05	17.52
4.86	15.00	10.76	22.00	44.86	33.67
0.0	0.0	18.67	13.14	20.57	23.48
0.0	20.43	4.62	33.14	52.33	12.00
3.00	11.76	25.19	56.81	31.19	6.00
0.0	3.90	25.00	0.0	70.62	22.67
8.67	10.14	12.19	18.29	80.67	30.38
29.90	17.05	6.19	10.19	36.71	33.48
24.52	47.48	0.0	76.57	72.86	23.86
27.57	13.33	13.24	67.29	43.52	38.29
43.19	18.76	12.71	35.81	5.71	57.33
29.67	57.57	5.05	46.05	31.10	0.0
6.86	17.05	6.19	10.19	36.71	33.48
0.0	18.52	25.86	55.00	40.90	22.33
24.29	34.24	11.95	32.43	8.33	21.62
13.14	5.43	0.0	42.76	57.05	50.29
6.62	7.14	9.43	28.76	18.52	18.52

Table A1.8 continued

NEONATES	7 DAYS	14 DAYS	18 DAYS	21 DAYS	ADULT
23.81	0.0	14.81	20.95	13.00	40.57
17.05	3.38	0.52	34.48	62.81	61.76
8.67	25.00	22.24	0.0	86.71	32.52
28.71	14.57	20.00	25.76	43.43	27.05
15.05	0.0	10.33	40.81	27.81	13.86
18.90	32.29	16.57	25.86	23.24	29.71
20.52	0.0	2.62	10.81	63.52	40.05
0.0	21.29	28.81	51.52	36.19	6.10
21.90	22.86	16.38	24.48	25.71	18.14
15.67	25.00	0.0	20.90	31.19	43.90
19.10	10.67	9.29	18.67	36.38	57.71
34.38	21.86	12.29	0.57	0.52	16.86
29.90	6.29	15.57	16.57	86.76	56.48
4.19	17.95	10.48	21.19	34.00	24.10
15.86	27.24	23.86	38.76	32.00	20.71
14.19	19.19	13.05	34.05	54.86	14.81
15.24	6.43	49.00	24.76	65.33	50.19
0.0	32.00	50.52	78.38	84.00	12.67
12.29	34.19	32.71	26.00	54.76	3.33
18.95	7.05	39.67	33.05	48.29	57.38
24.00	16.05	49.19	49.67	52.29	18.95
0.0	19.19	9.67	19.29	55.33	35.62
25.62	6.86	4.10	13.67	27.86	40.10
41.00	2.29	18.62	45.81	45.43	0.0
31.95	10.81	9.90	45.67	27.48	23.43
20.67	26.10	7.24	17.86	66.33	28.14
2.76	2.33	19.62	25.24	33.29	49.33
10.90	11.57	11.10	42.43	25.14	29.24
18.10	4.38	2.71	32.43	59.10	19.43
0.0	30.76	17.67	24.38	62.10	43.48
0.0	16.29	34.62	52.62	36.14	0.0
8.05	32.95	35.38	63.76	25.38	35.48
0.0	38.05	18.48	32.81	58.71	10.38
20.95	30.81	7.48	18.43	51.90	14.05
4.57	10.86	21.95	26.48	34.62	44.29
0.0	8.67	12.81	34.81	50.76	35.95
11.19	41.10	6.29	26.71	27.62	27.24
14.29	11.24	13.43	48.81	51.90	20.10
18.29	9.90	14.67	40.43	53.71	21.24
24.19	21.00	12.33	42.81	25.14	10.24
16.24	11.33	20.57	48.90	43.62	6.71
3.10	6.48	17.24	10.10	34.67	14.90
28.10	3.19	3.48	18.33	32.90	35.00
0.0	4.24	6.24	40.95	22.67	33.67
10.95	0.0	9.14	29.19	72.43	37.86
12.57	0.0	4.67	20.00	55.05	39.62
29.81	9.52	12.62	39.86	24.14	24.19
11.90	26.29	0.0	21.10	90.52	39.10
33.48	6.81	13.67	47.48	17.14	36.62
16.05	25.52	50.62	65.86	43.57	52.00

Table A1.9 Surface Density of Peripheral Couplings ($\mu\text{m}^2/\mu\text{m}^2$)

NEONATES	7 DAYS	14 DAYS	18 DAYS	21 DAYS	ADULT
0.0104	0.0202	0.0429	0.0038	0.1318	0.0755
0.0064	0.0264	0.0307	0.0468	0.1096	0.0525
0.0052	0.0801	0.0176	0.0336	0.0530	0.0010
0.0032	0.0127	0.0369	0.0200	0.0845	0.0749
0.0106	0.0289	0.0389	0.0465	0.0924	0.0707
0.0193	0.0136	0.0067	0.0183	0.0868	0.0806
0.0051	0.0043	0.0270	0.0702	0.0422	0.0941
0.0120	0.0275	0.0312	0.0675	0.0353	0.0406
0.0046	0.0192	0.0121	0.0338	0.0796	0.0486
0.0093	0.0298	0.0189	0.0451	0.0520	0.1213
0.0084	0.0290	0.0091	0.0266	0.0667	0.0414
0.0115	0.0215	0.0403	0.0286	0.0534	0.0778
0.0060	0.0117	0.0138	0.0036	0.0501	0.0339
0.0083	0.0343	0.0245	0.0373	0.0472	0.0812
0.0037	0.0214	0.0366	0.0186	0.0234	0.0434
0.0043	0.0629	0.0019	0.0318	0.0319	0.0259
0.0480	0.0494	0.0	0.0047	0.0034	0.0373
0.0560	0.0358	0.0226	0.0240	0.1080	0.0397
0.0538	0.0330	0.0162	0.0113	0.0476	0.0365
0.0118	0.0641	0.0546	0.0128	0.0406	0.0205
0.0050	0.0143	0.0039	0.0384	0.0633	0.0397
0.0194	0.0648	0.0104	0.0544	0.0826	0.0285
0.0121	0.0075	0.0051	0.0603	0.0420	0.0384
0.0091	0.0215	0.0145	0.0884	0.0975	0.0543
0.0150	0.0044	0.0454	0.0275	0.1286	0.0
0.0068	0.0	0.0381	0.0534	0.0730	0.1008
0.0209	0.0067	0.0422	0.0967	0.0778	0.0761
0.0300	0.0288	0.0101	0.0331	0.0639	0.0331
0.0048	0.0244	0.0350	0.0533	0.0573	0.0258
0.0228	0.0274	0.0318	0.0708	0.1051	0.0406
0.0103	0.0157	0.0328	0.0190	0.0766	0.0264
0.0270	0.0257	0.0066	0.0647	0.0526	0.0504
0.0597	0.0120	0.0166	0.0922	0.0318	0.0754
0.0130	0.0131	0.0209	0.0507	0.0691	0.0726
0.0511	0.0301	0.0282	0.0448	0.0531	0.0626
0.0	0.0	0.0235	0.0352	0.0799	0.0664
0.0	0.0226	0.0093	0.0689	0.0774	0.0499
0.0036	0.0093	0.0300	0.0962	0.0619	0.0128
0.0	0.0077	0.0426	0.0	0.0855	0.0584
0.0130	0.0167	0.0263	0.0203	0.1052	0.0361
0.0243	0.0232	0.0075	0.0191	0.0520	0.0590
0.0386	0.0621	0.0	0.1600	0.0711	0.0441
0.0267	0.0195	0.0165	0.0658	0.0550	0.0882
0.0480	0.0190	0.0117	0.0566	0.0094	0.0957
0.0226	0.0679	0.0085	0.0474	0.0524	0.0
0.0134	0.0168	0.0075	0.0159	0.1092	0.1309
0.0	0.0253	0.0336	0.0592	0.0948	0.0440
0.0190	0.0268	0.0197	0.0517	0.0715	0.0400
0.0111	0.0043	0.0	0.0708	0.0783	0.1262
0.0085	0.0077	0.0117	0.0445	0.0459	0.0670

Table A1.9 continued

NEONATES	7 DAYS	14 DAYS	18 DAYS	21 DAYS	ADULT
0.0290	0.0	0.0173	0.0307	0.0291	0.0505
0.0140	0.0043	0.0110	0.0463	0.0797	0.0851
0.0093	0.0341	0.0224	0.0	0.0841	0.0591
0.0363	0.0186	0.0551	0.0589	0.0447	0.0653
0.0199	0.0	0.0104	0.0890	0.0440	0.0149
0.0201	0.0465	0.0946	0.0383	0.0562	0.0601
0.0173	0.0	0.0529	0.0314	0.0913	0.0595
0.0	0.0400	0.0236	0.0532	0.0919	0.0160
0.0153	0.0327	0.0230	0.0650	0.0781	0.0359
0.0120	0.0211	0.0	0.0966	0.0707	0.0810
0.0159	0.0217	0.0139	0.0519	0.0828	0.0701
0.0360	0.0174	0.0447	0.0012	0.0007	0.0501
0.0269	0.0097	0.0185	0.0383	0.0958	0.1055
0.0052	0.0159	0.0571	0.0580	0.0721	0.0507
0.0104	0.0238	0.0433	0.0654	0.0415	0.0443
0.0199	0.0140	0.0184	0.0321	0.1115	0.0350
0.0160	0.0054	0.0302	0.1059	0.0665	0.0729
0.0	0.0340	0.1100	0.0781	0.1057	0.0237
0.0074	0.0302	0.0322	0.0492	0.1582	0.0047
0.0184	0.0053	0.0437	0.0579	0.0892	0.0876
0.0318	0.0168	0.0513	0.0699	0.0862	0.0393
0.0	0.0262	0.0144	0.0346	0.1126	0.1738
0.0330	0.0102	0.0048	0.0650	0.0451	0.0525
0.0341	0.0027	0.0291	0.0885	0.1027	0.0
0.0303	0.0131	0.0130	0.2798	0.0497	0.0484
0.0100	0.0340	0.0089	0.0219	0.0887	0.1136
0.0029	0.0034	0.0271	0.0304	0.0626	0.0586
0.0095	0.0092	0.0140	0.0932	0.0945	0.0413
0.0241	0.0077	0.0036	0.0317	0.0514	0.0249
0.0	0.0335	0.0196	0.0631	0.0475	0.0845
0.0	0.0170	0.0314	0.0578	0.0622	0.0
0.0154	0.0359	0.0283	0.0575	0.0551	0.0468
0.0	0.0266	0.0344	0.0639	0.0555	0.0298
0.0480	0.0221	0.0110	0.0206	0.0734	0.0239
0.0147	0.0120	0.0207	0.0269	0.0347	0.0510
0.0	0.0113	0.0121	0.0583	0.0726	0.0806
0.0114	0.0359	0.0117	0.0811	0.0476	0.0407
0.0158	0.0125	0.0143	0.0580	0.0662	0.0315
0.0174	0.0077	0.0293	0.0373	0.0719	0.0550
0.0366	0.0145	0.0390	0.0561	0.0222	0.0161
0.0228	0.0175	0.0443	0.0637	0.0739	0.0132
0.0032	0.0189	0.0310	0.0126	0.0497	0.0234
0.0247	0.0030	0.0093	0.0252	0.0448	0.0637
0.0	0.0119	0.0079	0.0442	0.0596	0.1066
0.0151	0.0	0.0083	0.0518	0.0658	0.0452
0.0082	0.0	0.0040	0.0359	0.0610	0.0695
0.0287	0.0108	0.0150	0.0349	0.0232	0.0471
0.0137	0.0398	0.0	0.0263	0.0847	0.0366
0.0276	0.0089	0.0343	0.0574	0.0407	0.0588
0.0194	0.0192	0.0439	0.0632	0.0586	0.0868

Table A1.10 Boundary Trace of Internal Couplings (mm)

NEONATES	7 DAYS	14 DAYS	18 DAYS	21 DAYS	ADULT
0.0	0.0	0.0	0.0	11.24	14.62
0.0	0.0	2.33	6.24	0.0	0.0
0.0	0.0	5.43	11.10	0.0	12.05
0.0	0.0	6.67	6.1	12.0	10.1
0.0	4.10	0.0	6.9	25.24	0.0
0.0	4.10	1.62	7.38	6.05	15.48
0.0	0.0	5.19	23.19	9.76	0.0
0.0	0.0	0.0	0.0	32.0	0.0
0.0	0.0	3.19	15.67	10.67	11.81
0.0	0.0	0.0	12.57	16.52	0.0
0.0	0.0	7.62	0.0	15.90	4.29
0.0	1.24	5.62	6.0	12.48	0.0
0.0	0.0	0.0	0.0	0.0	0.0
0.0	0.0	0.0	0.0	32.90	0.0
0.0	0.0	4.86	8.19	11.29	0.0
0.0	2.95	0.0	8.10	0.0	10.76
0.0	3.29	0.0	0.0	18.24	16.81
0.0	0.0	3.67	4.24	26.05	0.0
0.0	5.00	0.0	7.43	0.0	5.90
0.0	9.29	0.0	5.57	14.05	0.0
0.0	0.0	9.00	2.71	14.0	9.90
0.0	0.0	0.0	0.0	0.0	24.00
0.0	0.0	8.29	14.38	19.43	0.0
0.0	0.0	0.0	10.24	24.00	8.00
0.0	0.0	0.0	0.0	8.81	0.0
0.0	0.0	8.62	10.48	16.52	25.10
0.0	0.0	7.0	8.95	9.95	5.76
0.0	0.0	0.0	15.19	6.33	23.62
0.0	0.0	0.0	9.05	16.57	13.62
0.0	0.0	6.10	10.14	14.38	0.0
0.0	0.0	0.0	2.33	17.24	21.24
0.0	0.0	3.67	21.48	7.38	3.71
0.0	0.0	0.0	3.29	0.0	10.24
0.0	0.0	8.38	11.24	17.10	0.0
0.0	0.0	0.0	10.76	0.0	16.71
0.0	0.0	3.71	6.38	0.0	12.52
0.0	0.0	0.0	8.76	21.19	15.30
0.0	0.0	5.05	0.0	18.67	10.95
0.0	0.0	31.10	0.0	16.38	8.76
0.0	0.0	0.0	16.57	19.43	16.81
0.0	0.0	6.43	1.81	11.33	0.0
0.0	7.48	0.0	0.0	2.86	6.38
0.0	0.0	0.0	7.52	0.0	12.24
0.0	4.14	16.00	5.29	3.19	14.48
0.0	0.0	0.0	0.0	0.0	0.0
0.0	0.0	0.0	10.52	3.43	19.29
0.0	0.0	3.43	7.33	0.0	24.86
0.0	0.0	0.0	0.0	4.33	13.38
0.0	0.0	0.0	10.29	0.0	14.43
0.0	3.00	2.29	10.43	4.86	28.90

Table A1.10 continued

NEONATES	7 DAYS	14 DAYS	18 DAYS	21 DAYS	ADULT
0.0	0.0	1.86	2.95	10.48	28.05
0.0	0.0	3.90	7.24	10.05	11.33
0.0	0.0	9.05	0.0	12.14	7.81
0.0	0.0	3.81	0.0	10.71	0.0
0.0	0.0	0.0	6.71	10.90	0.0
0.0	0.0	0.0	0.0	10.81	0.0
0.0	0.0	0.0	0.0	0.0	26.29
0.0	0.0	0.0	21.52	6.00	10.00
0.0	5.00	6.90	0.0	0.0	0.0
0.0	0.0	0.0	8.57	10.86	11.76
0.0	0.0	0.0	7.38	7.71	0.0
0.0	0.0	0.0	7.86	7.67	16.81
0.0	0.0	3.14	0.0	11.52	10.00
0.0	0.0	0.0	11.24	15.14	16.05
0.0	0.0	2.76	10.43	8.33	11.95
0.0	0.0	0.0	7.67	14.52	0.0
0.0	0.0	12.24	4.95	21.86	15.62
0.0	0.0	9.10	12.62	0.0	0.0
0.0	0.0	0.0	0.0	17.43	9.90
0.0	0.0	3.43	0.0	16.76	9.62
0.0	2.14	0.0	4.00	9.57	0.0
0.0	0.0	2.19	10.62	0.0	33.14
0.0	0.0	0.0	4.19	3.19	9.95
0.0	0.0	0.0	15.52	10.62	0.0
0.0	0.0	0.0	5.81	0.0	19.67
0.0	0.0	0.0	6.76	18.67	11.67
0.0	0.0	0.0	6.14	8.00	53.86
0.0	0.0	1.90	0.0	18.00	15.43
0.0	0.0	3.24	0.0	7.67	15.43
0.0	0.0	3.29	8.62	19.33	11.14
0.0	0.0	0.0	9.00	0.0	0.0
0.0	0.0	8.90	12.62	8.48	20.95
0.0	0.0	10.52	14.62	15.81	14.90
0.0	0.0	0.0	3.29	0.0	10.33
0.0	8.76	0.0	0.0	7.29	13.62
0.0	7.81	3.19	0.0	27.90	20.38
0.0	0.0	0.0	8.24	12.33	0.0
0.0	7.14	0.0	5.90	3.81	23.38
0.0	0.0	0.48	0.0	10.48	10.29
0.0	0.0	0.0	7.52	23.14	9.71
0.0	0.0	0.0	4.14	13.52	4.52
0.0	0.0	0.0	7.00	8.62	7.38
0.0	0.0	0.0	13.38	0.0	10.43
0.0	0.0	0.0	0.0	14.09	5.95
0.0	0.0	0.0	0.0	18.33	0.0
0.0	0.0	0.0	16.14	0.0	20.00
0.0	0.0	0.0	0.0	0.0	42.86
0.0	0.0	0.0	7.05	16.10	20.05
0.0	0.0	0.0	0.0	0.0	25.90
0.0	0.0	3.19	14.76	8.62	11.81
0.0	0.0	5.24	2.52		
0.0	0.0	0.0			

Table A1.11 Surface Density of Internal Couplings ($\mu\text{m}^2/\mu\text{m}^2$)

NEONATES	7 DAYS	14 DAYS	18 DAYS	21 DAYS	ADULT
0.0	0.0	0.0	0.0	0.0165	0.0147
0.0	0.0	0.0046	0.0114	0.0	0.0
0.0	0.0	0.0096	0.0087	0.0	0.0142
0.0	0.0	0.0165	0.0046	0.0116	0.0162
0.0	0.0030	0.0	0.0054	0.0391	0.0
0.0	0.0042	0.0015	0.0085	0.0161	0.0288
0.0	0.0	0.0053	0.0206	0.0171	0.0
0.0	0.0	0.0	0.0	0.0323	0.0
0.0	0.0	0.0025	0.0165	0.0122	0.0181
0.0	0.0	0.0	0.0122	0.0199	0.0
0.0	0.0	0.0130	0.0	0.0223	0.0088
0.0	0.0012	0.0166	0.0088	0.0149	0.0
0.0	0.0	0.0	0.0	0.0	0.0
0.0	0.0	0.0	0.0	0.0539	0.0
0.0	0.0	0.0085	0.0077	0.0110	0.0
0.0	0.0086	0.0	0.0131	0.0	0.0154
0.0	0.0050	0.0	0.0	0.0157	0.0238
0.0	0.0	0.0189	0.0077	0.0434	0.0
0.0	0.0059	0.0	0.0080	0.0	0.0079
0.0	0.0129	0.0	0.0052	0.0163	0.0
0.0	0.0	0.0064	0.0036	0.0156	0.0260
0.0	0.0	0.0	0.0	0.0	0.0365
0.0	0.0	0.0090	0.0205	0.0200	0.0
0.0	0.0	0.0	0.0165	0.0336	0.0108
0.0	0.0	0.0	0.0	0.0218	0.0
0.0	0.0	0.0084	0.0132	0.0192	0.0923
0.0	0.0	0.0083	0.0080	0.0176	0.0127
0.0	0.0	0.0	0.0115	0.0101	0.0298
0.0	0.0	0.0	0.0121	0.0216	0.0110
0.0	0.0	0.0066	0.0092	0.0301	0.0
0.0	0.0	0.0	0.0013	0.0338	0.0298
0.0	0.0	0.0037	0.0442	0.0190	0.0077
0.0	0.0	0.0	0.0059	0.0	0.0270
0.0	0.0	0.0071	0.0174	0.0162	0.0
0.0	0.0	0.0	0.0219	0.0	0.0311
0.0	0.0	0.0047	0.0171	0.0	0.0355
0.0	0.0	0.0	0.0182	0.0313	0.0635
0.0	0.0	0.0060	0.0	0.0370	0.0234
0.0	0.0	0.0531	0.0	0.0198	0.0226
0.0	0.0	0.0	0.0184	0.0253	0.0200
0.0	0.0	0.0078	0.0034	0.0161	0.0
0.0	0.0098	0.0	0.0	0.0028	0.0118
0.0	0.0	0.0	0.0074	0.0	0.0282
0.0	0.0042	0.0148	0.0084	0.0052	0.0242
0.0	0.0	0.0	0.0	0.0	0.0
0.0	0.0	0.0	0.0165	0.0102	0.0754
0.0	0.0	0.0045	0.0079	0.0	0.0489
0.0	0.0	0.0	0.0	0.0376	0.0248
0.0	0.0	0.0	0.0170	0.0	0.0362
0.0	0.0032	0.0028	0.0161	0.0120	0.1046

Table A1.11 continued

NEONATES	7 DAYS	14 DAYS	18 DAYS	21 DAYS	ADULT
0.0	0.0	0.0022	0.0043	0.0235	0.0349
0.0	0.0	0.0041	0.0097	0.0128	0.0156
0.0	0.0	0.0091	0.0	0.0118	0.0142
0.0	0.0	0.0105	0.0	0.0110	0.0
0.0	0.0	0.0	0.0147	0.0173	0.0
0.0	0.0	0.0	0.0	0.0261	0.0
0.0	0.0	0.0	0.0	0.0	0.0390
0.0	0.0	0.0	0.0222	0.0152	0.0263
0.0	0.0072	0.0097	0.0	0.0	0.0
0.0	0.0	0.0	0.0396	0.0246	0.0217
0.0	0.0	0.0	0.0205	0.0176	0.0
0.0	0.0	0.0	0.0171	0.0100	0.0500
0.0	0.0	0.0037	0.0	0.0127	0.01878
0.0	0.0	0.0	0.0307	0.0321	0.0337
0.0	0.0	0.0050	0.0176	0.0108	0.0255
0.0	0.0	0.0	0.0072	0.0295	0.0
0.0	0.0	0.0075	0.0212	0.0223	0.0227
0.0	0.0	0.0198	0.0126	0.0	0.0
0.0	0.0	0.0	0.0	0.0504	0.0141
0.0	0.0	0.0038	0.0	0.0310	0.0147
0.0	0.0023	0.0	0.0056	0.0158	0.0
0.0	0.0	0.0033	0.0191	0.0	0.1617
0.0	0.0	0.0	0.0200	0.0052	0.0130
0.0	0.0	0.0	0.0300	0.0240	0.0
0.0	0.0	0.0	0.0356	0.0	0.0406
0.0	0.0	0.0	0.0083	0.0250	0.0471
0.0	0.0	0.0026	0.0074	0.0151	0.0639
0.0	0.0	0.0041	0.0	0.0679	0.0218
0.0	0.0	0.0043	0.0084	0.0067	0.0197
0.0	0.0	0.0	0.0233	0.0148	0.0217
0.0	0.0	0.0081	0.0139	0.0	0.0
0.0	0.0	0.0084	0.0132	0.0184	0.0277
0.0	0.0061	0.0	0.0064	0.0149	0.0428
0.0	0.0056	0.0	0.0	0.0	0.0176
0.0	0.0	0.0030	0.0	0.0073	0.0157
0.0	0.0092	0.0	0.0138	0.0399	0.0457
0.0	0.0	0.0	0.0179	0.0213	0.0
0.0	0.0	0.0005	0.0	0.0049	0.0366
0.0	0.0	0.0	0.0069	0.0140	0.0267
0.0	0.0	0.0	0.0054	0.0204	0.0153
0.0	0.0	0.0	0.0091	0.0229	0.0089
0.0	0.0	0.0	0.0167	0.0124	0.0116
0.0	0.0	0.0	0.0	0.0	0.0190
0.0	0.0	0.0	0.0	0.0371	0.0189
0.0	0.0	0.0	0.0286	0.0167	0.0
0.0	0.0	0.0	0.0	0.0	0.0351
0.0	0.0	0.0	0.0062	0.0	0.0835
0.0	0.0	0.0037	0.0	0.0151	0.0188
0.0	0.0	0.0132	0.0178	0.0	0.0416
0.0	0.0	0.0	0.0024	0.0116	0.0197

APPENDIX 2

Example of the rankings for cell diameter and the application of the Kruskal-Wallis test.

Table A2.1 Rankings of Cell Diameter Values from Table A1.4.

NEONATES	7 DAYS	14 DAYS	18 DAYS	21 DAYS	ADULT
103.5	91.0	469.5	304.5	333.0	578.0
63.0	161.0	408.5	250.0	507.0	574.0
107.0	23.0	237.0	22.0	460.0	526.0
24.0	73.5	483.5	113.0	424.0	532.0
168.0	421.0	256.5	168.0	384.0	508.0
186.0	176.0	2.0	214.0	495.0	548.0
29.0	184.0	61.0	339.0	452.0	588.0
304.5	155.5	298.0	262.5	307.5	579.0
94.5	138.5	47.0	198.5	488.5	569.0
163.5	239.5	136.0	277.5	345.5	546.5
6.0	98.0	408.5	502.0	448.5	594.0
123.5	225.0	402.5	500.0	494.0	538.0
221.0	121.5	367.0	399.5	501.0	576.0
15.5	339.0	128.0	440.0	488.5	586.0
70.5	147.0	147.0	443.5	378.0	582.0
94.5	36.5	133.5	369.0	485.0	512.0
349.0	76.5	217.5	145.0	477.0	524.0
267.5	121.5	3.0	284.5	391.5	535.0
48.5	262.5	239.5	364.5	492.0	523.0
20.0	76.5	39.5	161.0	558.5	585.0
275.5	194.5	138.5	469.5	143.5	532.0
229.0	180.0	405.0	384.0	262.5	505.0
364.5	133.5	320.5	396.0	473.0	513.5
282.0	327.0	481.5	262.5	496.5	530.0
189.0	141.5	198.5	180.0	349.0	555.0
27.5	42.5	345.5	174.0	399.5	540.0
11.0	70.5	150.5	294.0	466.0	599.0
7.5	161.0	119.5	355.0	396.0	567.0
39.5	279.5	101.0	113.0	479.0	510.0
202.0	147.0	198.5	416.0	450.5	546.5
17.5	113.0	189.0	430.5	329.0	525.0
359.5	214.0	371.5	369.0	176.0	561.0
221.0	221.0	313.0	391.5	471.5	532.0
73.5	81.0	333.0	459.0	463.0	598.0
107.0	13.0	113.0	288.0	252.5	572.0
7.5	313.0	480.0	433.0	411.5	504.0
128.0	21.0	464.0	384.0	446.0	565.0
320.5	225.0	158.0	424.0	339.0	528.5
150.5	53.0	357.0	359.5	481.5	580.0
194.5	81.0	58.0	491.0	498.5	553.0
205.5	138.5	374.0	414.0	401.0	541.0
168.0	31.5	419.0	233.0	364.5	515.0
163.5	76.5	189.0	171.0	438.0	528.5
288.0	58.0	333.0	171.0	378.0	511.0
210.5	361.0	184.0	327.0	353.5	577.0
288.0	189.0	419.0	313.0	474.5	592.0
196.0	233.0	221.0	427.0	288.0	503.0
133.5	202.0	378.0	273.0	294.0	563.0
128.0	119.5	304.5	362.0	391.5	516.0
313.0	117.0	351.5	320.5	304.5	554.0

Table A2.1 continued

NEONATES	7 DAYS	14 DAYS	18 DAYS	21 DAYS	ADULT
371.5	53.0	31.5	237.0	432.0	550.5
405.0	189.0	300.0	233.0	244.5	570.0
477.0	241.5	67.5	387.5	457.0	542.5
31.5	17.5	98.0	441.5	98.0	544.0
184.0	256.5	443.5	11.0	378.0	575.0
14.0	11.0	202.0	487.0	118.0	566.0
83.0	91.0	291.0	453.0	244.5	593.0
67.5	86.5	105.0	448.5	467.0	596.0
123.5	408.5	446.0	1.0	128.0	557.0
333.0	158.0	474.5	405.0	330.0	590.0
45.0	237.0	353.5	323.0	436.0	571.0
398.0	171.0	477.0	267.5	107.0	496.5
64.0	317.5	72.0	384.0	217.5	597.0
79.0	277.5	165.5	391.5	192.5	542.5
262.5	15.5	424.0	125.0	267.5	493.0
39.5	225.0	341.5	210.5	313.0	416.0
45.0	60.0	270.5	313.0	158.0	539.0
294.0	101.0	345.5	435.0	113.0	521.0
45.0	53.0	345.5	39.5	259.0	595.0
141.5	58.0	113.0	320.5	176.0	506.0
9.0	336.0	88.5	180.0	244.5	518.5
180.0	53.0	101.0	455.0	288.0	550.5
65.0	109.0	34.5	67.5	282.0	520.0
84.5	67.5	408.5	486.0	275.5	587.0
180.0	19.0	133.5	91.0	381.0	527.0
5.0	241.5	214.0	391.5	450.5	564.0
53.0	343.0	267.5	471.5	301.5	517.0
165.5	248.5	324.5	86.5	282.0	534.0
88.5	4.0	413.0	113.0	391.5	568.0
48.5	324.5	402.5	498.5	419.0	581.0
94.5	62.0	84.5	221.0	434.0	518.5
143.5	294.0	252.5	128.0	454.0	584.0
53.0	337.0	229.0	273.0	256.5	536.5
94.5	428.5	153.5	441.5	387.5	560.0
244.5	27.5	153.5	439.0	374.0	550.5
357.0	252.5	468.0	430.5	461.0	550.5
138.5	411.5	173.0	333.0	256.5	490.0
81.0	378.0	369.0	317.5	307.5	522.0
229.0	53.0	428.5	208.5	205.5	583.0
313.0	357.0	284.5	465.0	384.0	591.0
103.5	298.0	248.5	247.0	349.0	573.0
150.5	252.5	458.0	208.5	396.0	545.0
327.0	214.0	150.5	36.5	422.0	536.5
205.5	155.5	42.5	279.5	270.5	509.0
235.0	214.0	298.0	416.0	364.5	483.5
229.0	229.0	273.0	309.0	426.0	556.0
31.5	446.0	205.5	437.0	513.5	589.0
25.5	192.5	25.5	351.5	462.0	558.5
76.5	131.0	34.5	374.0	301.5	600.0
198.5	341.5	262.5	294.0	456.0	562.0

The sum of the rankings for the various postnatal ages was:

neonate = 15473.5, 7 day = 17554.0, 14 day = 25302.5,
18 day = 30807.0, 21 day = 36315.5, adult = 54847.5.

Using the Kruskal-Wallis formula to test for significant differences in average cell diameter.

$$H = 12/N(N + 1) \sum R_j^2/n_j - 3(N + 1) = 12/600(601) \times (15473.5^2 + 17554.0^2 + 25302.5^2 + 30807.0^2 + 36315.5^2 + 54847.5^2)/100 - 3(601) = 609.95.$$

This is significant at $p < .01$. Correcting for ties will increase H. This increases the level of significance.

Similarly H values were determined for the other parameters. The results of the tests are reported in Tables 1 - 3 and in Figure 38 and Figure 39.

B30372